HHS Public Access

Author manuscript

Eur J Med Chem. Author manuscript; available in PMC 2022 July 05.

Published in final edited form as:

Eur J Med Chem. 2021 July 05; 219: 113402. doi:10.1016/j.ejmech.2021.113402.

4-4-(Anilinomethyl)-3-[4-(trifluoromethyl)phenyl]-1*H*-pyrazol-1-ylbenzoic acid derivatives as potent anti-gram-positive bacterial agents

Raj KC. Hansa[a], **M.K. Khan**[a], **M.M. Frangie**[a], **D.F. Gilmore**[b], **R.S. Shelton**[c], **A.V. Savenka**[c], **A.G. Basnakian**[c,d], **S.L. Shuttleworth**[e], **M.S. Smeltzer**[e], **M.A. Alam**[a,*]

[a]Department of Chemistry and Physics, College of Science and Mathematics, Arkansas State University, Jonesboro, AR, 72467, USA

[b]Department of Biological Sciences, College of Science and Mathematics, Arkansas State University, Jonesboro, AR, 72467, USA

[c]Department of Pharmacology and Toxicology, University of Arkansas for Medical Sciences, 4301 W. Markham St., Little Rock, AR, 72205, USA

[d]Central Arkansas Veterans Healthcare System, W. 7th St., Little Rock, AR, 72205, USA

[e]Department of Microbiology and Immunology, Department of Orthopaedic Surgery, Center for Microbial Pathogenesis and Host Inflammatory Responses University of Arkansas for Medical Sciences, 4301 W. Markham, Little Rock, AR, 72205, USA

Abstract

A collection of potent antimicrobials consisting of novel 1,3-bis-benzoic acid and trifluoromethyl phenyl derived pyrazoles has been synthesized and tested for antibacterial activity. The majority of trifluoromethyl phenyl derivatives are highly potent growth inhibitors of Gram-positive bacteria and showed low toxicity to human cultured cells. In particular, two compounds (**59** and **74**) were selected for additional studies. These compounds are highly effective against *Staphylococcus aureus* as shown by a low minimum inhibitory concentration (MIC), a bactericidal effect in time-kill assays, moderate inhibition of biofilm formation as well as biofilm destruction, and a bactericidal effect against stationary phase cells representing non-growing persister cells. Multistep resistance assays showed a very low tendency for *S. aureus* and *Enterococcus faecalis* to develop resistance through mutation. Additionally, *in vivo* mouse model studies showed no harmful effects at doses up to 50 mg/kg using 14 blood plasma organ toxicity markers or TUNEL assay in liver and kidney. Investigations into the mode of action by performing macromolecular synthesis inhibition studies showed a broad range of inhibitory effects, suggesting targets that have a global effect on bacterial cell function.

*Corresponding author. malam@astate.edu (M.A. Alam).

Declaration of competing interest

The authors declare that they have no known competing financial interests or personal relationships that could have appeared to influence the work reported in this paper.

Appendix A. Supplementary data

Supplementary data to this article can be found online at https://doi.org/10.1016/j.ejmech.2021.113402.

Keywords

Antimicrobial; Pyrazole; *Staphylococcus aureus*; *Enterococcus*; MRSA; Toxicity; Antibiotics

1. Introduction

ESKAPE (*Enterococcus faecium*, *Staphylococcus aureus*, *Klebsiella pneumoniae*, *Acinetobacter baumannii*, *Pseudomonas aeruginosa*, and *Enterobacter* spp) bacteria are causing the majority of nosocomial infections in the United States and these pathogens are effectively escaping the current arsenal of antibiotics [1]. *S. aureus* infections are caused by various strains including methicillin-sensitive *S. aureus* (MSSA), methicillin-resistant *S aureus* (MRSA), vancomycin-intermediate *S. aureus* (VISA), and vancomycin-resistant *S. aureus* (VRSA) strains. MRSA strains have emerged as one of the most menacing pathogens of humans [2–4]. Although MRSA infections have the most notoriety, any *S. aureus* infection can be dangerous and potentially lethal [5]. Hospitals are hotbeds for highly drug-resistant pathogens such as MRSA, increasing the risk of hospitalization kills instead of cures [6]. We are reporting several newly synthesized compounds as potent anti-MRSA agents, an exciting discovery because MRSA has emerged as a major multidrug-resistant pathogen in nosocomial infections and is bypassing HIV in terms of fatality rate [7]. MRSA is one of the most common drug-resistant bacteria. One in three people carry *S. aureus* in their nares, usually without any health concern, but 2% of those carry MRSA strains that can pose a serious threat. *S. aureus* can cause a variety of serious or fatal problems including bacteremia, pneumonia, endocarditis, osteomyelitis, skin infections, and sepsis [8]. Often, the failure of antibiotic therapy against *S. aureus* is due to its acquisition of drug-resistance genes and its ability to adopt a non-growing, persister phenotype that increases drug resistance [9].

Bacterial biofilms are small bacterial communities held together by an extracellular matrix. The biofilm matrix makes bacterial populations tolerant to harsh conditions and resistant to antibacterial treatments [10,11]. In addition, biofilms act as a dangerous reservoir of persisters, which can be a nidus for re-infection [12]. An estimated 17 million new biofilm-associated infections are reported each year, resulting in up to 550,000 fatalities and an estimated $94 billion cost annually [13]. Biofilms are one of the most concerning health threats, and biofilm-forming microbes cause almost 80% of nosocomial infections [14]. Additionally, bacterial biofilm in medical devices is a major concern and causes numerous fatal infections [15]. Due to the importance of controlling biofilms to manage microbial infections, there have been increased efforts towards the inhibition of biofilm formation and destruction of preformed biofilms by small molecules [15,16]. *S. aureus* is a biofilm-producing pathogen, notorious for causing persistent chronic infections due to its ability to resist antibiotic treatments [17]. *S. aureus* and *S. epidermidis* biofilms cause about 40–50% of prosthetic heart valve, 50–70% of catheter biofilm infections, and 87% of bloodstream infections [18].

2. Results and discussion

2.1. Synthesis of pyrazole-derived anilines

Due to the menace of *S. aureus* pathogens, a number of papers have been reported to find novel antibiotics to treat MSSA, MRSA, and VRSA infections [19–23]. In a continuation of our effort to find novel pyrazole derivatives as potent antimicrobial agents, we have reported the synthesis of pyrazole-derivatives as potent antimicrobial agents [24–27]. Pyrazole-derived anilines and hydrazones have been found as anti-MRSA [28] and anti-*A. baumannii* [24,29] agents respectively. To increase the solubility, we designed and synthesized 1,3-bisbenzoic acid-derived pyrazole aldehyde (**P1**). Hydrazone derivatives of this aldehyde have shown potent narrow-spectrum activity, selectively inhibiting the growth of *A. baumannii* with minimum inhibitory concentration (MIC) values as low as 0.78 μg/ml [24]. In this article, we report the synthesis and antimicrobial studies of aniline derivatives of 1,3-bisbenzoic acid-derived pyrazole aldehyde (**P1**, Scheme 1). Reductive amination of this aldehyde with different amines resulted in the formation of pyrazole-derived anilines (**1–40** and **41–79**). The Hantzsch ester was found to be a better reducing agent than $NaBH_4$ and $NaBH_3CN$ for this methodology. The reaction of 1,3-dibenzoic acid-derived pyrazole aldehyde (**P1**) and electron-donating and withdrawing substituted derivatives of aniline formed the expected products (**1–11**) efficiently. Sulfanilamide and its derivatives have been known as antimicrobial agents for several decades [30]. We also synthesized three sulfonamide derivatives (**12–14**). Disubstituted aniline derivatives containing electron-donating (**15–17**), electron-withdrawing (**18–23**), and mixed substituents (**24–28**) were synthesized for antimicrobial studies. Trimethoxy substituted product (**29**) was obtained in a very good yield. To further, explore the structure activity relationship (SAR), 2-aminopyridine derivatives (**30–39**) were also synthesized by the same reductive amination using the Hantzsch ester. The 2-aminopiperazine derivative (40) was synthesized in this series. Surprisingly, none of these compounds (**1–40**) showed any significant activity against the 17 tested strains of Gram-positive and Gram-negative bacteria.

2.2. Antimicrobial studies

To find potent antimicrobial agents, we synthesized trifluoromethyl substituted pyrazole aldehyde (**P2**), which on reaction with different aniline derivatives afforded the desired products in a very good average yield (Scheme 2). Most of these compounds showed potent activity against the tested Gram-positive strains. The *N*-phenyl substituted compound (**41**) showed moderate activity against the tested strains with an MIC value as low as 3.12 μg/ml (Table 1). Halogen substitution (**42–47**) increased the activity of the resultant compounds significantly and the bromo-substituted compounds (**46 and 47**) were most active with MIC value as low as 0.78 μg/ml. The trifluoromethyl substituent (**48**) also showed potent activity. The sulfonamide substituent almost eliminated the activity of resultant compounds (**49**), which indicates that hydrophobic halogen substituent is required for the antibacterial activity. The trifluoromethyl substituent resulted in a potent molecule (**50**) with MIC values 0.78–3.125 μg/ml. Dihalogenated compounds (**51–57**) were potent growth inhibitors of tested Gram-positive strains. 3-Chloro-4-methyl aniline derivative (**58**) inhibited the growth of tested bacteria efficiently. Fluoro-trifluoromethyl substituted aniline resulted in the most potent compound (**59**) of the series. Other trifluoromethyl substituted products (**60–66**) also

showed potent activity with MIC values as low as sub μg/ml concentration. Carboxylic acid substituent eliminated the activity of the resultant compound (**67**) whereas the morpholine substituents produced a highly potent molecule (**68**). The trisubstituted aniline derivatives (**69–77**), except the hydroxy-substituted **78**, showed potent antimicrobial activity. The tetrasubstituted product (**79**) is one of the most potent molecules of the series and inhibited the growth of all the tested bacteria with MIC values of 0.78 μg/ml. The inactivity of compounds **49, 67, and 78** indicates that hydrogen bond donating polar groups in the aniline moiety eliminated the antimicrobial property of the compounds.

with MIC value as low as 0.78 μg/ml. The trifluoromethyl substituent (**48**) also showed potent activity. The sulfonamide substituent almost eliminated the activity of resultant compounds (**49**), which indicates that hydrophobic halogen substituent is required for the antibacterial activity. The trifluoromethyl substituent resulted in a potent molecule (**50**) with MIC values 0.78–3.125 μg/ml. Dihalogenated compounds (**51–57**) were potent growth inhibitors of tested Gram-positive strains. 3-Chloro-4-methyl aniline derivative (**58**) inhibited the growth of tested bacteria efficiently. Fluoro-trifluoromethyl substituted aniline resulted in the most potent compound (**59**) of the series. Other trifluoromethyl substituted products (**60–66**) also showed potent activity with MIC values as low as sub μg/ml concentration. Carboxylic acid substituent eliminated the activity of the resultant compound (**67**) whereas the morpholine substituents produced a highly potent molecule (**68**). The trisubstituted aniline derivatives (**69–77**), except the hydroxy-substituted **78**, showed potent antimicrobial activity. The tetrasubstituted product (**79**) is one of the most potent molecules of the series and inhibited the growth of all the tested bacteria with MIC values of 0.78 μg/ml. The inactivity of compounds **49, 67, and 78** indicates that hydrogen bond donating polar groups in the aniline moiety eliminated the antimicrobial property of the compounds.

Based on the antimicrobial activity of the compounds, we can decipher a good Structure Activity Relationship (SAR) as shown in Fig. 1. Carboxylic group on '**A**' ring eliminated the activity of the compounds (**1–40**) irrespective of the substituents on the aniline moiety ('**B**' ring). Trifluoromethyl substituent (CF_3) on the '**A**' ring resulted the formation of potent compounds. Choice of substituents on the aniline moiety is important for the potency of compounds. Anilines with polar protic substituents resulted the formation of almost inactive compounds (e.g. **49** and **78**). Small lipophilic groups such as fluoro (F), chloro (Cl), and methyl (CH_3) on the aniline moiety increase activity of the resultant compounds and these groups show synergistic effects with CF_3 substituent.

2.3. Cytotoxicity of potent antimicrobials

To select molecules for further antimicrobial studies, the most potent molecules were tested for their possible toxicity for human embryonic kidney (HEK293) cells. We found several molecules with a very good selectivity factor. The selectivity factors of compounds **59** and **74** are as high as 13 and 33 respectively. Although some other compounds had better selectivity, compounds **59** and **74** were selected for further studies for their comparatively low lipophilicity and high potency across the tested strains. Tested compounds with higher toxicity for HEK293 cells are not shown in Fig. 2.

2.4. Biofilm inhibition and destruction studies

In our quest to find biofilm inhibitors and preformed biofilm eliminators [25,31], we tested potent compounds for their ability to inhibit and destroy *S. aureus* and *E. faecalis* biofilms (Fig. 3). Compound **59** inhibited 90% of the biofilm formation at 2xMIC concentration and this compound retained its biofilm inhibition ability at MIC and 0.5xMIC concentrations. Compound **74** inhibited the biofilm formation by greater than 85% at 2xMIC concentration but its ability to inhibit the biofilm formation was reduced significantly at lower concentrations. In biofilm destruction studies, compound **59** eliminated almost 70% and 55% preformed biofilms at 2x and 1xMIC respectively and its ability to eliminate the preformed biofilm decreased significantly at 0.5xMIC concentration. A similar elimination property for compound **74** was observed. Thus, compound **59** is better than the positive control vancomycin for its ability to inhibit and eliminate *S. aureus* biofilms (Fig. 3). Similar experiments were conducted against *E. faecalis* biofilm. Compound **59** inhibited almost 90%, 85% and 75% biofilm formation at 2x, 1x and 0.5x MIC respectively. Compound **79** inhibited nearly 80% biofilm formation at 2xMIC and the ability to inhibit biofilm decreased at 1x and 0.5xMIC. We observed that compound **59** outperformed the inhibition capacity of the control drug vancomycin, which inhibited around ~75% in at 2xMIC. The biofilm destruction capacity of compound **59** at 2xMIC was 85% and 75% at 1xMIC while 0.5xMIC potency diminished significantly. Compound **74** was seen to destroy about 75% of preformed biofilm at 2xMIC and its capacity decreased with decreasing the concentration. Thus, compound **59** performed better in preformed biofilm destruction than the positive control, which destroyed around 70% and 75% at 2x and 1xMIC, respectively. Lead compounds (**59** and **75**) and vancomycin have shown >95% biofilm inhibition and destruction at 4x and 8xMIC (data not shown).

2.5. Destruction of catheter-associated biofilm

After finding compound **59** as a potent inhibitor and eliminator of biofilms, we tested its antibacterial efficacy in the context of an established biofilm using an *in vitro* model of catheter-associated biofilm formation and the methicillin-sensitive clinical isolate of *S. aureus* UAMS-1 (Fig. 4). The activity of compound **59** (MIC = 2 μg/ml) was compared against vancomycin based on its breakpoint MIC (≥2 μg/ml). Both compound **59** and vancomycin were studied at 20xMIC values (40 μg/ml) as described by us previously [32]. As shown in Fig. 4, molecule **(59)** showed activity comparable if not greater than that observed with vancomycin. Specifically, after 2 days of exposure, average CFU counts were 4.74×10^5 and 1.16×10^7 for **59** and vancomycin, respectively. The CFU count of untreated biofilms was 1.53×10^8. Thus, compound **59** was 25 times more potent than vancomycin in eliminating viable bacteria in catheter-associated biofilm of this strain.

2.6. Activity against persisters

Stationary phase cells of *S. aureus* are tolerant to conventional antibiotics [33,34]. We also demonstrated tolerance to conventional antibiotics vancomycin and gentamicin at 67xMIC against *S. aureus* ATCC 700699. We studied the ability of compounds **59** and **74** to kill persister cells of MRSA (Sa99). Persister cells in these experiments were represented by stationary phase cells from an overnight culture. High concentrations of conventional

antibiotics vancomycin and gentamicin (at 64xMIC) did not affect the viability of MRSA persisters whereas our compounds **59** and **74** were observed to be effective against persister cells at the lower concentration of 16xMIC (Fig. 5A). Therefore, we conducted persister kill assays against MRSA using these compounds at various MIC levels. We observed that compound **59** caused ~4-log reduction at 16xMIC and ~3, 2, and 1-log reduction at 8, 4, and 2xMIC respectively within 4 h. Compound **74** caused ~2-log reduction at 16xMIC and ~1-log reduction at 8, 4, and 2xMIC respectively (Fig. 5B).

2.7. Multistep resistance studies

Many antibiotics fail because of the ability of bacteria to develop resistance against antibiotics, through either mutation or horizontal gene transfer. The likelihood of a bacterium developing resistance through mutation can be tested using a multi-step resistance assay. *S. aureus* strains (MSSA and MRSA) were exposed to compounds **59** and **74**, and to positive control antibiotics ciprofloxacin and vancomycin at sub-lethal concentration. As shown in Fig. 6A and Fig. 6b, both staphylococcal strains started developing resistance to vancomycin on the 6th passage and showed no further change after the 10th passage. MRSA began developing resistance to ciprofloxacin whereas resistance to ciprofloxacin in the MSSA was delayed until the 7th passage. In both cases, however, further resistance developed rapidly, with bacteria becoming 16-fold more resistant within two weeks of the start of the experiment. In contrast, the MICs for **59** and **74** against MRSA doubled at the 9th and 10th passages respectively with one additional doubling during the 21 passages. Against MSSA, MIC values for **59** and **74** doubled on the 8th and 14th passages, respectively, without any further change. MRSA developed very quick resistance against the ciprofloxacin treatment. MIC for vancomycin double and quadrupled on 7th and 10th passages respectively. Although *E. faecalis* showed little increase in resistance to positive control antibiotics, after passages 3 and 8 for ciprofloxacin and after passage 7 for vancomycin, there was no increase in resistance against compounds **59** and **74** through the 14th passage.

2.8. Time kill assay

Time kill assays were performed with compounds **59** and **74** at 4xMIC concentration to observe their bactericidal activity against planktonic bacteria over time. Fig. 7 shows results for those compounds along with those for positive control vancomycin and negative control DMSO against two strains of *S. aureus*. Both compounds showed bactericidal activity against the tested strains. Compound **59** eliminated more than 3 log values of both the strains within 4 h of treatment. Compound **74** displayed similar activity by 4 h against *S. aureus* ATCC 33591 and by 6 h against *S. aureus* ATCC 700699 strain. Both of these bacteria are MRSA strains. Vancomycin, our positive control and the drug of choice for treatment of serious MRSA infections, displayed bactericidal activity and decreased bacterial concentration below detectable limits after 8 h of treatment for both strains.

2.9. Activity against clinical isolates

After finding the promising compound (**59**) to be a potent growth inhibitor of *S. aureus* and *E. faecalis* both in planktonic and biofilm contexts, this molecule was tested for its potency

against 18 clinical isolates as shown in Table 2. This compound is very potent against the *E. faecalis* isolates, is several times better than the positive controls oxacillin and vancomycin, and is comparable to meropenem potency. The activity of compound **59** against the *E. faecium* strains shows that this molecule could be a potential treatment for *E. faecium* infections that are otherwise non-treatable with all three positive controls. *S. aureus* clinical isolates were also inhibited with MIC values as low as 2 μg/ml by this potent compound (**59**).

2.10. In vivo toxicity studies

The absence of toxicity in cultured cells does not indicate that the compound is not toxic *in vivo*. Therefore, after testing the compound against human cell lines, we determined a potential toxicity of compound **59** in mice (Fig. 8). We chose the doses of 5, 20, and 50 mg/kg because they were used for our compounds in previous studies [24,35]. Acute *in vivo* effects of a single intraperitoneal injection of the compound were assessed 24 h later by 14 key parameters for organs' functions as described in Fig. 8. This measurement showed that none of the organ function markers indicated toxicity by the used criteria. Most of the tests after acute administration of the compound showed no significant difference from the control samples (vehicle, saline injection). In particular, a normal concentration of blood plasma albumin indicated no harm to the liver and kidneys. Unaffected blood urea nitrogen (BUN), createnine, sodium, and potassium concentrations indicated no toxicity to the kidneys of the treated animals. A normal concentration of amylase indicated that this potent antibacterial agent did not adversely affect the pancreatic function. A normal alkaline phosphatase (ALP) concentration in blood was a key indicator of a healthy liver and bones. This treatment exposure showed an unaffected level of ALP. Normal alanine transaminase (ALT) and glucose levels at up to 50 mg/kg treatment further confirm the tolerance of this compound by the liver. Altogether, the liver injury was not confirmed by any liver injury markers, such as total bilirubin, ALP, ALT, and others. Calcium and phosphorus levels indicated the normal function of several organs such as the liver, kidney, and bones. Unaffected total protein and globulin levels indicate a healthy liver and kidney, and immune system respectively. Thus, this compound (**59**) is non-toxic in therapeutic doses and seems to be very safe for further drug development.

While the organ function tests by blood markers are the most important, we wanted to make sure there was no structural organ damage induced by the new compound. For this, we tested the potential damage to the liver and kidneys, the organs most commonly affected by toxic compounds, and applied the TUNEL assay, which is the most sensitive and universal assay for irreversible cell death [36]. We used the well-established liver toxin acetaminophen and the kidney toxin cisplatin as positive controls. The data shown in Fig. 9 clearly demonstrated the absence of any structural injury (cell death detected by TUNEL-positivity) to the liver or kidney in the tested animals 24 h after IP injection with 50 mg/kg dose.

2.11. Mechanism of action (MoA) studies

Many compounds function by having a discernible inhibition of key enzymes and processes such as peptidoglycan or protein synthesis and radioactivity labelled precursors are widely used to determine the mechanism of action (MoA) of new molecular entities [37]. The MoA

of the potent molecule **59** was explored by performing macromolecular synthesis inhibition assays in *S. aureus* ATCC 29213 at multiples of the MIC as shown in Fig. 10. The treatment of *S. aureus* resulted in increasing inhibition of DNA synthesis from approximately 44% at 0.25xMIC to 100% inhibition at 4xMIC. This result compares with 86.2% inhibition for the positive control drug ciprofloxacin at 8xMIC. This potent compound (**59**) inhibited RNA synthesis in a dose-dependent fashion, with 15.5% inhibition observed at 0.25xMIC, and increasing inhibition was seen with increasing concentration of the compound with 98% inhibition at 4xMIC. The control drug rifampicin showed 76.3% inhibition at 8xMIC. Effects on cell wall synthesis were observed at higher doses with this compound, and less of a dose-response was observed. At 2xMIC, compound **59** demonstrated cell wall inhibition of 39.5%. At higher concentrations (4x to 8xMIC), cell wall inhibition levels were >80%. In comparison, the positive control drug vancomycin demonstrated 87.3% inhibition at 8xMIC. This compound showed inhibition of lipid synthesis at low doses with good dose-response. At the low dose, 0.25xMIC, 20.7% inhibition of lipid synthesis of was seen, and inhibition reached 56.2% at MIC and to near 100% at 4xMIC. The control drug cerulenin showed 71.9% inhibition at 8xMIC in this assay. Effects on protein synthesis for this novel agent (**59**) was substantial and nearly 100% protein synthesis was inhibited at 4xMIC. The protein synthesis inhibitor linezolid exhibited 70.7% inhibition at 8xMIC. These results are consistent with a mode of action against a target with wide ranging effects, such as disruption of ATP synthesis. Alternatively, there may be several individual and specific targets that also produce widespread inhibition. Either way, these results are very significant as it less likely that bacteria can develop resistance against these molecules, which have a fundamental or multiple mode of mechanism of action [38].

3. Conclusion

The synthesis and antimicrobial studies of 79 novel compounds led to the discovery of trifluoromethyl-substituted compounds as potent anti-Gram-positive bacterial agents. Further optimization helped to find compounds with halogens and the trifluormethyl group in the aniline substituent of the pyrazole moiety as the most promising compounds. While activity against *S. aureus* alone makes these compounds of considerable interest, the potent activity against clinical isolates of *E. faecium* make these molecules promising candidates to treat VRE infections. The activity of these compounds against biofilms and persisters also make them promising potential antibiotics. Both their potent antimicrobial effects as well as the lack of apparent *in vivo* toxicity of compound **59** up to 50 mg/kg shows the suitability of these compounds for further drug development. It is less likely that bacteria will develop resistance agianst these molecules which have multipe modes of mechanism of action. ADMET and *in vivo* antimicrobial studies will be reported in due course.

4. Experimental protocols

4.1. General methods

All of the reactions were carried out under air atmosphere in round-bottom flasks. Commercially available solvents, reagents, and substrates were purchased from Fisher Scientific (Hanover Park, IL, USA.) and Oakwood chemical (Estill, SC, USA) and used

directly. ^{1}H and ^{13}C NMR spectra were recorded on Varian Mercury (300 MHz for ^{1}H and 75 MHz for ^{13}C). Brucker Apex II-FTMS system was used to record mass spectra. Chemical shifts (^{1}H and ^{13}C) are reported in parts per million (ppm) referenced to the residual solvent peak. Abbreviations used to describe the peak signals in ^{1}H and ^{13}C NMR data are s (singlet), d (doublet), dd (double doublet), t (triplet), q (quartet), br (broad), and m (multiplet).

4.2. General method for the synthesis of pyrazole aldehyde (P1 and P2)

Pyrazole-derived aldehydes (**P1** and **P2**) were synthesized according to our reported procedures [24,29]. A solution of acetophenones (10 mmol) and hydrazinobenzoic acid (10.5 mmol, 1.59 g) in ethanol (50 ml) in a round-bottom flask fitted with a reflux condensor was heated to reflux for 8 h. The reaction mixture was brought to room temperature and the solvent was removed in vacuo. The product, hydrazone, was further dried in vacuo to remove the traces of solvent. *N,N*-Dimethylformamide (30 ml) was added to dossolve the solid hydrazone and the solution in a sealed round-bottom flask was cooled in ice for 15 min. $POCl_3$ (50 mmol, 4.67 ml) was added dropwise over aperiod of 10 min. The reaction mixture was vented by putting a needle in the septum. The reaction was stirred for 15 min under ice and further stirred for 30 min at room temperature followed by heating at 85 °C in an oild bath for 8 h. The hot reaction mixture was poured onto ice in a 500 ml beaker. The reaction mixture in ice/water was stirred for 8 h to precipited the product. The solid product was filtered and washed repeatedly with water to get the pure products (**P1** and **P2**). After drying the product in vacuo, these aldehyde derivatives were subjected to next step without any purification.

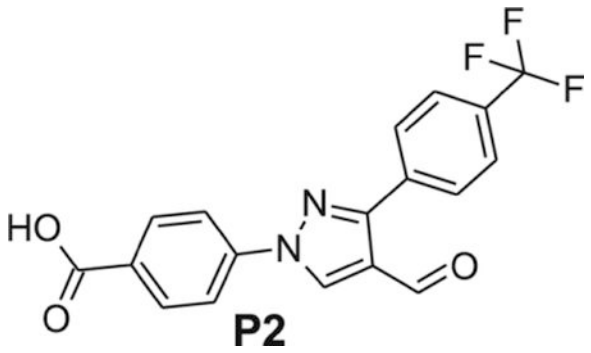

P2

4-[4-formyl-3-[4-(trifluoromethyl)phenyl]pyrazol-1-yl]benzoic acid (P2).— Yellowish solid; yield 99%; ^{1}H NMR, 300 MHz (DMSO-d_6); δ 10.0 (s, 1H), 9.50 (s, 1H), 8.19–8.11 (m, 6H), 7.87 (d, J = 8.1 Hz, 2H); ^{13}C NMR 75 MHz (DMSO-d_6): δ 184.9, 166.9, 151.5, 141.8, 136.9, 135.45 (^{4}J = 0.75 Hz), 131.4, 130.1, 129.86 (^{2}J = 31.7 Hz), 129.83, 125.8 (m), 124.5 (^{1}J = 270 Hz), 123.2, 119.3, HRMS (ESI-FTMS Mass (*m/z*): calcd for $C_{18}H_{11}F_3N_2O_3$ $[M+H]^+$ = 361.0794, found 361.0791.

4.3. General procedure for the reductive amination

Pyrazole-derived aldehyde (**P1** or **P2**, 1 mmol) and the aniline derivative (1.05 mmol) in toluene were refluxed by using Deen-Stark condenser for 8 h, and then the reaction was cooled to room temperature and the Hantzch ester (2 mmol) was added and the reaction

mixture was heated to reflux for 8 h. Toluene was distilled out and ethanol (~2 ml) was added to the reaction mixture and 10% HCl (~25 ml) was added to precipitate the product. Filtration followed by recrystallization with methanol gave the pure products.

4.3.1. Experimental data—

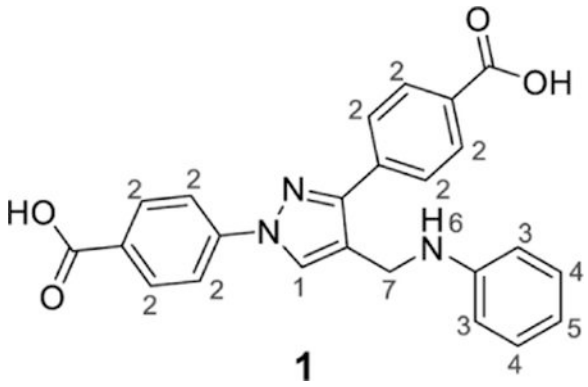

1

4-[4-(Anilinomethyl)-1-(4-carboxyphenyl)pyrazol-3-yl]benzoic acid (1).: Brownish yellow solid; yield 79%; ^{1}H NMR 300 MHz (DMSO-d_6): δ 8.71 (s, 1H, H-1), 8.06–7.95 (m, 8H, H-2), 7.09 (t, J = 7.1 Hz, 2H, H-3), 6.67 (d, J = 7.62 Hz, 2H, H-4), 6.57 (t, J = 6.84 Hz, 1H, H-5), 6.00 (br s, 1H, H-5), 4.29 (s, 2H, H-7); ^{13}C NMR 75 MHz (DMSO-d_6): δ 167.5, 167.1, 150.5, 148.9, 142.7, 137.1, 131.5, 130.6, 130.1, 129.3, 128.7, 127.8, 121.0, 118.1, 116.7, 112.8, 38.6. HRMS (ESI-FTMS Mass (*m/z*): calcd for $C_{24}H_{19}N_3O_4$ $[M+H]^+$ = 414.1448, found 414.1452.

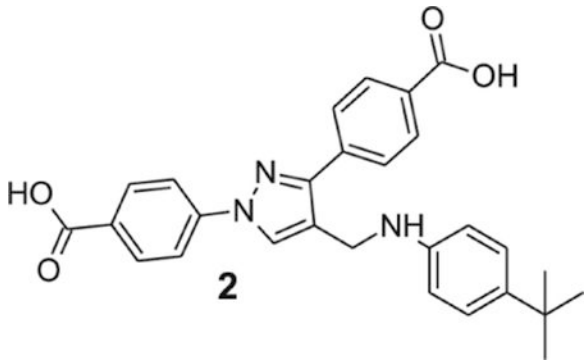

2

4-[4-[(4-*tert*-butylanilino)methyl]-1-(4-carboxyphenyl)pyrazol-3-yl]benzoic acid (2).: Yellowish solid; yield 76%; ^{1}H NMR, 300 MHz (DMSO-d_6): δ 8.71 (s, 1H), 8.08–7.95 (m, 9H), 7.11 (d, J = 8.46 Hz, 2H), 6.60 (d, J = 8.49 Hz, 2H), 4.28 (s, 2H), 1.20 (s, 9H); ^{13}C NMR 75 MHz (DMSO-d_6): δ 167.5, 167.1, 146.6, 142.7, 138.9, 137.2, 131.4, 130.6, 130.1, 129.2, 128.7, 127.8, 125.9, 121.3, 118.1, 112.6, 39.0, 33.9, 31.9. HRMS (ESI-FTMS Mass (*m/z*): calcd for $C_{28}H_{27}N_3O_4$ $[M+H]^+$ = 470.2074, found 470.2068.

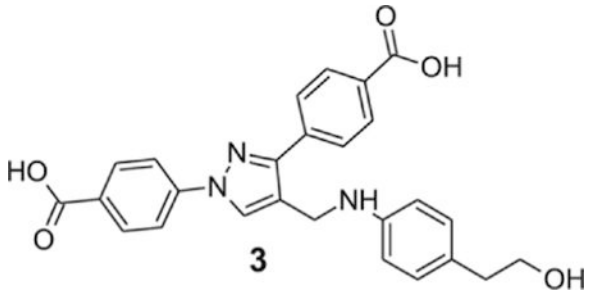

3

4-[1-(4-carboxyphenyl)-4-[[4-(2-hydroxyethyl)anilino]methyl]pyrazol-3-yl]benzoic acid (3).: Yellowish solid; yield 76%; ^{1}H NMR, 300 MHz (DMSO-d_6): δ 8.71 (s, 1H), 8.09–7.95 (m, 8H), 6.94 (d, J = 8.19 Hz, 2H), 6.60 (d, J = 8.22 Hz, 2H), 5.84 (br s, 1H), 4.27 (s, 2H), 3.50 (t, J = 7.2 Hz, 2H), 2.56 (t, J = 7.2 Hz, 2H); ^{13}C NMR 75 MHz (DMSO-d_6); δ 167.5, 167.1, 150.5, 147.2, 142.7, 137.2, 131.5, 130.6, 130.1, 130.0, 129.7, 128.7, 127.8, 127.3, 121.2, 118.1, 112.9, 63.2, 38.9, 38.8. HRMS (ESI-FTMS Mass (*m/z*): calcd for $C_{26}H_{23}N_3O_5$ $[M+H]^+$ = 458.1710, found 458.1714.

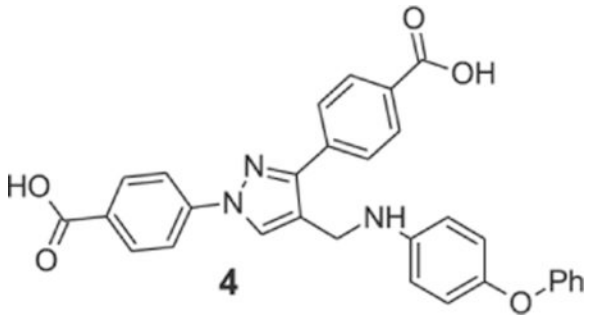

4

4-[1-(4-carboxyphenyl)-4-[(4-phenoxyanilino)methyl]pyrazol-3-yl]benzoic acid (4).: Yellowish solid; yield 90%; ^{1}H NMR, 300 MHz (DMSO-d_6): δ 8.74 (s, 1H), 8.07–7.99 (m, 8H), 7.29–7.27 (m, 2H), 6.99–6.27 (m, 1H), 6.99–6.85 (m, 3H), 6.72 (d, J = 8.61 Hz, 3H), 5.99 (br s, 1H), 4.30 (s, 2H); ^{13}C NMR 75 MHz (DMSO-d_6): δ 167.5, 167.1, 159.2, 150.5, 146.4, 145.9, 142.7, 137.1, 131.5, 130.5, 130.1, 128.7, 127.8, 122.2, 121.4, 120.9, 118.1, 116.9, 113.9, 38.9. HRMS (ESI-FTMS Mass (*m/z*): calcd for $C_{30}H_{23}N_3O_5$ $[M+H]^+$ = 506.1710, found 506.1699.

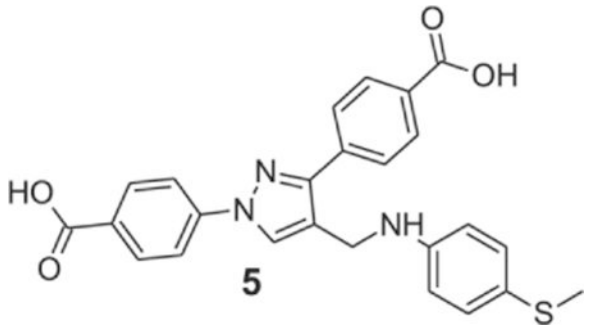

5

4-[1-(4-carboxyphenyl)-4-[(4-methylsulfanylanilino)methyl]pyrazol-3-yl]benzoic acid (5).: Brownish yellow solid; yield 91%; ^{1}H NMR, 300 MHz (DMSO-d_6): δ 8.70 (s, 1H),

8.09–7.93 (m, 8H), 7.12 (d, J = 8.34 Hz, 2H), 6.65 (d, J = 8.4 Hz, 2H), 4.28 (s, 2H), 2.33 (s, 3H); ^{13}C NMR 75 MHz (DMSO-d_6): δ 167.5, 167.1, 150.5, 147.7, 142.7, 137.1, 131.5, 130.9, 130.6, 130.1, 129.2, 128.7, 127.8, 122.8, 120.8, 118.1, 113.6, 38.6, 18.4. HRMS (ESI-FTMS Mass (*m/z*): calcd for $C_{25}H_{21}N_3O_4S$ $[M+H]^+$ = 460.1326, found 460.1324.

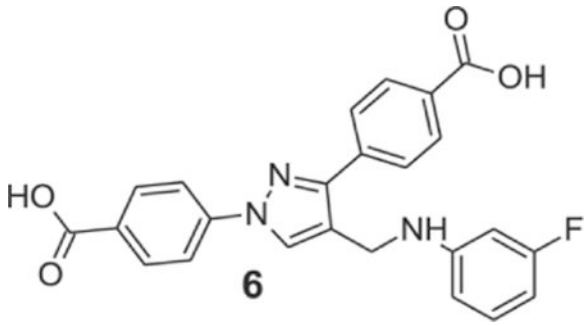

4-[1-(4-carboxyphenyl)-4-[(3-fluoroanilino)methyl]pyrazol-3-yl]benzoic acid (6).: Yellowish solid; yield 84%; ^{1}H NMR, 300 MHz (DMSO-d_6): δ 8.73 (s, 1H), 8.12–7.93 (m, 8H), 7.13–7.05 (m, 1H), 6.51–6.48 (m, 2H), 6.43 (s, 1H), 6.34 (t, J = 7.26 Hz, 1H), 4.30 (s, 2H); ^{13}C NMR 75 MHz (DMSO-d_6); δ 167.6, 167.2, 163.8 (^1J = 238.0 Hz), 150.9 (^3J = 11.0 Hz), 150.5, 142.6, 137.0, 131.4, 130.7, 130.6, 130.1, 129.3 (^3J = 7.6 Hz), 128.9, 127.8, 120.4, 118.1, 109.1, 102.6 (^2J = 21.2 Hz), 99.0 (^2J = 24.7 Hz), 38.5. HRMS (ESI-FTMS Mass (*m/z*): calcd for $C_{24}H_{18}FN_3O_4$ $[M+H]^+$ = 432.1354, found 432.1364.

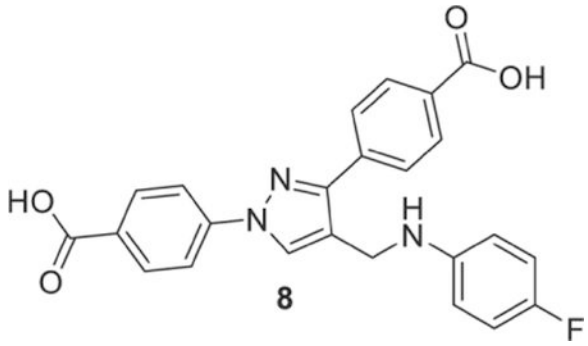

4-[1-(4-carboxyphenyl)-4-[(4-fluoroanilino)methyl]pyrazol-3-yl]benzoic acid (7).: Yellowish solid; yield 73%; ^{1}H NMR, 300 MHz (DMSO-d_6): δ 8.69 (s, 1H), 8.05–7.93 (m, 8H), 6.93 (t, J = 8.58 Hz, 2H), 6.66 (s, 2H), 4.26 (s, 2H); 13C NMR 75 MHz (DMSO-d_6); δ 167.5, 167.1, 155.0 (^1J = 229.8 Hz), 150.6, 145.5, 142.7, 137.1, 131.5, 130.5, 130.1, 130.0, 128.7, 127.8, 120.8, 118.2, 115.7 (^2J = 21.8 Hz), 113.7 (^3J = 7.11 Hz), 38.9. HRMS (ESI-FTMS Mass (*m/z*): calcd for $C_{24}H_{18}FN_3O_4$ $[M+H]^+$ = 432.1354, found 432.1350.

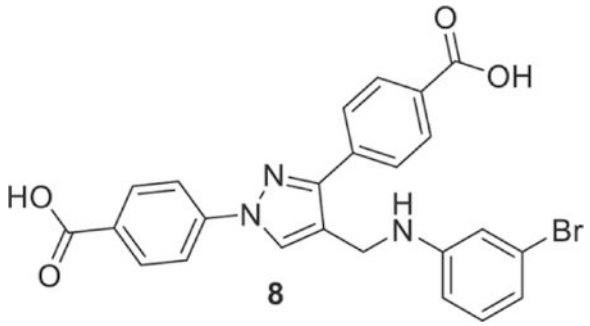

4-[4-[(3-bromoanilino)methyl]-1-(4-carboxyphenyl)pyrazol-3-yl]benzoic acid (8).: Yellowish solid; yield 72%; ^{1}H NMR, 300 MHz (DMSO-d_6): δ 8.73 (s, 1H), 8.07–7.93 (m, 8H), 7.03 (t, J = 7.6 Hz, 1H), 6.83 (s, 1H), 6.72–6.64 (m, 2H), 6.35 (s, 1H), 4.31 (s, 2H); ^{13}C NMR 75 MHz (DMSO-d_6): δ 167.6, 167.2, 150.5, 142.4, 136.8, 131.4, 131.2, 130.1, 129.6, 127.7, 122.8, 120.3, 118.9, 118.1, 114.9, 111.6, 38.4. HRMS (ESI-FTMS Mass (*m/z*): calcd for $C_{24}H_{18}BrN_3O_4$ $[M+H]^+$ = 492.0553, found 492.0561.

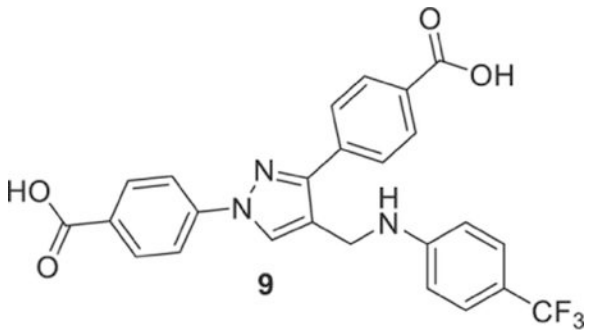

4-[1-(4-carboxyphenyl)-4-[[4-(trifluoromethyl)anilino]methyl]pyrazol-3-yl]benzoic acid (9).: Brownish yellow; yield 81%; ^{1}H NMR, 300 MHz (DMSO-d_6): δ 8.73 (s, 1H), 8.09–7.92 (m, 8H), 7.40 (d, J = 8.46, 2H), 6.77 (d, J = 8.49 Hz, 3H), 4.37 (s, 2H); ^{13}C NMR 75 MHz (DMSO-d_6): δ 167.5, 167.1, 151.7, 150.5, 142.6, 137.0, 131.5, 130.7, 130.6, 130.1, 128.8, 127.8, 126.7 (^{3}J = 3.51 Hz), 125.7 (^{1}J = 268.1 Hz), 120.2, 118.2, 116.2 (^{2}J = 31.5 Hz), 112.1, 38.2. HRMS (ESI-FTMS Mass (*m/z*): calcd for $C_{25}H_{18}F_3N_3O_4$ $[M+H]^+$ = 482.1322, found 482.1310.

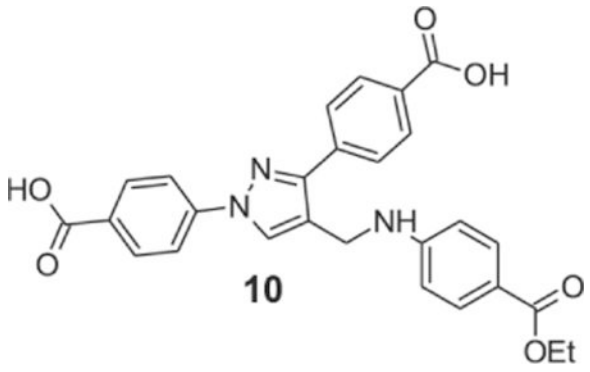

4-[1-(4-carboxyphenyl)-4-[(4-ethoxycarbonylanilino)methyl]pyrazol-3-yl]benzoic acid (10).: Yellowish solid; yield 83%; ^{1}H NMR, 300 MHz (DMSO-d_6): δ 8.71 (s, 1H), 8.08–7.90 (m, 8H), 7.70 (d, J = 8.49 Hz, 2H), 6.93 (br s, 1H), 6.69 (d, J = 8.49 Hz, 2H), 4.38 (s, 2H), 2.49 (s, 2H), 1.25 (t, J = 7.08 Hz, 3H); ^{13}C NMR 75 MHz (DMSO-d_6); δ 167.5, 167.1, 166.3, 152.7, 150.5, 142.6, 136.9, 131.4, 131.3, 130.7, 130.1, 128.8, 127.8, 120.0, 118.2, 117.1, 111.7, 60.0, 38.9, 38.0, 14.8. HRMS (ESI-FTMS Mass (*m/z*): calcd for $C_{27}H_{23}N_3O_6$ $[M+H]^+$ = 486.1660, found 486.1651.

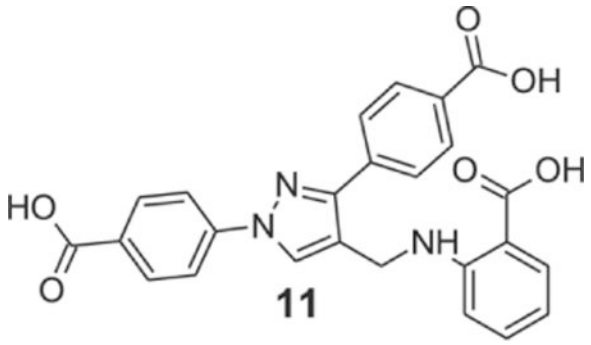

11

2-[[1,3-bis(4-carboxyphenyl)pyrazol-4-yl]methylamino]benzoic acid (11).: Yellowish solid; yield 72%; ^{1}H NMR, 300 MHz (DMSO-d_6): δ 8.72 (s, 1H), 8.06–7.94 (m, 8H), 7.51 (s, 1H), 7.25 (s, 1H), 7.20 (d, J = 9.84 Hz, 2H), 6.89 (d, J = 7.02 Hz, 1H), 6.34 (br s, 1H), 4.34 (s, 2H); ^{13}C NMR 75 MHz (DMSO-d_6): δ 168.3, 167.5, 167.1, 150.5, 148.9, 142.6, 137.1, 131.8, 131.5, 130.6, 130.1, 129.5, 128.8, 127.8, 120.7, 118.2, 117.6, 116.8, 113.5, 39.0, 38.6. HRMS (ESI-FTMS Mass (*m/z*): calcd for $C_{25}H_{19}N_3O_6$ $[M+H]^+$ = 458.1347, found 458.1349.

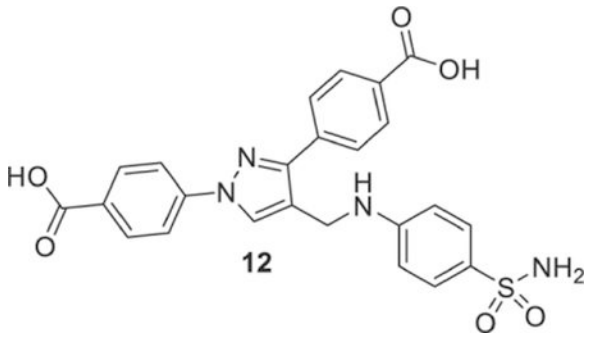

12

4-[1-(4-carboxyphenyl)-4-[(4-sulfamoylanilino)methyl]pyrazol-3-yl]benzoic acid (12).: Yellowish solid; yield 85%; ^{1}H NMR, 300 MHz (DMSO-d_6): δ 8.73 (s, 1H), 8.06–7.92 (m, 8H), 7.54 (d, J = 8.58 Hz, 2H), 6.96 (s, 2H), 6.81 (s, 1H), 6.73 (d, J = 8.67 Hz, 2H), 4.39 (s, 2H); ^{13}C NMR 75 MHz (DMSO-d_6); δ 167.5, 167.1, 151.4, 150.5, 142.6, 137.0, 131.5, 131.1, 130.8, 130.1, 130.0, 129.3, 129.0, 127.8, 120.2, 118.2, 111.6, 38.2. HRMS (ESI-FTMS Mass (*m/z*): calcd for $C_{24}H_{20}N_4O_6S$ $[M+H]^+$ = 493.1176, found 493.1168.

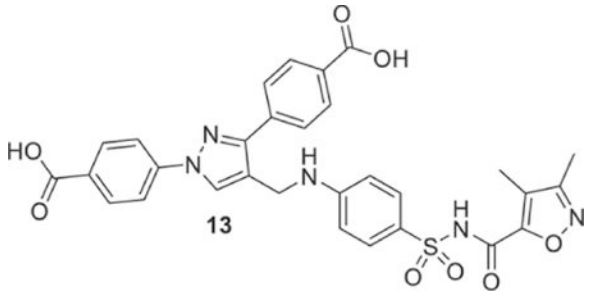

4-[1-(4-carboxyphenyl)-4-[[4-[(3,4-dimethylisoxazole-5-carbonyl) sulfamoyl]anilino]methyl]pyrazol-3-yl]benzoic acid (13).: Yellowish solid; yield 92%; ^{1}H NMR, 300 MHz (DMSO-d_6): δ 8.73 (s, 1H), 8.10–7.91 (m, 8H), 7.44 (d, J = 8.79 Hz, 2H), 7.09 (s, 1H), 6.75 (d, J = 8.85 Hz, 2H), 4.41 (s, 2H), 2.05 (s, 3H), 1.58 (s, 3H); ^{13}C NMR 75 MHz (DMSO-d_6): δ 167.5, 167.1, 161.6, 156.7, 152.5, 150.5, 142.6, 137.0, 131.5, 130.6, 130.1, 129.0, 128.8, 127.8, 125.7, 119.9, 118.2, 111.9, 104.7, 38.0, 10.7, 6.2. HRMS (ESI-FTMS Mass (*m/z*): calcd for $C_{30}H_{25}N_5O_8S$ $[M+H]^+$ = 616.1497, found 588.1549.

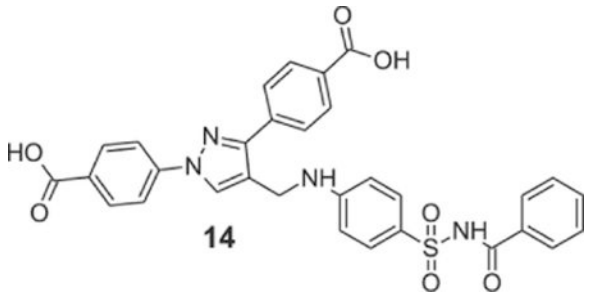

4-[4-[[4-(benzoylsulfamoyl)anilino]methyl]-1-(4-carboxyphenyl)pyrazol-3-yl]benzoic acid (14).: Yellowish solid; yield 89%; ^{1}H NMR, 300 MHz (DMSO-d_6): δ 8.75 (s, 1H), 8.09–7.92 (m, 8H), 7.84 (d, J = 7.41 Hz, 2H), 7.72 (d, J = 8.70 Hz, 2H), 7.59 (d, J = 7.23, 1H), 7.46 (d, J = 7.71 Hz, 2H), 7.14 (s, 1H), 6.78 (d, J = 8.85 Hz, 2H), 4.41 (s, 2H); ^{13}C NMR 75 MHz (DMSO-d_6): δ 167.5, 167.1, 165.6, 152.8, 150.5, 142.6, 137.0, 133.3, 132.4, 131.4, 130.7, 130.3, 130.2, 128.9, 128.8, 127.8, 125.1, 119.9, 118.5, 118.2, 111.5, 38.1. HRMS (ESI-FTMS Mass (*m/z*): calcd for $C_{31}H_{24}N_4O_7S$ $[M+H]^+$ = 597.1438, found 597.1442.

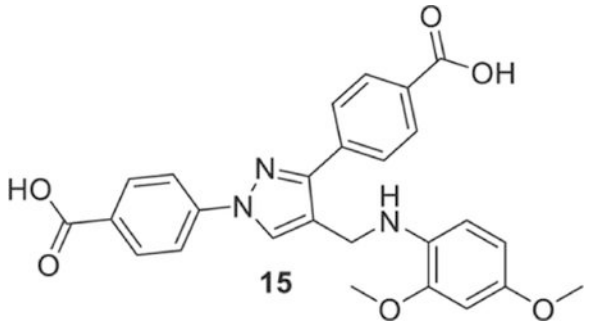

4-[1-(4-carboxyphenyl)-4-[(2,4-dimethoxyanilino)methyl]pyrazol-3-yl]benzoic acid (15).: Yellowish solid; yield 97%; ^{1}H NMR, 300 MHz (DMSO-d_6): δ 8.64 (s, 1H), 8.08–7.94 (m, 9H), 6.55–6.48 (m, 2H), 6.34 (d, J = 8.49 Hz, 1H), 4.31 (s, 2H), 3.72 (s, 3H), 3.64 (S, 3H); ^{13}C NMR 75 MHz (DMSO-d_6): δ 167.5, 167.1, 152.0, 150.4, 148.1, 142.7, 137.2, 132.3, 131.4, 130.6, 130.1, 129.9, 128.7, 127.8, 121.5, 118.2, 110.9, 104.3, 99.5, 55.8, 55.7, 39.0. HRMS (ESI-FTMS Mass (*m/z*): calcd for $C_{26}H_{23}N_3O_6$ $[M+H]^+$ = 474.1660, found 474.1651.

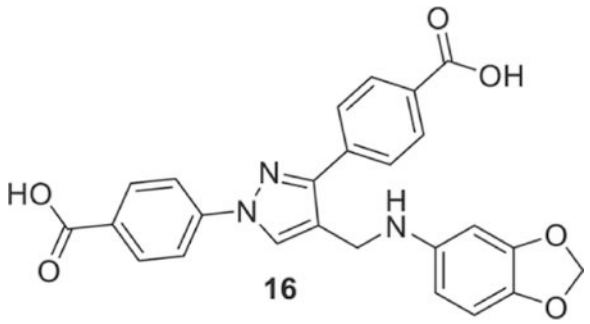

16

4-[4-[(1,3-benzodioxol-5-ylamino)methyl]-1-(4-carboxyphenyl)pyrazol-3-yl]benzoic acid (16): Yellowish solid; Yield 83%; ^{1}H NMR, 300 MHz (DMSO-d_6):δ8.64 (s, 1H), 8.08–7.94 (m, 9H), 6.55–6.48 (m, 2H), 6.34 (d, J = 8.49 Hz, 1H), 4.31 (s, 2H), 3.72 (s, 3H), 3.64 (S, 3H); ^{13}C NMR 75 MHz (DMSO-d_6): δ 167.5, 167.1, 150.5, 148.1, 144.8, 142.7, 138.8, 137.1, 131.5, 130.6, 130.1, 128.7, 127.8, 121.0, 118.1, 108.9, 104.0, 100.4, 95.9, 39.0. HRMS (ESI-FTMS Mass (*m/z*): calcd for $C_{26}H_{23}N_3O_6$ $[M+H]^+$ = 458.1347, found 458.1345.

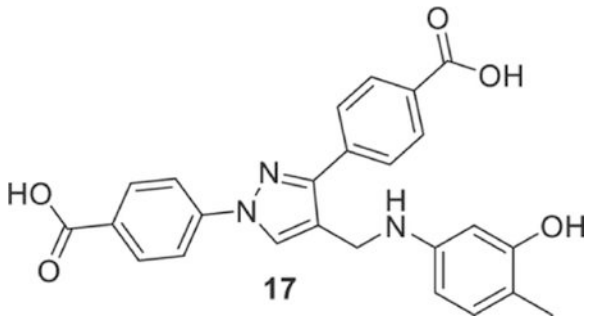

17

4-[1-(4-carboxyphenyl)-4-[(3-hydroxy-4-methyl-anilino)methyl]pyrazol-3-yl]benzoic acid (17).: Yellowish Solid; Yield 91%; ^{1}H NMR 300 MHz (DMSO-d_6): δ 8.65 (s, 1H), 8.09–7.94 (m, 8H), 6.75 (d, J = 8.01 Hz, 2H), 6.16 (s, 1H), 6.07 (d, J = 8.01 Hz, 1H), 4.22 (s, 2H), 1.96 (s, 3H); ^{13}C NMR 75 MHz (DMSO-d_6): δ 167.5, 167.1, 156.2, 150.5, 148.2, 142.7, 137.2, 131.5, 131.1, 130.6, 130.1, 129.9, 128.7, 127.8, 121.4, 118.1, 112.1, 104.1, 100.1, 39.0, 15.7. HRMS (ESI-FTMS Mass (*m/z*): calcd for $C_{25}H_{21}N_3O_5$ $[M+H]^+$ = 444.1554, found 444.1563.

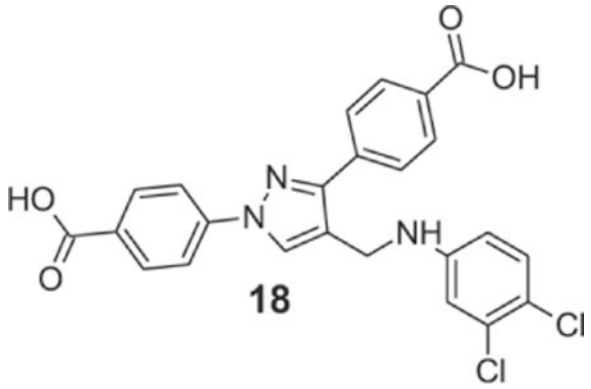

18

4-[1-(4-carboxyphenyl)-4-[(3,4-dichloroanilino)methyl]pyrazol-3-yl]benzoic acid (18).: Yellowish Solid; Yield 92%; ^{1}H NMR, 300 MHz (DMSO-d_6): δ 8.70 (s, 1H), 8.09–7.91 (m, 8H), 7.27 (d, J = 8.79 Hz 1H), 6.85 (s, 1H), 6.65 (d, J = 8.73 Hz, 1H), 6.50 (br s, 1H), 4.33 (s, 2H); ^{13}C NMR 75 MHz (DMSO-d_6): δ 167.5, 167.1, 150.5, 148.9, 142.6, 137.0, 131.7, 131.5, 130.9, 130.6, 130.1, 129.9, 128.8, 127.8, 120.2, 118.2, 117.2, 113.4, 113.2, 38.4. HRMS (ESI-FTMS Mass (*m/z*): calcd for $C_{24}H_{17}Cl_2N_3O_4$ $[M+H]^+$ = 482.0669, found 482.0662.

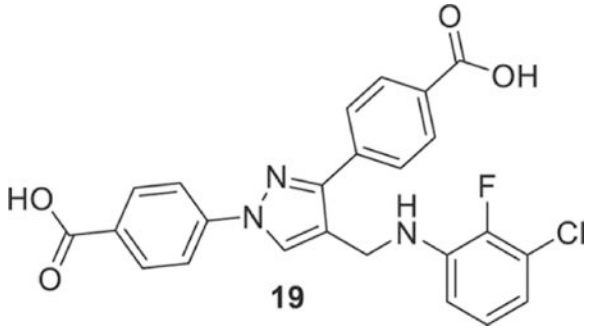

19

4-[1-(4-carboxyphenyl)-4-[(3-chloro-2-fluoro-anilino)methyl]pyrazol-3-yl]benzoic acid (19).: Yellowish solid; Yield 90%; ^{1}H NMR, 300 MHz (DMSO-d_6): δ 8.63 (s, 1H), 8.12–7.93 (m, 8H), 6.93 (t, J = 7.71 Hz, 1H), 6.68 (t, J = 7.8 Hz, 1H), 6.29 (br s, 1H), 4.44 (s, 2H); ^{13}C NMR 75 MHz (DMSO-d_6): δ 167.5, 167.1, 150.3, 146.7 (^{1}J = 239.1 Hz), 142.7, 138.2 (^{3}J = 11.2 Hz), 137.1, 131.4, 130.6, 130.1, 129.7, 128.7, 127.9, 125.6 (^{4}J = 4.1 Hz), 120.8, 119.6 (^{3}J = 14.6 Hz), 118.2, 116.6, 111.4, 38.6. HRMS (ESI-FTMS Mass (*m/z*): calcd for $C_{24}H_{17}ClFN_3O_4$ $[M+H]^+$ = 466.0964, found 466.0954.

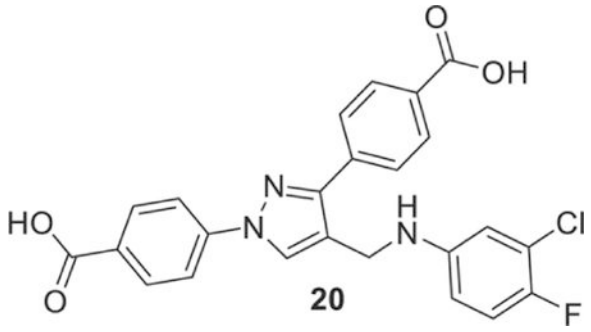

20

4-[1-(4-carboxyphenyl)-4-[(3-chloro-4-fluoro-anilino)methyl]pyrazol-3-yl]benzoic acid (20).: Yellowish solid; Yield 72%; ^{1}H NMR, 300 MHz (DMSO-d_6): δ 8.73 (s, 1H), 8.16–7.93 (m, 8H), 7.13 (t, J = 9.09 Hz, 1H), 6.79–6.77 (m, 1H), 6.64 (m, 1H), 6.29 (br s, 1H), 4.29 (s, 2H); ^{13}C NMR 75 MHz (DMSO-d_6); δ 167.5, 167.1, 151.3, 150.6, 148.2, 146.4, 142.6, 137.0, 131.5, 130.6, 130.1, 128.8, 127.8, 120.4, 119.8 (^{2}J = 18.0 Hz), 118.2, 117.39, (^{2}J = 21.3 Hz), 113.05, 112.5 (^{4}J = 6.0 Hz), 38.8. HRMS (ESI-FTMS Mass (*m/z*): calcd for $C_{24}H_{17}ClFN_3O_4$ $[M+H]^+$ = 466.0964, found 466.0954.

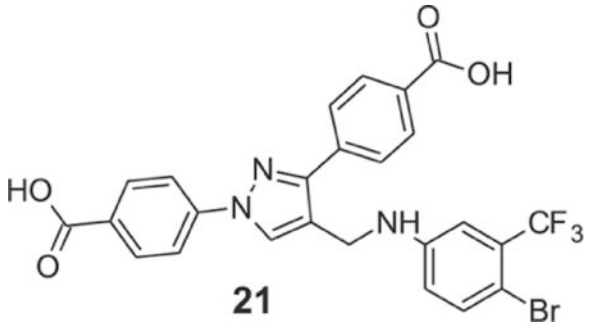

21

4-[4-[[4-bromo-3-(trifluoromethyl)anilino]methyl]-1-(4-carboxyphenyl)pyrazol-3-yl]benzoic acid (21).: Yellowish Soild; Yield 82%; ^{1}H NMR, 300 MHz (DMSO-d_6): δ 8.72 (s, 1H), 8.06–7.91 (m, 8H), 7.50 (d, J = 8.64 Hz, 1H), 7.08 (s, 1H), 6.81–6.77 (m, 2H), 4.36 (s, 2H); ^{13}C NMR 75 MHz (DMSO-d_6): δ 167.5, 167.1, 150.5, 148.3, 142.6, 136.9, 135.7, 131.5, 130.6, 130.1, 129.9, 128.9 (^{2}J = 29.7 Hz), 128.8, 127.8, 123.5 (^{1}J = 271.4 Hz), 120.0, 118.2, 116.7, 112.2 (^{3}J = 5.5 Hz), 102.9, 38.3. HRMS (ESI-FTMS Mass (*m/z*): calcd for $C_{25}H_{17}BrF_3N_3O_4$ $[M+H]^+$ = 560.0427, found 560.0418.

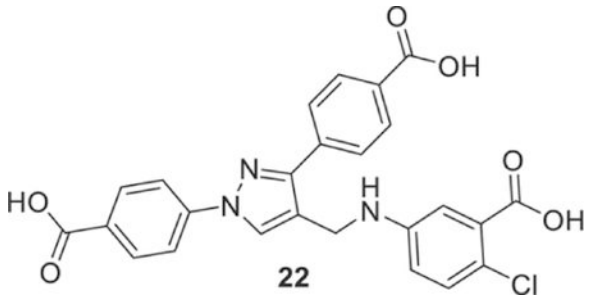

22

5-[[1,3-bis(4-carboxyphenyl)pyrazol-4-yl]methylamino]-2-chloro-benzoic acid (22).: Yellowish solid; Yield 97%; ^{1}H NMR, 300 MHz (DMSO-d_6): δ 8.71 (s, 1H), 8.03–7.94 (m, 8H), 7.18 (s, 1H), 7.02 (s, 1H), 6.76 (s, 1H), 6.46 (s, 1H), 4.31 (s, 2H); ^{13}C NMR 75 MHz (DMSO-d_6); δ 167.9, 167.6, 167.2, 150.5, 147.6, 142.6, 137.0, 132.6, 131.4, 131.2, 130.8, 130.1, 129.2, 128.9, 127.8, 120.4, 118.2, 117.9, 115.9, 114.3, 38.5. HRMS (ESI-FTMS Mass (*m/z*): calcd for $C_{25}H_{18}ClN_3O_6$ $[M+H]^+$ = 492.0957, found 492.0963.

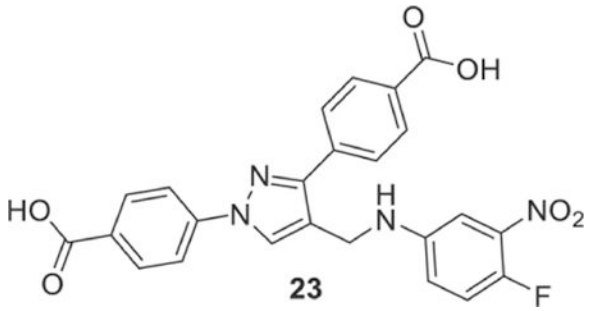

23

4-[1-(4-carboxyphenyl)-4-[[4-fluoro-3-(nitromethyl)anilino]methyl]pyrazol-3-yl]benzoic acid (23).: Yellowish Solid; Yield 84%; ^{1}H NMR, 300 MHz (DMSO-d_6): δ 8.74 (s, 1H), 8.09–7.93 (m, 8H), 7.35–7.28 (m, 2H), 7.05 (s, 1H), 6.65 (br s, 1H), 4.38 (s, 2H); ^{13}C NMR 75 MHz (DMSO-d_6): δ 167.5, 167.1, 150.5, 146.8 (^{1}J = 248.1 Hz), 145.8, 142.6, 137.5 (^{3}J = 8.24 Hz), 137.0, 131.4, 130.7, 130.1, 129.3, 128.8, 127.8, 120.1, 119.7 (^{4}J = 6.86 Hz), 119.1 (^{2}J = 21.3 Hz), 118.2, 107.3, 38.7. HRMS (ESI-FTMS Mass (*m/z*): calcd for $C_{24}H_{17}FN_4O_6$ $[M+H]^+$ = 477.1205, found 477.1207.

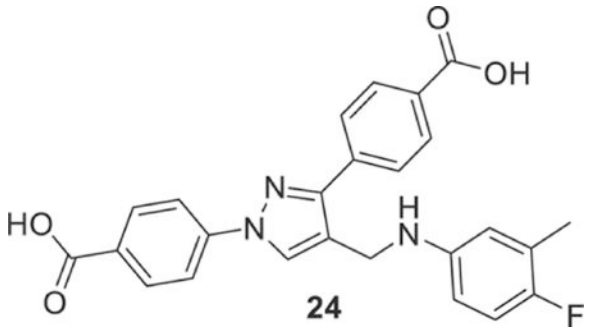

24

4-[1-(4-carboxyphenyl)-4-[(4-fluoro-3-methyl-anilino)methyl]pyrazol-3-yl]benzoic acid (24).: Yellowish solid; Yield 78%; ^{1}H NMR, 300 MHz (DMSO-d_6): δ 8.70 (s, 1H), 8.06–7.94 (m, 8H), 6.86 (t, J = 8.94 Hz, 1H), 6.53 (s, 1H), 6.48 (s, 1H), 4.24 (s, 2H), 2.1 (s, 3H); ^{13}C NMR 75 MHz (DMSO-d_6): δ 167.5, 167.1, 153.5 (^{1}J = 229.2 Hz), 150.6, 145.4, 142.7, 137.1, 131.4, 130.6, 130.1, 128.7, 127.8, 124.6, 124.3, 120.9, 118.1, 115.4 (^{2}J = 22.5 Hz), 115.1 (^{4}J = 3.6 Hz), 111.1 (^{3}J = 7.2 Hz), 39.0, 14.9. HRMS (ESI-FTMS Mass (*m/z*): calcd for $C_{25}H_{20}FN_3O_4$ $[M+H]^+$ = 446.1511, found 446.1506.

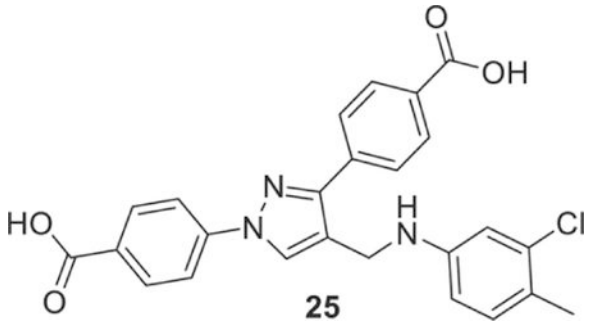

25

4-[1-(4-carboxyphenyl)-4-[(3-chloro-4-methyl-anilino)methyl]pyrazol-3-yl]benzoic acid (25).: Yellowish Solid; Yield 73%; ^{1}H NMR, 300 MHz (DMSO-d_6): δ 8.72 (s, 1H), 8.09–7.93 (m, 8H), 7.03 (d, J = 8.25 Hz, 1H), 6.70 (s, 1H), 6.56 (d, J = 6.96 Hz, 1H), 6.13 (br s, 1H), 4.28 (s, 2H), 2.1 (s, 3H); ^{13}C NMR 75 MHz (DMSO-d_6); δ 167.5, 167.1, 150.6, 148.3, 142.7, 137.1, 133.9, 131.8, 131.5, 130.6, 130.1, 129.3, 128.8, 127.8, 122.3, 120.7, 118.1, 112.6, 111.9, 38.6, 18.9. HRMS (ESI-FTMS Mass (*m/z*): calcd for $C_{25}H_{20}ClN_3O_4$ $[M+H]^+$ = 462.1215, found 462.1210.

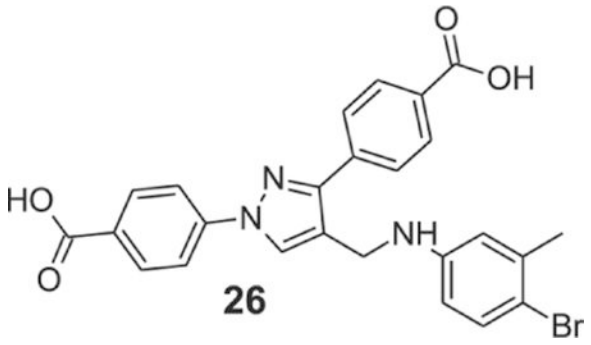

26

4-[4-[(4-bromo-3-methyl-anilino)methyl]-1-(4-carboxyphenyl)pyrazol-3-yl]benzoic acid (26).: Yellowish Solid; yield 74%; ^{1}H NMR, 300 MHz (DMSO-d_6): δ 8.69 (s, 1H), 8.09–7.92 (m, 8H), 7.22 (d, J = 8.58 Hz, 1H), 6.64 (s, 1H), 6.45 (d, J = 8.61 Hz, 1H), 6.15 (br s, 1H), 4.27 (s, 2H), 2.20 (s, 3H); ^{13}C NMR 75 MHz (DMSO-d_6); δ 167.5, 167.1, 150.6, 148.4, 142.6, 137.5, 137.1, 132.5, 131.5, 130.6, 130.1, 130.0, 128.7, 127.8, 120.7, 118.2, 115.1, 112.5, 110.1, 38.5, 23.1. HRMS (ESI-FTMS Mass (*m/z*): calcd for $C_{25}H_{20}BrN_3O_4$ $[M+H]^+$ = 506.0710, 508.0691, found 508.0711.

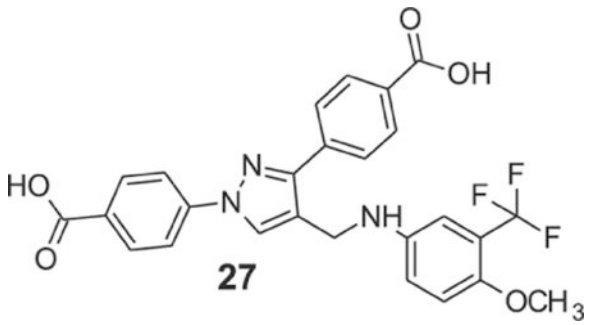

27

4-[1-(4-carboxyphenyl)-4-[[4-methoxy-3-(trifluoromethyl)anilino]methyl]pyrazol-3-yl]benzoic acid (27).: Yellowish solid; yield 79%; ^{1}H NMR, 300 MHz (DMSO-d_6): δ 8.72 (s, 1H), 8.12–7.94 (m, 8H), 7.05 (d, J = 8.79 Hz, 1H), 6.93–6.88 (m, 2H), 4.29 (s, 2H), 3.74 (s, 3H); ^{13}C NMR 75 MHz (DMSO-d_6): δ 167.5, 167.1, 150.6, 148.6, 142.8, 142.7, 137.1, 131.5, 130.6, 130.1, 129.9, 128.7, 127.8, 124.3 (^{1}J = 270.5 Hz), 120.7, 118.1, 117.6, 116.9, 114.8, 111.2 (^{3}J = 5.19 Hz), 56.8, 39.0. HRMS (ESI-FTMS Mass (*m/z*): calcd for $C_{26}H_{20}F_3N_3O_5$ $[M+H]^+$ = 512.1428, found 512.1423.

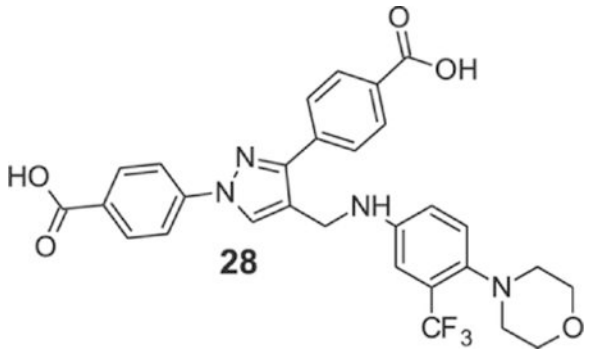

4-[1-(4-carboxyphenyl)-4-[[4-morpholino-3-(trifluoromethyl)anilino]methyl]pyrazol-3-yl]benzoic acid (28).: Yellowish solid; 89%; ^{1}H NMR, 300 MHz (DMSO-d_6): δ 8.74 (s, 1H), 8.09–7.93 (m, 8H), 7.36 (d, J = 8.31 Hz, 1H), 6.91–6.87 (m, 2H), 6.39 (br s, 1H), 4.33 (s, 2H), 3.64 (s, 4H), 2.72 (s, 4H); ^{13}C NMR 75 MHz (DMSO-d_6): δ 167.5, 167.1, 150.6, 146.6, 142.6, 140.9, 137.0, 131.4, 130.6, 130.1, 128.8, 127.8, 127.5, 127.1, 126.3, 124.7 (^{1}J = 270.5 Hz), 120.5, 118.2, 116.2, 110.3 (m), 67.2, 54.1, 38.7. HRMS (ESI-FTMS Mass (*m/z*): calcd for $C_{29}H_{25}F_3N_4O_5$ $[M+H]^+$ = 567.1850, found 567.1848.

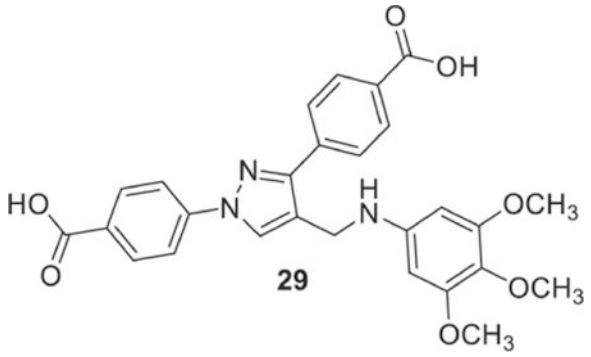

4-[1-(4-carboxyphenyl)-4-[(3,4,5-trimethylanilino)methyl]pyrazol-3-yl]benzoic acid (29).: Yellowish Solid; yield 88%; ^{1}H NMR, 300 MHz (DMSO-d_6): δ 8.74 (s, 1H), 8.10–7.96 (m, 8H), 5.98 (s, 2H), 4.29 (s, 2H), 3.67 (s, 6H), 3.52 (s, 3H); ^{13}C NMR 75 MHz (DMSO-d_6); δ 167.5, 167.1, 153.8, 150.6, 145.8, 142.7, 137.1, 131.5, 130.6, 130.1, 129.3, 128.7, 127.8, 121.0, 118.1, 90.6, 60.6, 55.9, 38.9. HRMS (ESI-FTMS Mass (*m/z*): calcd for $C_{27}H_{25}N_3O_7$ $[M+H]^+$ = 504.1765, found 504.1756.

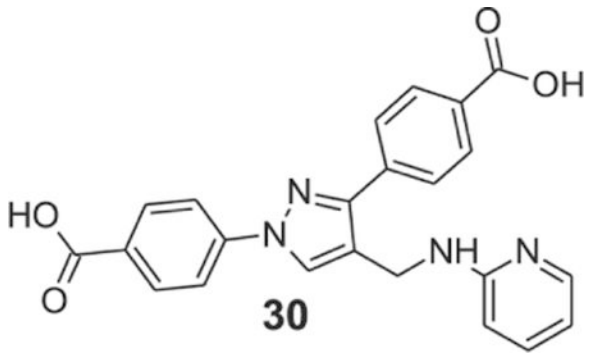

4-[1-(4-carboxyphenyl)-4-[(2-pyridylamino)methyl]pyrazol-3-yl]benzoic acid (30).: Yellowish solid; yield 87%; ^{1}H NMR, 300 MHz (DMSO-d_6): δ 8.67 (s, 1H), 8.13–7.93 (m, 9H), 7.39 (t, J = 6.99 Hz, 1H), 6.93 (s, 1H), 6.57–6.50 (m, 2H), 4.56 (s, 2H); ^{13}C NMR 75 MHz (DMSO-d_6): δ 167.5, 167.1, 158.7, 150.4, 147.8, 142.7, 137.2, 131.4, 130.5, 130.1, 129.9, 129.3, 128.7, 127.8, 121.4, 118.1, 112.4, 109.2, 39.3. HRMS (ESI-FTMS Mass (*m/z*): calcd for $C_{23}H_{18}N_4O_4$ $[M+H]^+$ = 415.1401, found 415.1401.

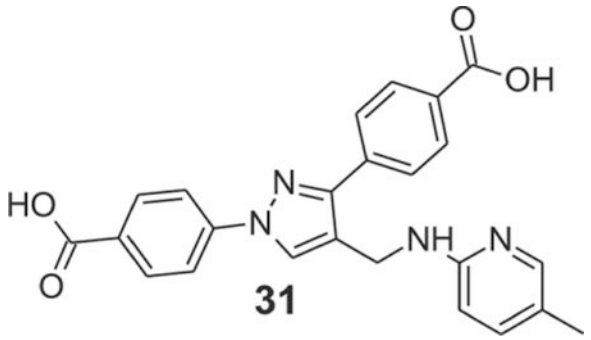

4-[1-(4-carboxyphenyl)-4-[[(5-methyl-2-pyridyl)amino]methyl]pyrazol-3-yl]benzoic acid (31).: Yellowish solid; yield 78%; ^{1}H NMR, 300 MHz (DMSO-d_6): δ 8.62 (s, 1H), 8.08–7.92 (m, 8H), 7.82 (s, 1H), 7.24 (d, J = 8.31 Hz, 1H), 6.68 (br s, 1H), 6.49 (d, J = 8.40 Hz, 1H), 4.51 (s, 2H), 2.09 (s, 3H): ^{13}C NMR 75 MHz (DMSO-d_6): δ 167.5, 167.1, 157.0, 150.4, 147.0, 142.7, 138.3, 137.2, 131.5, 130.5, 130.1, 129.8, 128.7, 127.8, 121.6, 120.7, 118.1, 108.9, 36.4, 17.4. HRMS (ESI-FTMS Mass (*m/z*): calcd for $C_{24}H_{20}N_4O_4$ $[M+H]^+$ = 429.1557, found 429.1551.

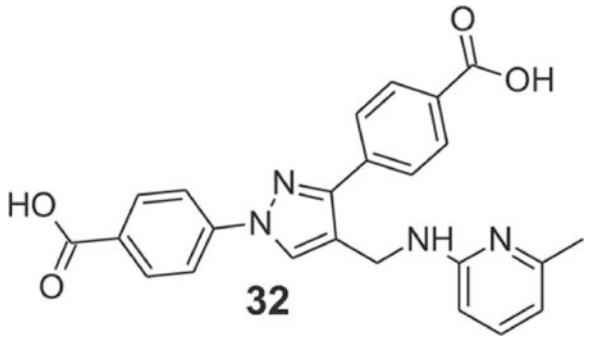

4-[1-(4-carboxyphenyl)-4-[[(6-methyl-2-pyridyl)amino]methyl]pyrazol-3-yl]benzoic acid (32).: Yellowish solid; yield 84%; ^{1}H NMR, 300 MHz (DMSO-d_6): δ 8.68 (s, 1H), 8.09–7.96 (m, 8H), 7.28 (t, J = 7.71 Hz, 1H), 6.81 (br s, 1H), 6.40–6.32 (m, 2H), 4.54 (s, 2H), 2.27 (s, 3H); ^{13}C NMR 75 MHz (DMSO-d_6): δ 167.5, 167.1, 158.3, 156.0, 150.5, 142.7, 137.5, 137.2, 131.5, 130.6, 130.1, 129.9, 128.7, 127.8, 121.5, 118.1, 111.4, 105.7, 36.1, 24.6. HRMS (ESI-FTMS Mass (*m/z*): calcd for $C_{24}H_{20}N_4O_4$ $[M+H]^+$ = 429.1557, found 429.1550.

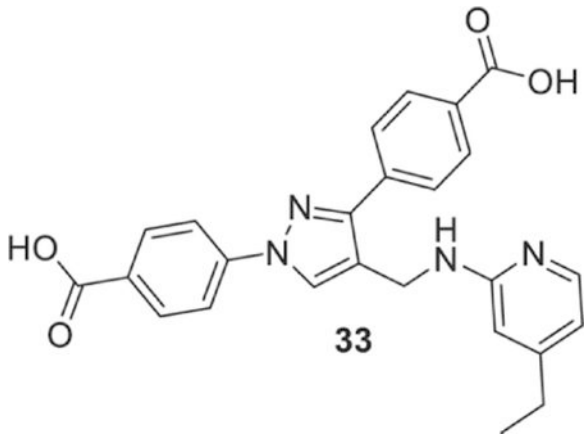

33

4-[1-(4-carboxyphenyl)-4-[[(4-ethyl-2-pyridyl)amino]methyl]pyrazol-3-yl]benzoic acid (33).: Yellowish solid; yield 75%; ^{1}H NMR, 300 MHz (DMSO-d_6): δ 8.66 (s, 1H), 8.12–7.89 (m, 9H), 6.84 (br s, 1H), 6.40 (s, 2H), 4.56 (s, 2H), 2.44 (d, J = 7.53 Hz, 2H), 1.11 (t, J = 7.50 Hz, 3H); ^{13}C NMR 75 MHz (DMSO-d_6): δ 167.6, 167.1, 159.0, 153.3, 150.4, 147.5, 142.7, 137.2, 131.4, 130.6, 130.1, 129.8, 128.7, 127.8, 121.6, 118.1, 112.9, 107.7, 36.3, 27.9, 14.6. HRMS (ESI-FTMS Mass (*m/z*): calcd for $C_{25}H_{22}N_4O_4$ $[M+H]^+$ = 443.1714, found 443.1712.

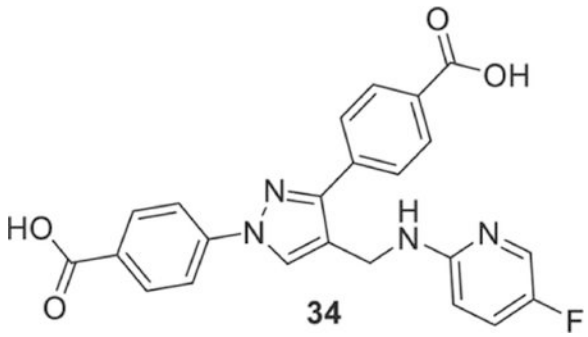

34

4-[1-(4-carboxyphenyl)-4-[[(5-fluoro-2-pyridyl)amino]methyl]pyrazol-3-yl]benzoic acid (34).: Yellowish solid; yield 74%; ^{1}H NMR, 300 MHz (DMSO-d_6): δ 8.66 (s, 1H), 8.09–7.91 (m, 8H), 7.40 (t, J = 2.88 Hz, 1H), 6.95 (s, 1H), 6.58 (d, J = 9.09 Hz, 1H), 4.53 (s, 2H); ^{13}C NMR 75 MHz (DMSO-d_6); δ 167.5, 167.1, 155.8, 153.1 (^{1}J = 236.5 Hz), 150.4, 142.6, 137.1, 133.8 (^{2}J = 23.67 Hz), 131.4, 130.7, 130.1, 129.9, 128.8, 127.7, 125.6 (^{2}J = 20.7 Hz), 121.3, 118.1, 109.8 (^{4}J = 3.79 Hz), 36.7. HRMS (ESI-FTMS Mass (*m/z*): calcd for $C_{23}H_{17}FN_4O_4$ $[M+H]^+$ = 433.1307, found 433.1307.

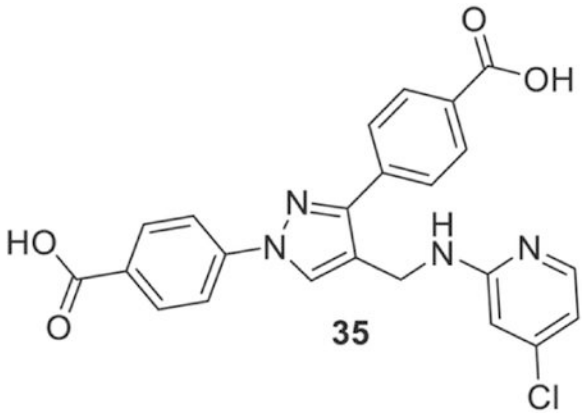

35

4-[1-(4-carboxyphenyl)-4-[[(4-chloro-2-pyridyl)amino]methyl]pyrazol-3-yl]benzoic acid (35).: Yellowish solid; Yield 79%; ^{1}H NMR, 300 MHz (DMSO-d_6); δ 8.67 (s, 1H), 8.09–7.91 (m, 9H), 7.25 (s, 1H), 6.61 (s, 2H), 4.57 (s, 2H); ^{13}C NMR 75 MHz (DMSO-d_6); δ 167.5, 167.1, 159.7, 150.3, 149.5, 142.9, 142.6, 137.1, 131.4, 130.6, 130.1, 129.9, 128.8, 127.7, 121.0, 118.2, 112.5, 108.0, 36.3. HRMS (ESI-FTMS Mass (*m/z*): calcd for $C_{23}H_{17}ClN_4O_4$ $[M+H]^+$ = 449.1011, 451.0984, found 449.1019.

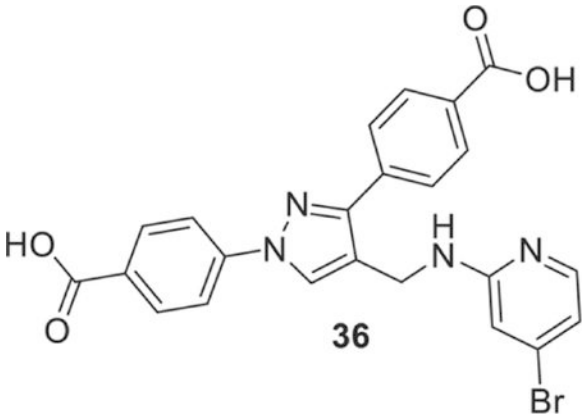

36

4-[4-[[(4-bromo-2-pyridyl)amino]methyl]-1-(4-carboxyphenyl)pyrazol-3-yl]benzoic acid (36).: Yellowish solid; Yield 82%; ^{1}H NMR, 300 MHz (DMSO-d_6); δ 8.67 (s, 1H), 8.13–7.89 (m, 9H), 7.23 (s, 1H), 6.77 (s, 1H), 6.72 (d, J = 5.34 Hz, 1H), 4.57 (s, 2H); ^{13}C NMR 75 MHz (DMSO-d_6); δ 167.5, 167.1, 159.6, 150.3, 149.4, 142.7, 137.1, 132.1, 131.4, 130.6, 130.1, 129.9, 128.7, 127.7, 121.0, 118.2, 115.2, 111.1, 36.2. HRMS (ESI-FTMS Mass (*m/z*): calcd for $C_{23}H_{17}BrN_4O_4$ $[M+H]^+$ = 493.0506, found 493.0502.

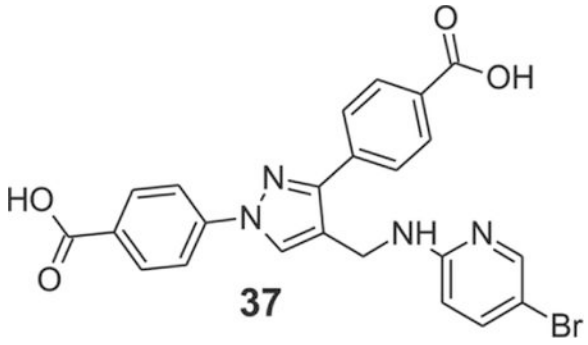

37

4-[4-[[(5-bromo-2-pyridyl)amino]methyl]-1-(4-carboxyphenyl)pyrazol-3-yl]benzoic acid (37).: Yellow solid; yield 92%; ^{1}H NMR, 300 MHz (DMSO-d_6): δ 8.62 (s, 1H), 8.05–7.91 (m, 8H), 7.54 (s, 1H), 7.20 (s, 1H), 6.54 (d, J = 8.70 Hz, 1H), 4.52 (s, 2H); ^{13}C NMR 75 MHz (DMSO-d_6): δ 167.5, 167.1, 157.5, 150.4, 148.0, 142.6, 139.4, 137.1, 131.4, 130.6, 130.1, 129.9, 128.7, 127.8, 121.0, 118.2, 111.2, 106.1, 36.3. HRMS (ESI-FTMS Mass (*m/z*): calcd for $C_{23}H_{17}BrN_4O_4$ $[M+H]^+$ = 495.0487, found 495.0481.

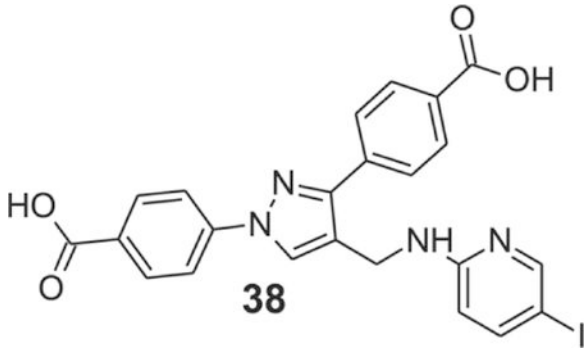

38

4-[1-(4-carboxyphenyl)-4-[[(5-iodo-2-pyridyl)amino]methyl]pyrazol-3-yl]benzoic acid (38).: Yellowish solid; Yield 89%; ^{1}H NMR, 300 MHz (DMSO-d_6): δ 8.66 (s, 1H), 8.17–7.90 (m, 9H), 7.63 (d, J = 8.70 Hz, 1H), 7.19 (s, 1H), 6.48 (d, J = 8.76 Hz, 1H), 4.53 (s, 2H); ^{13}C NMR 75 MHz (DMSO-d_6); δ 167.5, 167.1, 157.6, 153.1, 150.4, 144.3, 142.6, 137.1, 131.4, 130.6, 130.1, 129.9, 128.7, 127.8, 121.0, 118.2, 111.9, 76.7, 36.2. HRMS (ESI-FTMS Mass (*m/z*): calcd for $C_{23}H_{17}IN_4O_4$ $[M+H]^+$ = 541.0367, found 541.0361.

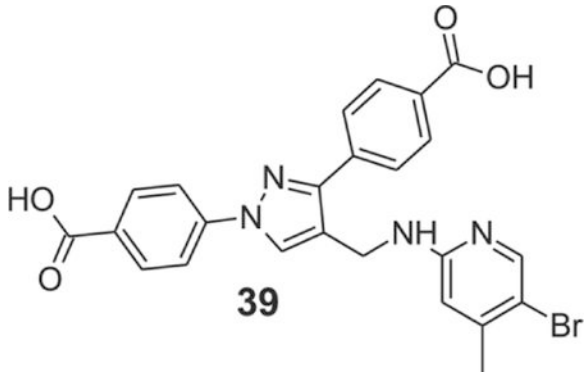

39

4-[4-[[(5-bromo-4-methyl-2-pyridyl)amino]methyl]-1-(4-carboxyphenyl)pyrazol-3-yl]benzoic acid (39).: Yellow solid; yield 85%; ^{1}H NMR, 300 MHz (DMSO-d_6): δ 8.65 (s, 1H), 8.08–7.91 (m, 9H), 7.09 (s, 1H), 6.53 (s, 1H), 4.53 (s, 2H), 2.18 (s, 3H); ^{13}C NMR 75 MHz (DMSO-d_6); δ 167.5, 167.1, 158.1, 150.3, 148.5, 146.4, 142.7, 137.1, 131.4, 130.5, 130.1, 129.9, 128.7, 127.7, 121.2, 118.1, 110.7, 109.6, 36.3, 22.2. HRMS (ESI-FTMS Mass (*m/z*): calcd for $C_{24}H_{19}BrN_4O_4$ $[M+H]^+$ = 509.0643, found 509.0640.

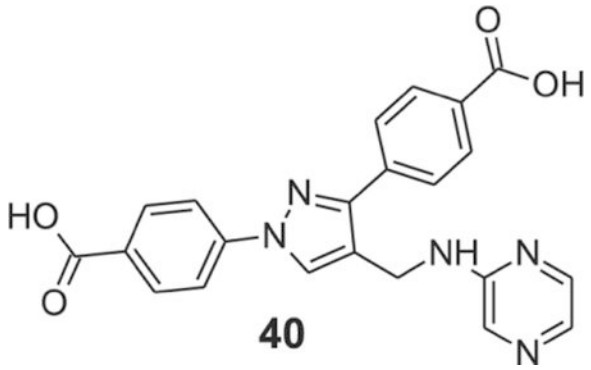

40

4-[1-(4-carboxyphenyl)-4-[(pyrazin-2-ylamino)methyl]pyrazol-3-yl]benzoic acid (40).: Yellow solid; yield 94%; ^{1}H NMR, 300 MHz (DMSO-d_6): δ 8.69 (s, 1H), 8.12–7.91 (m, 10H), 7.70 (s, 1H), 7.51 (s, 1H), 4.57 (s, 2H); ^{13}C NMR 75 MHz (DMSO-d_6): δ 167.5, 167.1, 155.0, 150.3, 148.5, 142.6, 141.9, 137.1, 134.1, 131.4, 130.5, 130.1, 130.0, 128.8, 127.8, 120.8, 118.2, 35.7. HRMS (ESI-FTMS Mass (*m/z*): calcd for $C_{22}H_{17}N_5O_4$ $[M+H]^+$ = 416.1353, found 416.1356.

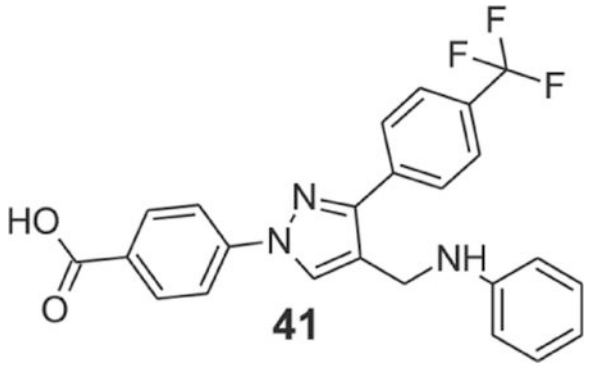

41

4-[4-(anilinomethyl)-3-[4-(trifluoromethyl)phenyl]pyrazol-1-yl]benzoic acid (41).: Yellowish solid; yield 79%; ^{1}H NMR, 300 MHz (DMSO-d_6): δ 8.87 (s, 1H), 8.10 (d, J = 8.70 Hz, 2H), 8.02–7.94 (m, 4H), 7.81 (d, J = 8.22 Hz, 2H), 7.20 (t, J = 7.77 Hz, 2H), 6.95 (d, J = 6.72 Hz, 2H), 6.86 (s, 1H), 4.42 (s, 2H); ^{13}C NMR 75 MHz (DMSO-d_6): δ 167.0, 150.9, 142.4, 136.5, 131.6, 131.4, 129.7, 129.1, 128.8, 128.7, 128.2, 125.9 (^{3}J = 3.6 Hz), 124.6 (^{1}J = 270.5 Hz), 118.9, 118.3, 116.7, 42.1, 39.9. HRMS (ESI-FTMS Mass (*m/z*): calcd for $C_{24}H_{18}F_3N_3O_2$ $[M+H]^+$ = 438.1423, found 438.1419.

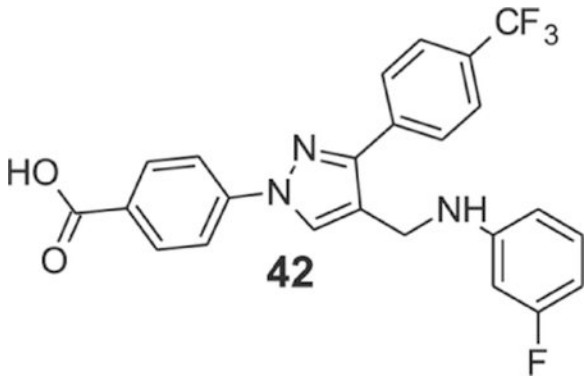

42

4-[4-[(3-fluoroanilino)methyl]-3-(*p*-tolyl)pyrazol-1-yl]benzoic acid (42).: Yellow solid; yield 88%; ^{1}H NMR, 300 MHz (DMSO-d_6): δ 8.79 (s, 1H), 8.10–8.03 (m, 6H), 7.84 (d, J = 8.22 Hz, 2H), 7.10 (q, J = 7.53 Hz, 7.71 Hz, 7.95 Hz, 1H), 6.52 (d, J = 8.58 Hz, 1H), 6.46 (s, 1H), 6.36 (t, J = 8.85 Hz, 1H), 4.31 (s, 2H); ^{13}C NMR 75 MHz (DMSO-d_6): δ 167.0, 163.8 (^{1}J = 238.1 Hz), 150.5 (^{3}J = 11.2 Hz), 150.2, 142.6, 136.9, 131.5, 130.7 (^{3}J = 10.2 Hz), 128.89, 128.8 (^{2}J = 31.4 Hz), 128.4, 126.0 (^{3}J = 3.63 Hz), 124.7 (^{1}J = 270.3 Hz), 120.1, 118.2, 109.5, 103.1 (^{2}J = 20 Hz), 99.6, 99.3, 38.7. HRMS (ESI-FTMS Mass (*m/z*): calcd for $C_{24}H_{17}F_4N_3O_2$ $[M+H]^+$ = 456.1330, found 456.1334.

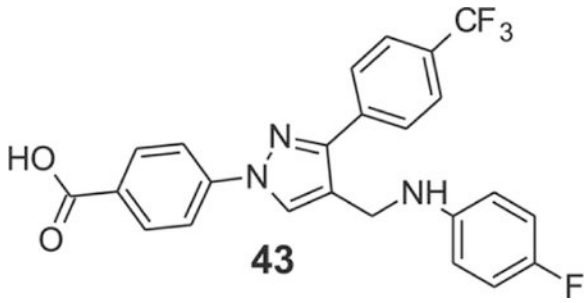

43

4-[4-[(4-fluoroanilino)methyl]-3-(*p*-tolyl)pyrazol-1-yl]benzoic acid (43).: Yellow solid; yield 82%; ^{1}H NMR, 300 MHz (DMSO-d_6): δ 8.76 (s, 1H), 8.07–8.02 (m, 6H), 7.84 (d, J = 7.98 Hz, 2H), 6.98 (s, 1H), 6.94 (d, J = 8.76 Hz, 1H), 6.70–6.65 (m, 2H), 5.96 (s, 1H), 4.26 (s, 2H); ^{13}C NMR 75 MHz (DMSO-d_6): δ 167.1, 156.6, 153.5, 150.1, 145.7, 142.6, 137.0, 131.4, 130.2, 129.0, 128.6, 128.4, 126.0 (^{3}J = 3.68 Hz), 124.7 (^{1}J = 270.4 Hz), 120.8, 118.2, 115.7 (^{2}J = 21.8 Hz), 113.7 (^{3}J = 7.33 Hz). HRMS (ESI-FTMS Mass (*m/z*): calcd for $C_{24}H_{17}F_4N_3O_2$ $[M+H]^+$ = 456.1330, found 456.1337.

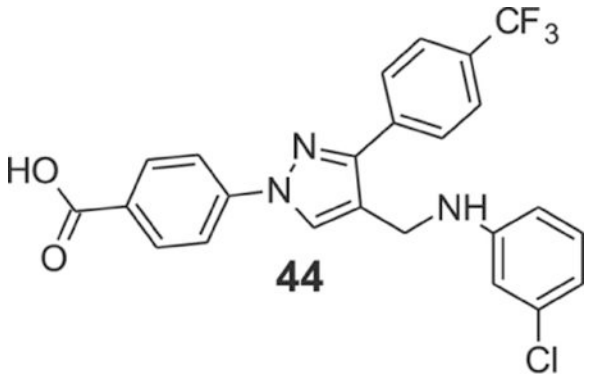

44

4-[4-[(3-chloroanilino)methyl]-3-(*p*-tolyl)pyrazol-1-yl]benzoic acid (44).: Yellowish solid; yield 83%; ^{1}H NMR, 300 MHz (DMSO-d_6): δ 8.75 (s, 1H), 8.29–7.92 (m, 6H), 7.83 (d, J = 7.29 Hz, 2H), 6.89 (d, J = 6.63 Hz, 1H), 6.69 (s, 1H), 6.60 (t, J = 8.64 Hz, 2H), 6.37 (s, 1H), 4.29 (s, 2H); ^{13}C NMR 75 MHz (DMSO-d_6): δ 167.1, 150.3, 150.2, 142.6, 136.9, 134.0, 131.5, 130.8, 130.3, 128.88, 128.8 (^{2}J = 31.7 Hz), 128.4, 126.1 (^{3}J = 3.69 Hz), 124.7 (^{1}J = 270.3 Hz), 120.3, 118.2, 116.0, 112.0, 111.4, 38.3. HRMS (ESI-FTMS Mass (*m/z*): calcd for $C_{24}H_{17}ClF_3N_3O_2$ $[M+H]^+$ = 472.1034, found 472.1024.

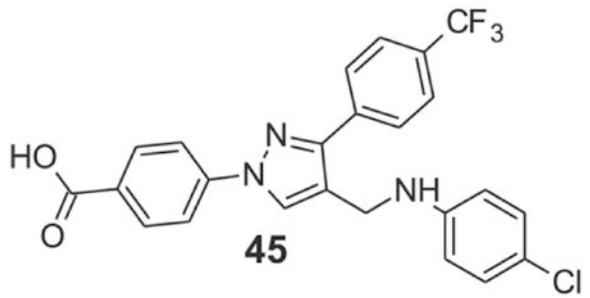

45

4-[4-[(4-chloroanilino)methyl]-3-(*p*-tolyl)pyrazol-1-yl]benzoic acid (45).: Yellow solid; yield 83%; ^{1}H NMR, 300 MHz (DMSO-d_6): δ 8.78 (s, 1H), 8.10–8.02 (m, 6H), 7.82 (d, J = 7.86 Hz, 2H), 7.13 (d, J = 8.67 Hz, 2H), 6.73 (s, 2H), 4.31 (s, 2H); ^{13}C NMR 75 MHz (DMSO-d_6): δ 167.0, 150.3, 145.9, 142.6, 136.8, 131.5, 130.6, 129.4, 129.1, 128.9, 128.7 (^{2}J = 31.5 Hz), 128.5, 126.0 (^{3}J = 3.75 Hz), 124.7 (^{1}J = 270.3 Hz), 121.9, 118.2, 115.9, 39.0. HRMS (ESI-FTMS Mass (*m/z*): calcd for $C_{24}H_{17}ClF_3N_3O_2$ $[M+H]^+$ = 472.1034, 474.1007, found 472.1026.

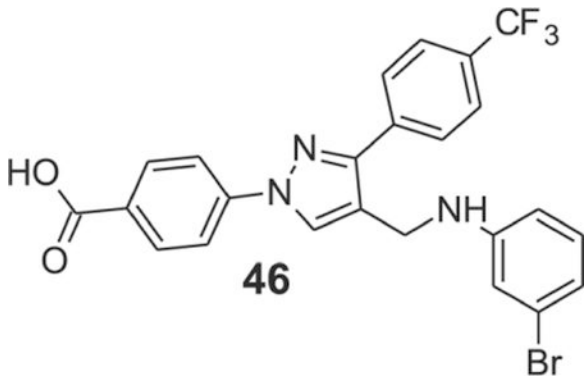

46

4-{4-[(3-bromoanilino)methyl]-3-[4-(trifluoromethyl)phenyl]-1H-pyrazol-1-yl}benzoic acid (46).: Yellow solid; yield 82%; ^{1}H NMR, 300 MHz (DMSO-d_6): δ 8.79 (s, 1H), 8.10–8.01 (m, 6H), 7.83 (d, J = 8.31 Hz, 2H), 7.04 (t, J = 8.01 Hz, 1H), 6.87 (s, 1H), 6.76–6.68 (m, 2H), 4.31 (s, 2H); ^{13}C NMR 75 MHz (DMSO-d_6); δ 167.0, 150.2, 150.0, 142.6, 136.8, 131.5, 130.4, 129.9, 128.9, 128.8 (^{2}J = 31.6 Hz), 128.4, 126.0 (^{3}J = 3.69 Hz), 124.7 (^{1}J = 270.2 Hz), 122.7, 120.0, 119.5, 118.2, 115.4, 112.2, 38.6. HRMS (ESI-FTMS Mass (*m/z*): calcd for $C_{24}H_{17}BrF_3N_3O_2$ $[M+H]^+$ = 516.0529, found 516.0523.

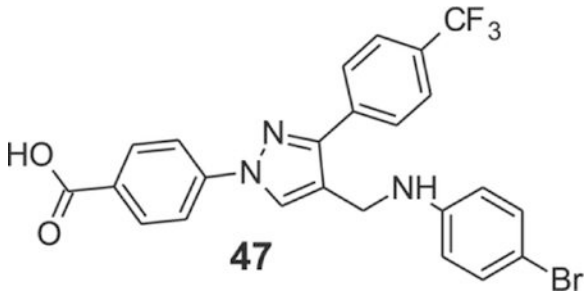

47

4-[4-[(4-bromoanilino)methyl]-3-[4-(trifluoromethyl)phenyl]pyrazol-1-yl]benzoic acid (47).: Yellow solid; Yield 72%; ^{1}H NMR, 300 MHz (DMSO-d_6); δ 8.75 (s, 1H), 8.10–8.03 (m, 6H), 7.83 (d, J = 8.28 Hz, 2H), 7.23 (d, J = 8.70 Hz, 2H), 6.64 (d, J = 8.76 Hz, 2H), 6.28 (s, 1H), 4.28 (s, 2H); 13C NMR 75 MHz (DMSO-d_6); δ 167.1, 150.1, 148.1, 142.6, 136.9, 131.8, 131.5, 130.3, 128.9, 128.8 (^{2}J = 31.6 Hz), 128.3, 126.0 (^{3}J = 3.60 Hz), 124.7 (^{1}J = 270.3 Hz), 120.4, 118.2, 114.7, 107.4, 38.5. HRMS (ESI-FTMS Mass (*m/z*): calcd for $C_{24}H_{17}BrF_3N_3O_2$ $[M+H]^+$ = 516.0529, found 516.0513.

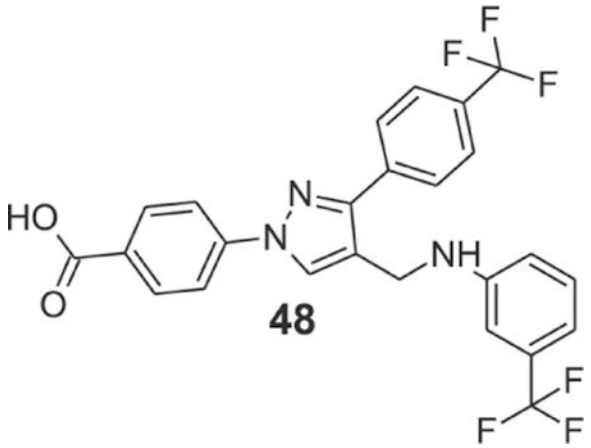

48

4-[4-[[3-(trifluoromethyl)anilino]methyl]-3-[4-(trifluoromethyl)phenyl]pyrazol-1-yl]benzoic acid (48).: Yellowish solid; yield 78%; ^{1}H NMR, 300 MHz (DMSO-d_6): δ 8.78 (s, 1H), 8.10–8.03 (m, 6H), 7.84 (d, J = 8.34 Hz, 2H), 7.30 (d, J = 7.8 Hz, 1H), 6.94–6.85 (m, 3H), 6.54 (s, 1H), 4.36 (s, 2H); ^{13}C NMR 75 MHz (DMSO-d_6): δ 167.1, 150.2, 149.3, 142.6, 136.8, 131.5, 130.3 (^{3}J = 4.03 Hz), 129.8, 128.8 (^{2}J = 31.6 Hz), 128.4, 126.7, 126.1 (m), 124.6 (^{1}J = 270.4 Hz), 123.2, 123.1, 120.2, 118.2, 116.0, 112.5 (^{3}J = 3.6 Hz), 108.7 (^{3}J = 3.6 Hz), 38.3. HRMS (ESI-FTMS Mass (*m/z*): calcd for $C_{25}H_{17}F_6N_3O_2$ $[M+H]^+$ = 506.1298, found 506.1296.

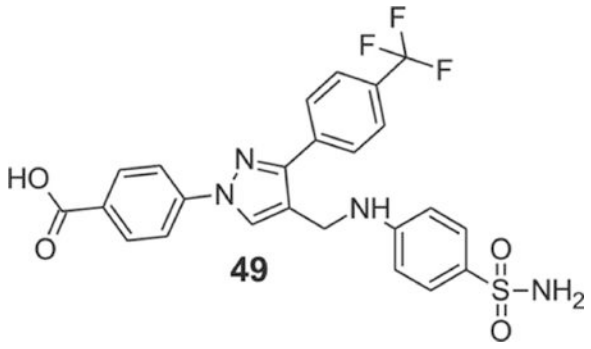

49

4-[4-[(4-sulfamoylanilino)methyl]-3-[4-(trifluoromethyl)phenyl]pyrazol-1-yl]benzoic acid (49).: Yellow solid; yield 88%; ^{1}H NMR, 300 MHz (DMSO-d_6); δ 8.76 (s, 1H), 8.10–8.02 (m, 6H), 7.84 (d, J = 8.34 Hz, 2H), 7.54 (d, J = 8.70 Hz, 2H), 6.97 (s, 2H), 6.81 (br s, 1H), 6.74 (d, J = 8.76 Hz, 2H), 4.38 (s, 2H); ^{13}C NMR 75 MHz (DMSO-d_6): δ 167.1, 151.3, 150.1, 142.5, 136.8, 131.5, 131.2, 130.3, 129.0, 128.8 (^{2}J = 31.5 Hz), 128.3, 127.8, 126.0 (^{3}J = 3.61 Hz), 124.7 (^{1}J = 270.3 Hz), 120.0, 118.2, 111.6, 38.1. HRMS (ESI-FTMS Mass (*m/z*): calcd for $C_{24}H_{19}F_3N_4O_4S$ $[M+H]^+$ = 517.1152, found 517.1151.

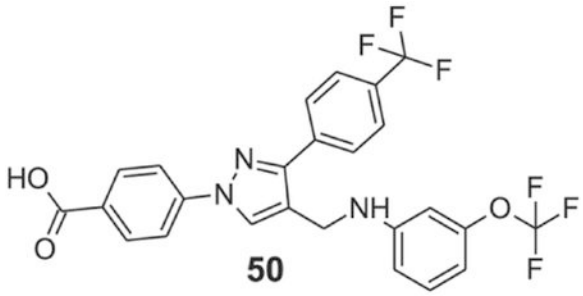

50

4-[4-[[3-(trifluoromethoxy)anilino]methyl]-3-[4-(trifluoromethyl)phenyl]pyrazol-1-yl]benzoic acid (50).: Yellow solid; yield 74%; ^{1}H NMR, 300 MHz (DMSO-d_6): δ 8.77 (s, 1H), 8.10–8.03 (m, 6H), 7.84 (d, J = 8.13 Hz, 2H), 7.19 (t, J = 8.10 Hz, 1H), 6.67 (d, J = 8.19 Hz, 1H), 6.59, 6.50 (d, J = 5.91 Hz, 2H), 4.31 (s, 2H); ^{13}C NMR 75 MHz (DMSO-d_6): δ 167.0, 150.6, 150.2, 150.0, 142.6, 136.9, 131.5, 130.8, 130.4, 128.88, 128.8 (^{2}J = 31.6 Hz), 128.4, 126.0 (^{3}J = 3.72 Hz), 124.7 (^{1}J = 270.3 Hz), 122.2, 120.2, 118.2, 111.6, 108.0, 104.7, 38.3. HRMS (ESI-FTMS Mass (*m/z*): calcd for $C_{25}H_{17}F_6N_3O_3$ $[M+H]^+$ = 522.1247, found 522.1252.

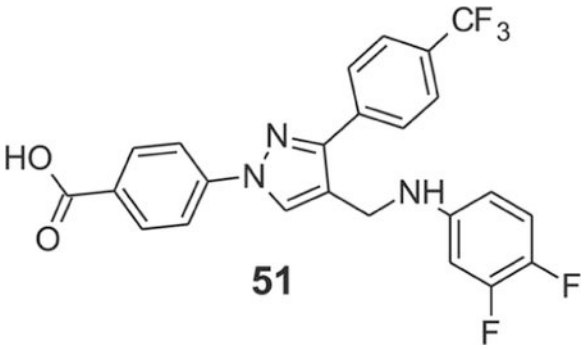

51

4-{4-[(3,4-difluoroanilino)methyl]-3-[4-(trifluoromethyl)phenyl]-1H-pyrazol-1-yl}benzoic acid (51).: Yellow solid; yield 87%; ^{1}H NMR, 300 MHz (DMSO-d_6): δ 8.77 (s, 1H), 8.10–8.03 (m, 6H), 7.83 (d, J = 8.25 Hz, 2H), 7.14 (q, J = 9.33 Hz, 1H), 6.66 (qd, J = 2.58 Hz, 1H), 6.45 (d, J = 8.85 Hz, 1H), 6.26 (s, 1H), 4.27 (s, 2H); ^{13}C NMR 75 MHz (DMSO-d_6): δ 167.1, 152.0 (^{3}J = 13.1 Hz), 150.1, 146.5 (^{3}J = 9.1 Hz), 146.5 (^{3}J = 9.1 Hz), 142.6, 140.2 (^{3}J = 12.5 Hz), 136.9, 131.5, 130.3, 128.9, 128.8 (^{2}J = 31.6 Hz), 128.4, 126.0 (^{3}J = 3.70 Hz), 124.7 (^{1}J = 270.3 Hz), 120.3, 118.2, 117.8 (^{3}J = 17.1 Hz), 108.4 (^{4}J = 2.82 Hz), 100.8 (^{2}J = 20.3 Hz), 38.8. HRMS (ESI-FTMS Mass (*m/z*): calcd for $C_{24}H_{16}F_5N_3O_2$ $[M+H]^+$ = 474.1235, found 474.1229.

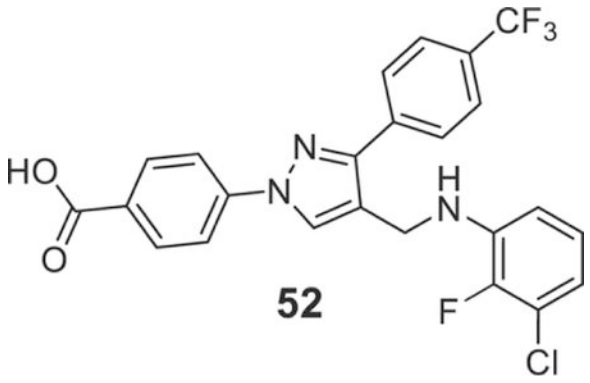

4-[4-[(3-chloro-2-fluoro-anilino)methyl]-3-[4-(trifluoromethyl)phenyl]pyrazol-1-yl]benzoic acid (52).: Yellow solid; yield 86%; ^{1}H NMR, 300 MHz (DMSO-d_6); δ 8.66 (s, 1H), 8.10–8.02 (m, 6H), 7.83 (d, J = 7.95 Hz, 2H), 6.93 (t, J = 7.86 Hz, 1H), 6.69 (t, J = 6.93 Hz, 2H), 6.31 (s, 1H), 4.44 (s, 2H); 13C NMR 75 MHz (DMSO-d_6): δ 167.1, 149.9, 146.7 (^{1}J = 239.2 Hz), 142.6, 138.2 (^{3}J = 11.2 Hz), 137.0, 131.4, 129.9, 128.8, 128.5, 128.4 (^{2}J = 31.5 Hz), 126.0 (^{3}J = 3.65 Hz), 125.6 (^{4}J = 4.16 Hz), 124.7 (^{1}J = 270.5 Hz), 120.7, 119.6 (^{3}J = 14.6 Hz), 118.2, 116.7, 111.6, 38.5. HRMS (ESI-FTMS Mass (*m/z*): calcd for $C_{24}H_{16}ClF_4N_3O_2$ $[M+H]^+$ = 490.0940, found 490.0932.

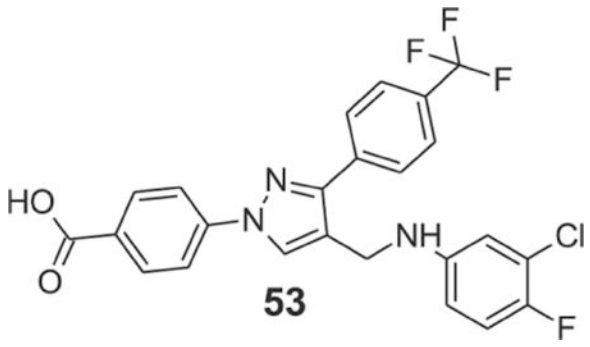

4-[4-[(3-chloro-4-fluoro-anilino)methyl]-3-[4-(trifluoromethyl)phenyl]pyrazol-1-yl]benzoic acid (53).: Yellow solid; yield 83%; ^{1}H NMR, 300 MHz (DMSO-d_6); δ 8.77 (s, 1H), 8.10–8.03 (m, 6H), 7.84 (d, J = 8.25 Hz, 2H), 7.14 (t, J = 9.18 Hz, 1H), 6.79 (dd, J = 2.76 Hz, 2.70 Hz, 1H), 6.66–6.62 (m, 1H), 6.25 (s, 1H), 4.29 (s, 2H); 13C NMR 75 MHz (DMSO-d_6); δ 167.1, 150.2, 149.7 (^{1}J = 232.5 Hz), 146.4, 142.6, 136.9, 131.5, 130.3, 128.9, 128.8 (^{2}J = 31.5 Hz), 128.4, 126.1 (^{3}J = 3.69 Hz), 124.7 (^{1}J = 270.5 Hz), 120.3, 119.8 (^{3}J = 18.0 Hz), 118.2, 117.4 (^{2}J = 21.1 Hz), 113.0, 112.5 (^{4}J = 6.32 Hz), 38.7. HRMS (ESI-FTMS Mass (*m/z*): calcd for $C_{24}H_{16}ClF_4N_3O_2$ $[M+H]^+$ = 490.0940, found 490.0937.

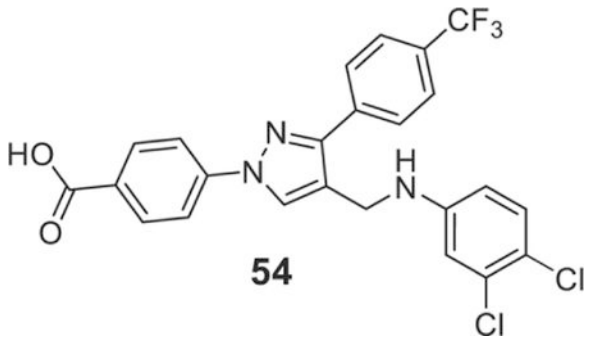

54

4-[4-[(3,4-dichloroanilino)methyl]-3-[4-(trifluoromethyl)phenyl]pyrazol-1-yl]benzoic acid (54).: Yellow solid; yield 73%; ^{1}H NMR, 300 MHz (DMSO-d_6): δ 8.74 (s, 1H), 8.09–8.01 (m, 6H), 7.82 (d, J = 7.98 Hz, 2H), 6.86 (s, 1H), 6.65 (d, J = 8.70 Hz, 1H), 6.53 (s, 1H), 4.30 (s, 2H); ^{13}C NMR 75 MHz (DMSO-d_6): δ 167.0, 150.1, 148.9, 142.6, 136.8, 131.7, 131.4, 130.9, 130.3, 128.9, 128.8 (^{2}J = 31.6 Hz), 128.4, 126.0 (^{3}J = 3.69 Hz), 124.7 (^{1}J = 270.4 Hz), 120.1, 118.2, 117.3, 113.5, 113.2, 38.4. HRMS (ESI-FTMS Mass (*m/z*): calcd for $C_{24}H_{16}Cl_2F_3N_3O_2$ $[M+H]^+$ = 506.0644, found 506.0632.

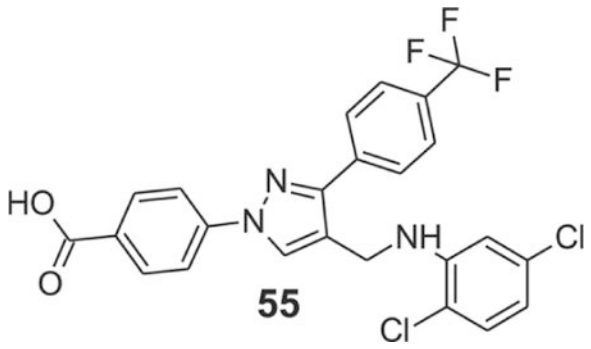

55

4-[4-[(2,5-dichloroanilino)methyl]-3-[4-(trifluoromethyl)phenyl]pyrazol-1-yl]benzoic acid (55).: Yellow solid; yield 82%; ^{1}H NMR, 300 MHz (DMSO-d_6); δ 8.65 (s, 1H), 8.10–8.02 (m, 6H), 7.83 (d, J = 8.13 Hz, 2H), 6.93 (t, J = 8.01 Hz, 1H), 6.69 (t, J = 7.44 Hz, 2H), 6.31 (s, 1H), 4.44 (s, 2H); 13C NMR 75 MHz (DMSO-d_6): δ 167.1, 149.9, 145.3, 142.6, 136.9, 133.0, 131.4, 130.5, 129.7, 129.5, 129.0, 128.8, 128.6, 126.0 (^{3}J = 3.64 Hz), 124.7 (^{1}J = 270.3 Hz), 120.5, 118.5, 118.2, 111.4, 38.4. HRMS (ESI-FTMS Mass (*m/z*): calcd for $C_{24}H_{16}Cl_2F_3N_3O_2$ $[M+H]^+$ = 506.0644, found 506.0651.

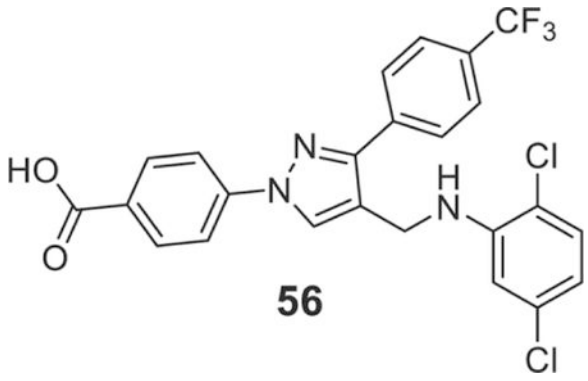

56

4-[4-[(3,5-dichloroanilino)methyl]-3-[4-(trifluoromethyl)phenyl]pyrazol-1-yl]benzoic acid (56).: Yellow solid; yield 93%; ^{1}H NMR, 300 MHz (DMSO-d_6); δ 8.77 (s, 1H), 8.10–8.01 (m, 6H), 7.84 (d, J = 8.19 Hz, 2H), 6.70 (s, 1H), 6.66 (s, 3H), 4.33 (s, 2H); ^{13}C NMR 75 MHz (DMSO-d_6): δ 167.1, 151.0, 150.2, 142.6, 136.8, 134.8, 131.5, 130.4, 128.9, 128.8 (^{2}J = 31.8 Hz), 128.4, 126.1 (^{3}J = 3.72 Hz), 124.7 (^{1}J = 270.4 Hz), 119.8, 118.3, 115.2, 110.8, 38.1. HRMS (ESI-FTMS Mass (*m/z*): calcd for $C_{24}H_{16}Cl_2F_3N_3O_2$ $[M+H]^+$ = 506.0644, found 506.0634.

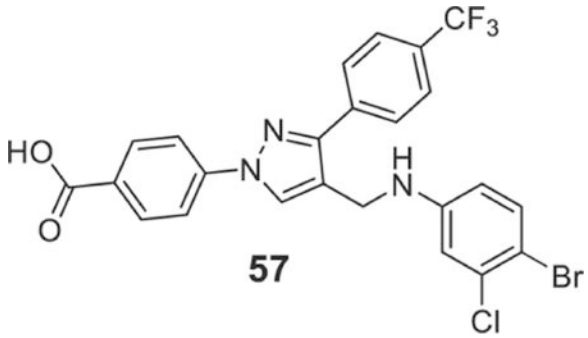

57

4-[4-[(4-bromo-3-chloro-anilino)methyl]-3-[4-(trifluoromethyl)phenyl]pyrazol-1-yl]benzoic acid (57).: Yellow solid; yield 83%; ^{1}H NMR, 300 MHz (DMSO-d_6): δ 8.75 (s, 1H), 8.10–8.01 (m, 6H), 7.83 (d, J = 8.28 Hz, 2H), 7.39 (d, J 8.79 Hz, 1H), 6.87 (s, 1H), 6.59 (d, J = 6.39, 2H), 4.31 (s, 2H); ^{13}C NMR 75 MHz (DMSO-d_6): δ 167.1, 150.1, 149.4, 142.6, 136.8, 134.0, 133.7, 131.4, 129.5, 128.8 (^{2}J = 31.6 Hz), 128.3, 126.1 (^{3}J = 3.67 Hz), 125.8 (^{3}J = 3.72 Hz), 124.7 (^{1}J = 270.3 Hz), 120.0, 119.3, 118.2, 113.6, 106.3, 38.3. HRMS (ESI-FTMS Mass (*m/z*): calcd for $C_{24}H_{16}BrClF_3N_3O_2$ $[M+H]^+$ = 492.1141, found 492.1148.

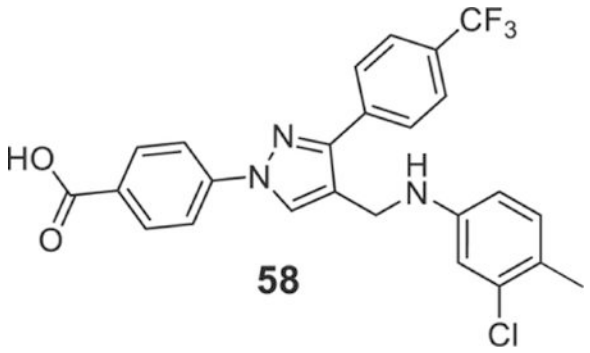

58

4-[4-[(3-chloro-4-methyl-anilino)methyl]-3-[4-(trifluoromethyl)phenyl]pyrazol-1-yl]benzoic acid (58).: Yellow solid; yield 94%; ^{1}H NMR, 300 MHz (DMSO-d_6): δ 8.75 (s, 1H), 8.06–8.05 (m, 6H), 7.84 (d, J = 7.86 Hz, 2H), 7.04 (d, J = 8.07 Hz, 1H), 6.71 (s, 1H), 6.57 (d, J = 8.34 Hz, 1H), 6.14 (s, 1H), 4.27 (s, 2H); ^{13}C NMR 75 MHz (DMSO-d_6): δ 167.1, 150.1, 148.3, 142.6, 136.9, 134.0, 131.8, 131.5, 130.3, 128.9, 128.8 (^{2}J = 31.6 Hz), 128.4, 126.0 (^{3}J = 3.68 Hz), 124.7 (^{1}J = 270.1 Hz), 122.4, 120.5, 118.2, 112.6, 111.9, 38.5, 18.9. HRMS (ESI-FTMS Mass (*m/z*): calcd for $C_{25}H_{19}ClF_3N_3O_2$ $[M+H]^+$ = 486.1191, 488.1163, found 486.1189.

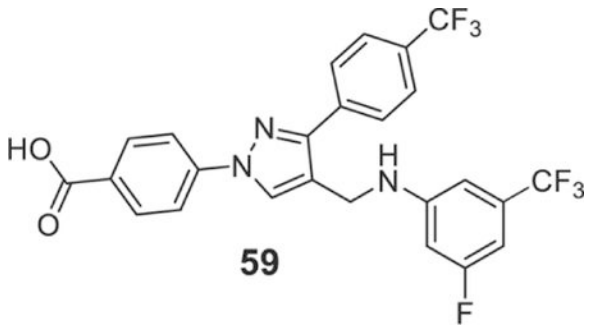

59

4-[4-[[3-fluoro-5-(trifluoromethyl)anilino]methyl]-3-[4-(trifluoromethyl)phenyl]pyrazol-1-yl]benzoic acid (59).: Light yellow solid; yield 95%; ^{1}H NMR, 300 MHz (DMSO-d_6): δ 8.80 (s, 1H), 8.10–8.02 (m, 6H), 7.84 (d, J = 8.04 Hz, 2H), 6.90 (s, 1H), 6.82 (s, 1H), 6.76 (s, 1H), 6.69 (d, J = 9.39 Hz, 1H), 4.37 (s, 2H); ^{13}C NMR 75 MHz (DMSO-d_6); δ 167.1, 163.7 (^{1}J = 240.3 Hz), 151.3 (^{3}J = 11.6 Hz), 150.2, 142.6, 136.8, 131.5, 130.4, 128.98, 128.9 (^{2}J = 31.5 Hz), 128.4, 126.1 (^{3}J = 3.6 Hz), 124.7 (^{1}J = 270.4 Hz), 119.7, 118.3, 105.8, 102.0, 101.7, 99.3, 99.0, 38.2. HRMS (ESI-FTMS Mass (*m/z*): calcd for $C_{25}H_{16}F_7N_3O_2$ $[M+H]^+$ = 524.1204, found 524.1198.

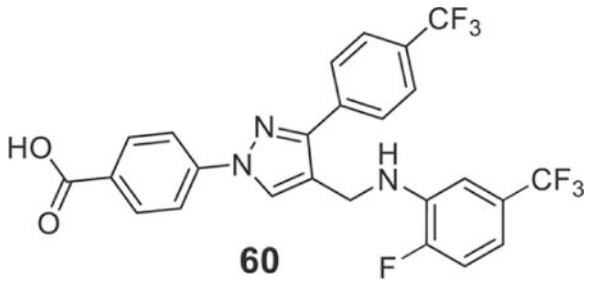

60

4-[4-[[2-fluoro-5-(trifluoromethyl)anilino]methyl]-3-[4-(trifluoromethyl)phenyl]pyrazol-1-yl]benzoic acid (60).: Yellow solid; yield 84%; ^{1}H NMR, 300 MHz (DMSO-d_6); δ 8.69 (s, 1H), 8.09–8.02 (m, 6H), 7.84 (d, J = 8.25 Hz, 2H), 7.27–7.22 (m, 1H), 6.97–6.90 (m, 2H), 6.42 (s, 1H), 4.50 (s, 2H); ^{13}C NMR 75 MHz (DMSO-d_6): δ 167.1, 153.1 (^{1}J = 244.1 Hz), 151.5, 142.6, 137.6, 137.5, 136.9, 131.4, 130.0, 129.0, 128.8, 128.6, 126.0 (^{3}J = 3.75 Hz), 124.7 (^{1}J = 270.4 Hz), 124.6 (^{1}J = 270.1 Hz), 120.4, 118.2, 115.4 (^{2}J = 19.6 Hz), 113.4 (m), 108 (m), 38.1. HRMS (ESI-FTMS Mass (*m/z*): calcd for $C_{25}H_{16}F_7N_3O_2$ $[M+H]^+$ = 524.1204, found 524.1200.

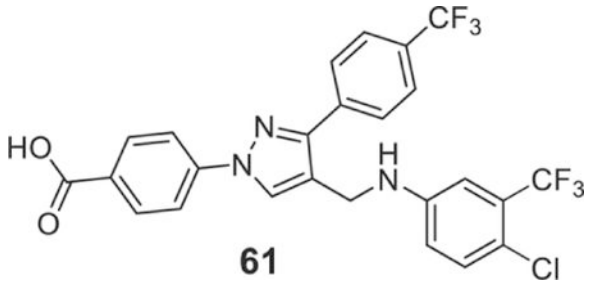

61

4-[4-[[4-chloro-3-(trifluoromethyl)anilino]methyl]-3-[4-(trifluoromethyl)phenyl]pyrazol-1-yl]benzoic acid (61).: Yellowish solid; yield 89%; ^{1}H NMR, 300 MHz (DMSO-d_6): δ 8.76 (s, 1H), 8.10–8.02 (m, 6H), 7.84 (d, J = 8.4 Hz, 2H), 7.38 (d, J = 8.82 Hz, 1H), 7.07 (d, J = 2.58 Hz, 1H), 6.89 (d, J = 8.85 Hz, 1H), 6.74 (s, 1H), 4.36 (s, 2H); ^{13}C NMR 75 MHz (DMSO-d_6); δ 167.1, 150.1, 147.9, 142.6, 136.8, 132.4, 131.5, 130.3, 128.9, 128.8 (^{2}J = 31.4 Hz), 128.4, 127.4, 126.13 (^{3}J = 3.66 Hz), 124.6 (^{1}J = 270 Hz), 120.0, 119.9, 118.2, 116.6, 116.1, 111.6 (^{3}J = 5.53 Hz), 38.3. HRMS (ESI-FTMS Mass (*m/z*): calcd for $C_{25}H_{16}ClF_6N_3O_2$ $[M+H]^+$ = 540.0908, found 540.0905.

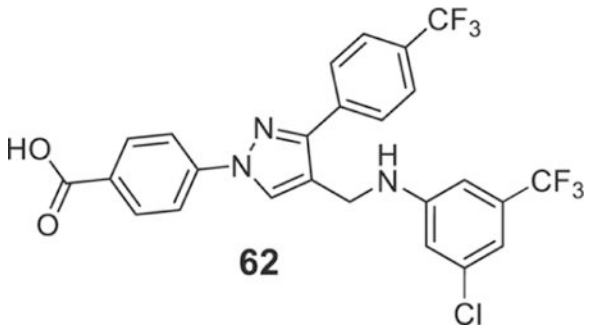

62

4-[4-[[3-chloro-5-(trifluoromethyl)anilino]methyl]-3-[4-(trifluoromethyl)phenyl]pyrazol-1-yl]benzoic acid (62).: Yellow solid; yield 78%; ^{1}H NMR, 300 MHz (DMSO-d_6): δ 8.79 (s, 1H), 8.11–8.01 (m, 6H), 7.84 (d, J = 8.22 Hz, 2H), 6.93 (d, J = 9.24 Hz, 1H), 6.88 (s, 3H), 4.40 (s, 2H); ^{13}C NMR 75 MHz (DMSO-d_6): δ 167.0, 150.6, 150.2, 142.6, 136.8, 135.0, 131.9, 131.5, 130.4, 128.94, 128.9 (^{2}J = 31.6 Hz), 128.4, 126.1 (^{3}J = 3.67 Hz), 124.7 (^{1}J = 270.0 Hz), 124.0 (^{1}J = 271.1 Hz), 119.7, 118.3, 114.8, 111.8 (m), 108 (m), 38.1. HRMS (ESI-FTMS Mass (*m/z*): calcd for $C_{25}H_{16}ClF_6N_3O_2$ $[M+H]^+$ = 540.0908, found 540.0905.

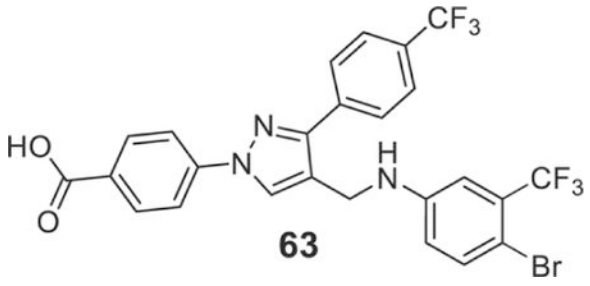

63

4-[4-[[4-bromo-3-(trifluoromethyl)anilino]methyl]-3-[4-(trifluoromethyl)phenyl]pyrazol-1-yl]benzoic acid (63).: Light yellow solid; yield 93%; ^{1}H NMR 300 MHz (DMSO-d_6): δ 8.77 (s, 1H), 8.10–8.02 (m, 6H), 7.84 (d, J = 7.74 Hz, 2H), 7.51 (d, J = 8.82 Hz, 1H), 7.08 (s, 1H), 6.83–6.77 (m, 2H), 4.36 (s, 2H); ^{13}C NMR 75 MHz (DMSO-d_6): δ 167.1, 150.1, 148.3, 142.6, 136.8, 135.7, 131.5, 130.3, 128.94, 128.9 (^{2}J = 29.8 Hz), 128.8 (^{2}J = 31.6 Hz), 128.4, 126.1 (^{3}J = 3.72 Hz), 125.4, 124.7 (^{1}J = 270.4 Hz), 119.9, 118.2, 116.8, 112.1 (m), 102.9, 38.2. HRMS (ESI-FTMS Mass (*m/z*): calcd for $C_{25}H_{16}BrF_6N_3O_2$ $[M+H]^+$ = 584.0403, 586.0384, found 584.0394.

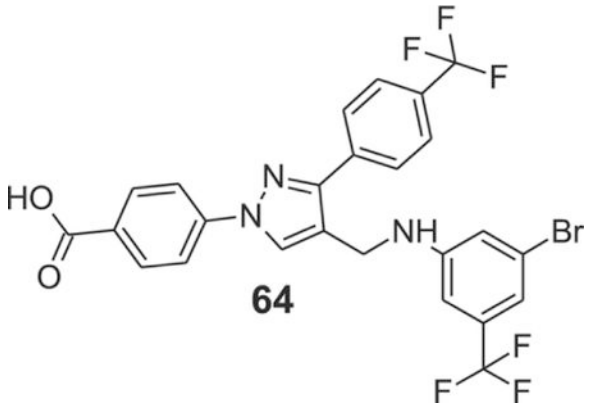

64

4-[4-[[3-bromo-5-(trifluoromethyl)anilino]methyl]-3-[4-(trifluoromethyl)phenyl]pyrazol-1-yl]benzoic acid (64).: Yellowish solid; yield 76%; ^{1}H NMR, 300 MHz (DMSO-d_6): δ 8.78 (s, 1H), 8.10–8.01 (m, 6H), 7.84 (d, J = 8.07 Hz, 2H), 7.08 (s, 1H), 7.00 (s, 1H), 6.94 (s, 1H), 6.85 (s, 1H), 4.38 (s, 2H); ^{13}C NMR 75 MHz (DMSO-d_6): δ 167.0,150.7, 150.2, 142.6, 136.8, 132.0, 131.6, 131.5, 130.4, 128.9, 128.8 (^{2}J = 31.5 Hz), 126.1 (^{3}J = 3.72 Hz), 124.6 (^{1}J = 270.1 Hz), 125.7, 123.3, 122.1, 118.3, 117.8,

114.5 (m), 108.0 (m), 38.1. HRMS (ESI-FTMS Mass (*m/z*): calcd for $C_{25}H_{16}BrF_6N_3O_2$ [M +H]$^+$ = 584.0403, found 584.0405.

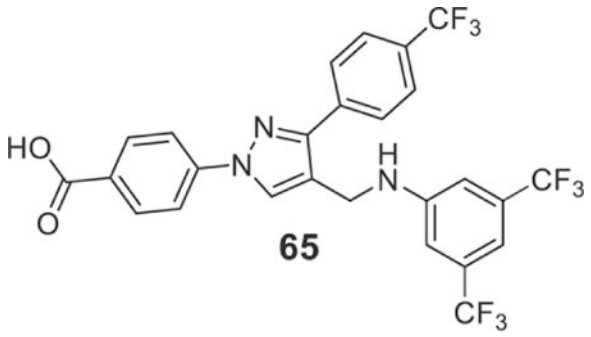

65

4-[4-[[3,5-bis(trifluoromethyl)anilino]methyl]-3-[4-(trifluoromethyl)phenyl]pyrazol-1-yl]benzoic acid (65).: Yellow solid; yield 97%; ^{1}H NMR, 300 MHz (DMSO-d_6): δ 8.81 (s, 1H), 8.11–8.02 (m, 6H), 7.84 (d, J = 7.86 Hz, 2H), 7.20 (s, 2H), 7.11–7.06 (m, 2H), 4.45 (s, 2H); ^{13}C NMR 75 MHz (DMSO-d_6): δ 167.0, 150.2, 150.0, 142.6, 136.8, 131.5, 131.1, 130.4, 128.98, 128.9 (^2J = 31.6 Hz), 128.4, 126.1 (^3J = 3.68 Hz), 124.7 (^1J = 270.4 Hz), 124.1 (^1J = 271.0 Hz), 119.6, 118.3, 112.0, 108.2, 38.1. HRMS (ESI-FTMS Mass (*m/z*): calcd for $C_{26}H_{16}F_9N_3O_2$ [M+H]$^+$ = 574.1172, found 574.1176.

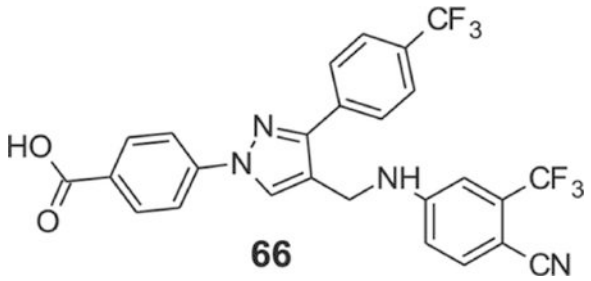

66

4-[4-[[4-cyano-3-(trifluoromethyl)anilino]methyl]-3-[4-(trifluoromethyl)phenyl]pyrazol-1-yl]benzoic acid (66).: Yellow solid; yield 98%; ^{1}H NMR, 300 MHz (DMSO-d_6): δ 8.81 (s, 1H), 8.11–8.02 (m, 6H), 7.84 (d, J = 7.86 Hz, 2H), 7.20 (s, 2H), 7.11–7.06 (m, 2H), 4.45 (s, 2H); ^{13}C NMR 75 MHz (DMSO-d_6); δ 167.0, 150.2, 150.0, 142.6, 136.8, 131.5, 131.1, 130.4, 128.98, 128.9 (^2J = 31.6 Hz), 128.4, 126.1 (^3J = 3.68 Hz), 124.7 (^1J = 270.4 Hz), 124.1 (^1J = 271.0 Hz), 119.6, 118.3, 112.0, 108.2, 38.1. HRMS (ESI-FTMS Mass (*m/z*): calcd for $C_{26}H_{16}F_6N_4O_2$ [M+H]$^+$ = 531.1250, found 531.1246.

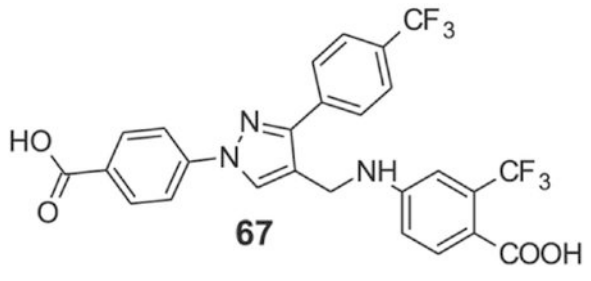

67

4-[[1-(4-carboxyphenyl)-3-[4-(trifluoromethyl)phenyl]pyrazol-4-yl]methylamino]-2-(trifluoromethyl)benzoic acid (67).: Yellow solid; Yield 96%; ^{1}H NMR, 300 MHz (DMSO-d_6): δ 8.78 (s, 1H), 8.10–8.01 (m, 6H), 7.84 (d, J = 8.31 Hz, 2H), 7.77 (d, J = 8.61 Hz, 1H), 7.19 (s, 1H), 7.08 (s, 1H), 6.86 (d, J = 8.76 Hz, 1H), 4.44 (s, 2H); ^{13}C NMR 75 MHz (DMSO-d_6); δ 167.1, 151.2, 150.1, 142.5, 136.8, 134.1, 131.4, 130.3, 129.5, 129.0, 128.9 (^{2}J = 31.7 Hz), 128.6, 128.4, 126.1 (^{3}J = 3.68 Hz), 125.2, 124.6 (^{1}J = 270.3 Hz), 124.1 (^{1}J = 271.7 Hz), 119.7, 118.2, 113.0, 111.4, 38.0. HRMS (ESI-FTMS Mass (*m/z*): calcd for $C_{26}H_{17}F_6N_3O_4$ $[M+H]^+$ = 550.1196, found 550.1197.

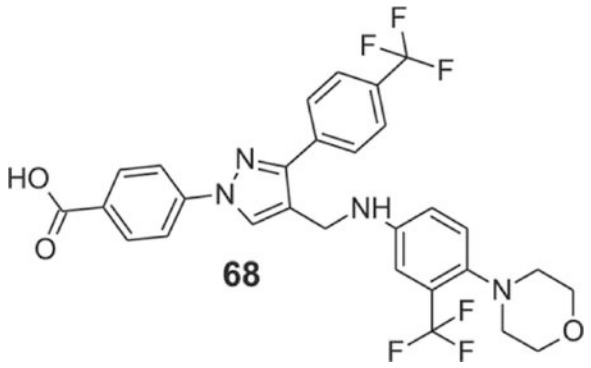

68

4-[4-[[4-morpholino-3-(trifluoromethyl)anilino]methyl]-3-[4-(trifluoromethyl)phenyl]pyrazol-1-yl]benzoic acid (68).: Yellow solid; yield 97%; ^{1}H NMR, 300 MHz (DMSO-d_6): δ 8.77 (s, 1H), 8.10–8.04 (m, 6H), 7.84 (d, J = 8.37 Hz, 2H), 7.36 (d, J = 8.28 Hz, 1H), 6.91 (s, 1H), 6.88 (s, 1H), 6.39 (br s, 1H), 4.32 (s, 2H), 3.65 (s, 4H), 2.72 (s, 4H); ^{13}C NMR 75 MHz (DMSO-d_6): δ 167.0, 150.2, 146.6, 142.6, 140.9, 136.9, 131.5, 130.1 (^{2}J = 32.8 Hz), 128.87, 128.8 (^{2}J = 31.7 Hz), 128.4, 126.3, 126.1 (^{3}J = 3.66 Hz), 124.7 (^{1}J = 270.4 Hz), 124.6 (^{1}J = 271.8 Hz), 120.4, 119.5, 118.2, 116.3, 110.3, 67.2, 54.1, 38.6. HRMS (ESI-FTMS Mass (*m/z*): calcd for $C_{29}H_{24}F_6N_4O_3$ $[M+H]^+$ = 591.1825, found 591.1823.

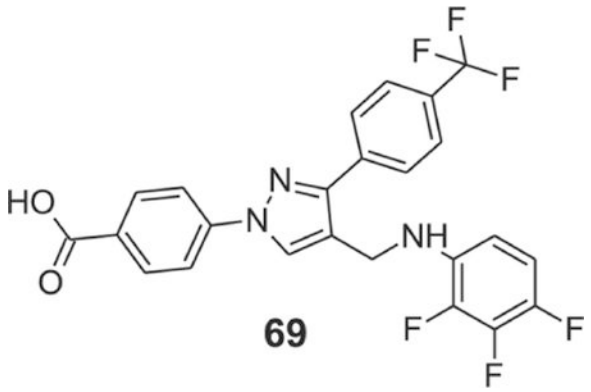

69

4-[4-[(2,3,4-trifluoroanilino)methyl]-3-[4-(trifluoromethyl)phenyl]pyrazol-1-yl]benzoic acid (69).: Yellow solid; yield 83%; ^{1}H NMR, 300 MHz (DMSO-d_6): δ 8.65 (s, 1H), 8.08–8.02 (m, 6H), 7.83 (d, J = 8.22 Hz, 2H), 7.03 (q, J = 9.51 Hz, 1H), 6.53 (br s, 1H), 6.21 (s, 1H), 4.42 (s, 2H); ^{13}C NMR 75 MHz (DMSO-d_6): δ 167.1, 149.9, 142.6, 136.9, 135.0,

134.9, 131.4, 130.1, 129.9, 129.4, 129.0, 128.8, 128.5, 126.0 (^3J = 3.72 Hz), 124.7 (^1J = 270.1 Hz), 120.7, 118.2, 111.9, 106.2, 38.6. HRMS (ESI-FTMS Mass (*m/z*): calcd for $C_{24}H_{15}F_6N_3O_2$ $[M+H]^+$ = 492.1141, found 492.1148.

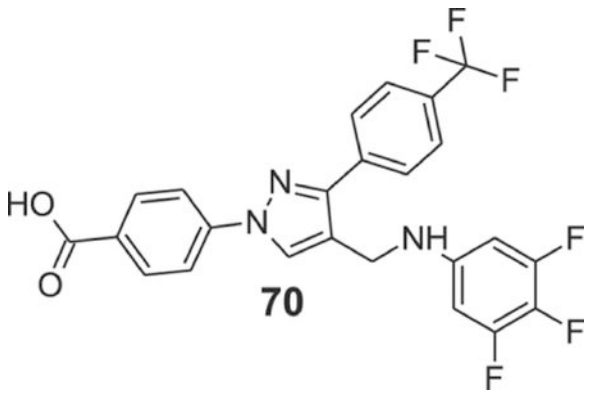

70

4-[4-[(3,4,5-trifluoroanilino)methyl]-3-[4-(trifluoromethyl)phenyl]pyrazol-1-yl]benzoic acid (70).: Yellow solid; yield 82%; ^{1}H NMR, 300 MHz (DMSO-d_6); δ 8.77 (s, 1H), 8.08–8.01 (m, 6H), 7.84 (d, *J* = 5.16 Hz, 2H), 6.54–6.49 (m, 3H), 4.28 (s, 2H); ^{13}C NMR 75 MHz (DMSO-d_6): δ 167.1, 153.1, 153.0, 150.2, 149.9, 145.5, 142.6, 136.8, 131.5, 128.9, 128.8 (^2J = 31.6 Hz), 128.4, 126.1 (^3J = 3.66 Hz), 124.7 (^1J = 270.4 Hz), 119.8, 118.3, 96.2 (^2J = 22.3 Hz), 38.5. HRMS (ESI-FTMS Mass (*m/z*): calcd for $C_{24}H_{15}F_6N_3O_2$ $[M+H]^+$ = 492.1141, found 492.1132.

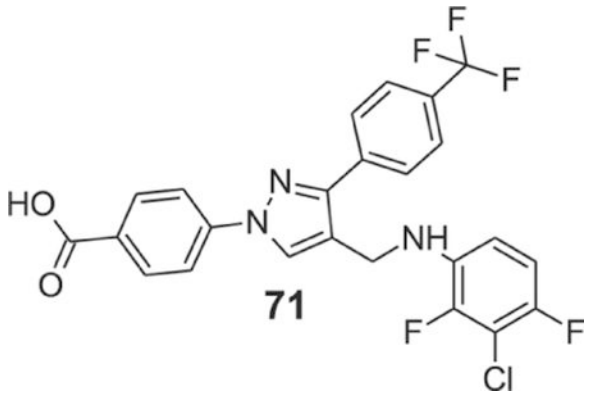

71

4-[4-[(3-chloro-2,4-difluoro-anilino)methyl]-3-[4-(trifluoromethyl)phenyl]pyrazol-1-yl]benzoic acid (71).: Yellow solid; Yield 90%; ^{1}H NMR, 300 MHz (DMSO-d_6): δ 8.65 (s, 1H), 8.07–8.01 (m, 6H), 7.83 (d, *J* = 8.28 Hz, 2H), 7.04 (t, *J* = 8.94 Hz, 1H), 6.74–6.66 (m, 1H), 4.43 (s, 2H); ^{13}C NMR 75 MHz (DMSO-d_6); δ 167.1, 149.9, 149.4 (^1J = 234.4 Hz), 146.9 (^1J = 244.6 Hz), 142.6, 136.9, 134.6 (^3J = 11.5 Hz), 131.4, 129.9, 129.3, 128.8 (^2J = 26.3 Hz), 128.5, 126.0 (^3J = 3.60 Hz), 124.7 (^1J = 270.4 Hz), 120.6, 118.2, 111.7 (^2J = 20.4 Hz), 110.5, 108.4 (q, ^2J = 18.1 Hz, 21.7 Hz), 38.6. HRMS (ESI-FTMS Mass (*m/z*): calcd for $C_{24}H_{15}F_6N_3O_2$ $[M+H]^+$ = 508.0846, found 508.0835.

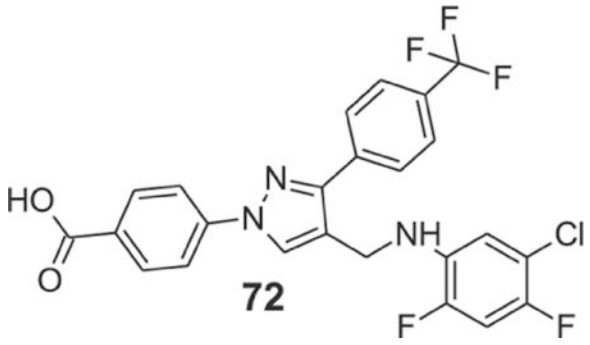

72

4-[4-[(5-chloro-2,4-difluoro-anilino)methyl]-3-[4-(trifluoromethyl)phenyl]pyrazol-1-yl]benzoic acid (72).: Yellow solid; yield 92%; ^{1}H NMR, 300 MHz (DMSO-d_6): δ 8.67 (s, 1H), 8.09–8.02 (m, 6H), 7.84 (d, J = 8.28 Hz, 2H), 7.37 (q, J = 9.36 Hz, J = 9.36 Hz, 1H), 6.88 (t, J = 7.89 Hz, 1H), 6.10 (s, 1H), 4.41 (s, 2H); ^{13}C NMR 75 MHz (DMSO-d_6); δ 167.1, 150.0, 149.2 (^{1}J = 241.6 Hz), 148.1 (^{1}J = 235.1 Hz), 142.6, 136.9, 134.7 (^{3}J = 11.2 Hz), 131.4, 129.9, 128.7, 128.5, 126.0 (^{3}J = 3.60 Hz), 124.7 (^{1}J = 270.4 Hz), 120.5, 118.2, 115.1 (^{4}J = 3.99 Hz), 114.9 (^{4}J = 3.89 Hz), 112.4 (^{4}J = 4.95 Hz), 105.1 (q, 2J = 24.5 Hz, 25.6 Hz), 38.5. HRMS (ESI-FTMS Mass (*m/z*): calcd for $C_{24}H_{15}F_6N_3O_2$ $[M+H]^+$ = 508.0846, found 508.0843.

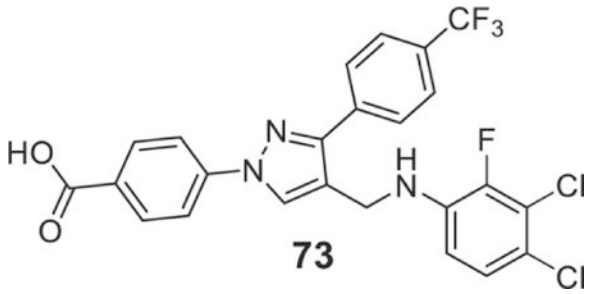

73

4-[4-[(3,4-dichloro-2-fluoro-anilino)methyl]-3-[4-(trifluoromethyl)phenyl]pyrazol-1-yl]benzoic acid (73).: Yellow solid; yield 98%; ^{1}H NMR, 300 MHz (DMSO-d_6): δ 8.64 (s, 1H), 8.08–8.01 (m, 6H), 7.84 (d, J = 8.31 Hz, 2H), 7.19 (d, J = 7.38 Hz, 1H), 6.71 (t, J = 8.91 Hz, 1H), 6.51 (br s, 1H), 4.47 (s, 2H); ^{13}C NMR 75 MHz (DMSO-d_6): δ 167.1, 149.8, 147.3 (^{1}J = 241.8 Hz), 142.6, 137.1, 136.9, 131.4, 129.8, 129.0, 128.7, 128.5, 126.0 (^{3}J = 3.65 Hz), 125.8 (^{4}J = 3.21 Hz), 124.7 (^{1}J = 270.4 Hz), 120.5, 118.8 (^{3}J = 16.9 Hz), 118.2, 117.6, 111.5 (^{4}J = 4.71 Hz), 38.4. HRMS (ESI-FTMS Mass (*m/z*): calcd for $C_{24}H_{15}Cl_2F_4N_3O_2$ $[M+H]^+$ = 524.0550, found 524.0543.

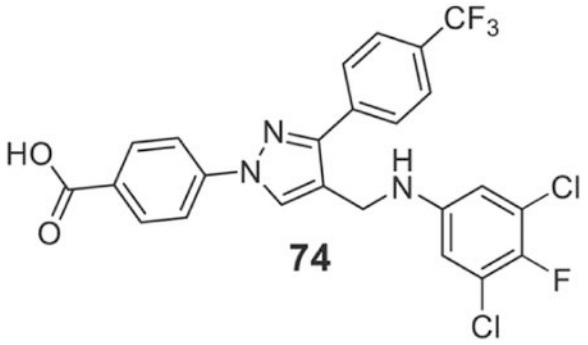

4-[4-[(3,5-dichloro-4-fluoro-anilino)methyl]-3-[4-(trifluoromethyl)phenyl]pyrazol-1-yl]benzoic acid (74).: Yellow solid; yield 86%; ^{1}H NMR, 300 MHz (DMSO-d_6): δ 8.74 (s, 1H), 8.09–8.01 (m, 6H), 7.83 (d, J = 8.31 Hz, 2H), 6.77 (d, J = 5.64 Hz, 2H), 6.49 (s, 1H), 4.30 (s, 2H); ^{13}C NMR 75 MHz (DMSO-d_6): δ 167.1, 150.2, 146.2 (^{4}J = 2.36 Hz), 145.2 (^{1}J = 233.6 Hz), 142.6, 136.8, 131.5, 130.3, 128.9, 128.8 (^{2}J = 31.6 Hz), 128.4, 126.1 (^{3}J = 3.66 Hz), 124.7 (^{1}J = 270.4 Hz), 121.5 (^{3}J = 17.7 Hz), 119.9, 118.2, 112.1, 38.4. HRMS (ESI-FTMS Mass (*m/z*): calcd for $C_{24}H_{15}Cl_2F_4N_3O_2$ $[M+H]^+$ = 524.0550, found 524.0553.

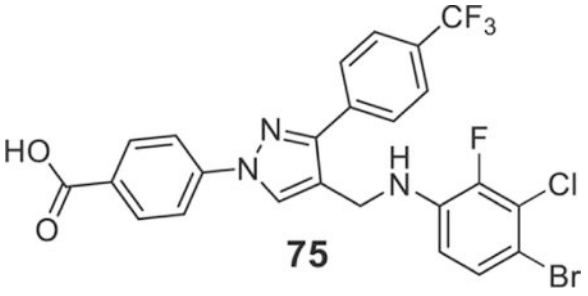

4-[4-[(4-bromo-3-chloro-2-fluoro-anilino)methyl]-3-[4-(trifluoromethyl)phenyl]pyrazol-1-yl]benzoic acid (75).: Yellow solid; yield 78%; ^{1}H NMR, 300 MHz (DMSO-d_6); δ 8.64 (s, 1H), 8.04–8.02 (m, 6H), 7.84 (d, J = 8.1 Hz, 2H), 7.30 (d, J = 8.91 Hz, 1H), 6.67 (t, J = 8.94 Hz, 1H), 6.54 (br s, 1H), 4.45 (s, 2H); ^{13}C NMR 75 MHz (DMSO-d_6); δ 167.1, 149.8, 147.3 (^{1}J = 242.6 Hz), 142.6, 137.4 (^{3}J = 11.9 Hz), 136.9, 131.4, 129.8, 128.8 (^{2}J = 31.7 Hz), 128.7, 128.5, 126.0 (^{3}J = 3.70 Hz), 124.7 (^{1}J = 270.4 Hz), 120.6, 120.5, 120.4, 118.2, 112.3 (^{4}J = 4.12 Hz), 106.4, 38.4. HRMS (ESI-FTMS Mass (*m/z*): calcd for $C_{24}H_{15}BrClF_4N_3O_2$ $[M+H]^+$ = 570.0025, found 570.0021.

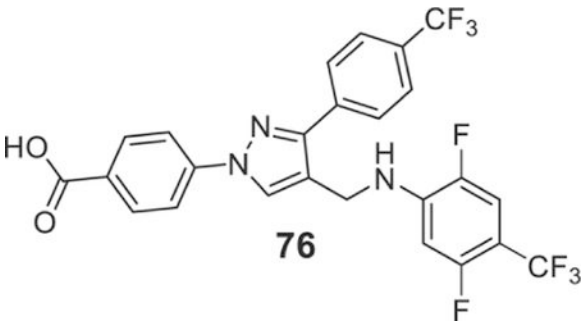

4-[4-[[2,5-difluoro-4-(trifluoromethyl)anilino]methyl]-3-[4-(trifluoromethyl)phenyl]pyrazol-1-yl]benzoic acid (76).: Yellow solid; yield 83%; ^{1}H NMR, 300 MHz (DMSO-d_6); δ 8.68 (s, 1H), 8.05–8.00 (m, 6H), 7.84 (d, J = 8.25 Hz, 2H), 7.42 (q, J = 6.72 Hz, J = 6.69 Hz, 1H), 7.09 (s, 1H), 6.81 (q, J = 6.93 Hz, J = 6.99 Hz, 1H), 4.52 (s, 2H); 13C NMR 75 MHz (DMSO-d_6): δ 167.1, 157.1 (^{1}J = 243.5 Hz), 149.9, 147.8, 144.6, 142.6, 142.1 (t, ^{3}J = 13.6 Hz, 12.8 Hz), 136.9, 131.4, 129.8, 129.0, 128.8, 128.5, 126.0 (^{3}J = 3.73 Hz), 124.7 (^{1}J = 270.3 Hz), 123.4 (^{1}J = 272.0 Hz), 119.8, 118.3, 112.7, 99.9 (^{2}J = 22.7 Hz), 38.1. HRMS (ESI-FTMS Mass (*m/z*): calcd for $C_{25}H_{15}F_8N_3O_2$ $[M+H]^+$ = 542.1109, found 542.1110.

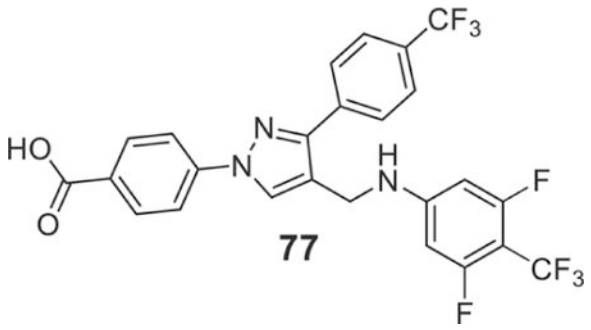

77

4-[4-[[3,5-difluoro-4-(trifluoromethyl)anilino]methyl]-3-[4-(trifluoromethyl)phenyl]pyrazol-1-yl]benzoic acid (77).: Yellow solid; yield 94%; ^{1}H NMR, 300 MHz (DMSO-d_6): δ 8.78 (s, 1H), 8.10–7.98 (m, 6H), 7.84 (d, J = 8.07 Hz, 2H), 7.45 (s, 1H), 6.52 (s, 1H), 6.47 (s, 1H), 4.41 (s, 2H); ^{13}C NMR 75 MHz (DMSO-d_6): δ 167.1, 153.8, 150.1, 142.5, 136.7, 131.5, 130.4, 129.0, 128.9 (^{2}J = 31.6 Hz), 128.4, 126.1 (^{3}J = 3.78 Hz), 124.6 (^{1}J = 270.2 Hz), 119.2, 118.3, 95.9, 95.6, 37.9. HRMS (ESI-FTMS Mass (*m/z*): calcd for $C_{25}H_{15}F_8N_3O_2$ $[M+H]^+$ = 542.1109, found 542.1104.

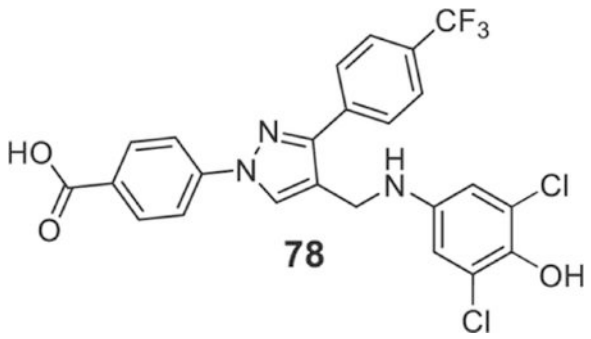

78

4-[4-[(3,5-dichloro-4-hydroxy-anilino)methyl]-3-[4-(trifluoromethyl)phenyl]pyrazol-1-yl]benzoic acid (78).: Yellow solid; yield 78%; ^{1}H NMR, 300 MHz (DMSO-d_6): δ 8.76 (s, 1H), 8.10–8.03 (m, 6H), 7.84 (d, J = 8.31 Hz, 2H), 6.69 (s, 2H), 6.00 (br s, 1H), 4.24 (s, 2H); ^{13}C NMR 75 MHz (DMSO-d_6): δ 167.1, 150.2, 143.3, 142.6, 139.8, 136.8, 131.5, 130.3, 128.9, 128.8 (^{2}J = 31.6 Hz), 128.4, 126.1 (^{3}J = 3.61 Hz), 124.7 (^{1}J = 270.3 Hz), 120.4, 118.2, 112.6, 38.8. HRMS (ESI-FTMS Mass (*m/z*): calcd for $C_{24}H_{16}Cl_2F_3N_3O_3$ $[M+H]^+$ = 522.0594, found 522.0589.

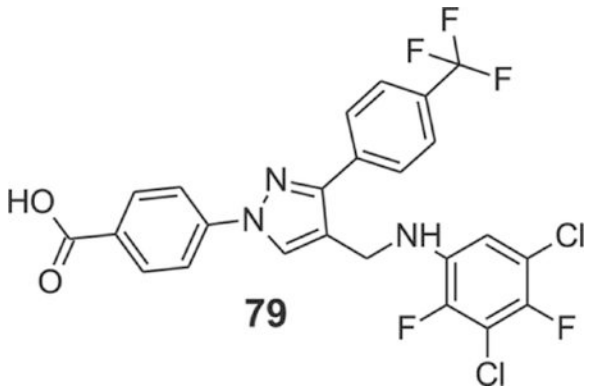

4-[4-[(3,5-dichloro-2,4-difluoro-anilino)methyl]-3-[4-(trifluoromethyl)phenyl]pyrazol-1-yl]benzoic acid (79).: Yellow solid; yield 98%; ^{1}H NMR, 300 MHz (DMSO-d_6); δ 8.66 (s, 1H), 8.05–8.02 (m, 6H), 7.85 (d, J = 8.37 Hz, 2H), 6.95–6.90 (m, 1H), 6.48 (s, 1H), 4.45 (s, 2H); ^{13}C NMR 75 MHz (DMSO-d_6): δ 167.1, 149.9, 145.7 (^{1}J = 243.0 Hz), 144.7 (^{1}J = 234.5 Hz), 142.6, 136.9, 134.9 (^{3}J = 10.1 Hz), 131.4, 129.8, 129.0, 128.7, 128.5, 126.0 (^{3}J = 3.77 Hz), 124.7 (^{1}J = 270.3 Hz), 120.3, 118.2, 116.2 (^{4}J = 3.96 Hz), 116.0 (^{4}J = 4.16 Hz), 110.3, 38.4. HRMS (ESI-FTMS Mass (*m/z*): calcd for $C_{24}H_{14}Cl_2F_5N_3O_2$ $[M+H]^+$ = 542.0456, found 542.0456.

4.4. Minimal inhibitory concentration (MIC) assay

The standard microdilution method, recommended by the Clinical and Laboratory Standards Institute (CLSI) was used to determine the MIC of the antibiotics. The starting concentration of compounds was 50 μg/ml and 2-fold dilution was done down the 96 honeycomb well plate column. The MIC assay was conducted in triplicates.

4.5. Cytotoxicity against HEK293 cell line

Cytotoxicity of the antibiotics was evaluated by using a human embryonic kidney cell line (HEK293). HEK293 cells were grown in Eagle's Minimum Essential Medium (EMEM) with 10% Fetal Bovine Serum (FBS) and incubated at 37 °C in the presence of 5% carbon dioxide. For cytotoxicity assays, HEK293 cells were cultured in 96-well black plates with 4000 cells per well and treated for 24 h with a range of concentrations of antibiotics dissolved in DMSO. Resazurin (40 μl of 0.15 mg/ml) was added per well and incubated for additional 4 h. Reduction of resazurin was measured with excitation at 560 nm and emission at 590 nm using Bio Tek™ Cytation™5 plate reader. IC_{50} values were determined through data processing using Graphpad Prism 7 for Windows, Version 7.04.

4.6. Biofilm inhibition and destruction studies

Biofilm inhibition and destruction activity were evaluated as described in a previous study [25]. Briefly for inhibition activity, an overnight culture of bacteria was suspended to 0.5 McFarland standard in sterile phosphate buffer saline (PBS) and diluted 1:100 in cation adjusted Muller Hilton broth (CAMHB) containing 1% glucose. This bacterial suspension (195 μl) plus 5 μl antibiotic (in DMSO) at 2xMIC, MIC, and 0.5xMIC concentration was added to wells in triplicates in a 96 well flat bottom plate. Broth only wells were maintained

as negative controls and bacterial suspension in broth with added DMSO served as a positive control. After 24 h of incubation at 35 °C, wells were washed with PBS thrice and dried in an oven at 60 °C for 15 min. Crystal violet (250 μl at 0.1% (w/v) concentration) was added to each well to stain cells. After 15 min, excess crystal violet was washed away with deionized water, and plates were dried in the oven. To solubilize biofilm-bound crystal violet, 250 μl of 33% acetic acid was added, then optical density was measured at 620 nm excitation using a Bio TekTM CytationTM 5 plate reader.

For destruction activity, mature biofilm was maintained in 96-well flat bottom plate by growing bacteria in CAMHB containing 1% glucose without the addition of antibiotics by incubation at 35 °C for 24 h. The wells were washed thrice by sterile PBS under aseptic conditions and fresh medium was added with antibiotics at 2xMIC, MIC, and 0.5xMIC concentration. Negative and positive controls were also maintained as in the inhibition activity assay. The plate was incubated for additional 24 h and washed, dried, stained with crystal violet, washed and acetic acid added to measure optical density as described above.

4.7. Catheter associated biofilm

Compound **59**, along with controls, was tested for the ability to destroy biofilm using an *in vitro* catheter model following an established protocol with some modification [32]. Briefly, 1 cm segments of 14 gauge fluorinated polyethylene propylene catheter (Introcan safety catheter; Braun, Bethlehem, PA) were coated with human plasma and placed into wells of a 12-well microtiter plate containing 2 ml of tryptic soy broth supplemented with glucose and NaCl (biofilm medium, BM) containing approximately 1×10^7 colony-forming units of the methicillin-sensitive *S. aureus* (MSSA) strain UAMS-1 as assessed based on an optical density of 0.05 at 600 nm. The plate was then incubated at 37 °C for 24 h with gentle shaking. As an untreated control, nine catheters were removed, rinsed three times with sterile phosphate buffered saline (PBS), and placed individually into 5 ml of sterile PBS. Three catheters were collected on days 0, 1, and 2 and processed as described below to determine the number of viable bacteria. An additional six catheters were placed individually into the wells of a 24-well microtiter plate containing 1 ml of either BM supplemented with DMSO with or without 40 μg/ml compound **59**. As a treatment control, an additional six catheters were exposed to BDM containing 40 μg/ml vancomycin. All plates were then incubated at 37 °C with gentle shaking. Catheters (n = 3) in each group were recovered at 24 h and 48 h and placed into 5 ml of sterile PBS. For catheters harvested at 48 h, the medium with or without added treatment was made fresh and replaced after 24 h to determine the concentration of adherent cells, the catheters were sonicated to remove adherent bacteria, diluted, and plated on tryptic soy agar without antibiotic selection to determine the total number of adherent bacteria as defined by CFUs per catheter.

4.8. Persister cell killing assay

A persister cell killing assay was performed following the methodology described by Kim et al. with some modifications [39]. *S. aureus* strain was grown to stationary phase in CAMHB medium by shaking at 200 rpm overnight at 35 °C. An aliquot of stationary phase culture (1 ml) was washed thrice with 1xPBS by centrifugation. After washing, the cells were diluted to ~ 5×10^8 CFU/ml (confirmed by plate count). Diluted persister cells (2 ml) plus

antibiotics at the desired concentration were incubated in sterile 10 × 75 mm plastic culture tubes at 35 °C with shaking at 200 rpm. At specific times, 400 μl aliquots were placed into microcentrifuge tubes and the cells washed and serially diluted in PBS. The diluted sample was plated on TSA agar plate with 5% sheep blood by the 6 × 6 drop plate method. Plates were incubated for 18–20 h at 35 °C, and then colonies were counted to calculate concentrations in CFU/ml. The experiment was performed in triplicates.

4.9. Time-kill assay

Time kill assay for test antibiotics against *S. aureus* ATCC 700699 and *S. aureus* ATCC 33591 strains was conducted using procedures published previously [31]. Briefly, a log-phase bacterial culture was diluted to ~5×10^6 CFU/ml in warm sterile CAMHB broth and was exposed to antibiotics at 4xMIC concentration then incubated at 35 °C. Samples of 20 μl were taken every 2 h, diluted 10 fold to $10^{-5,}$ and the 6 × 6 drop plate method was performed to determine viable CFU/ml after 18–24 h of incubation at 35 °C. Each antibiotic time-kill assay was conducted in triplicate.

4.10. In vivo toxicity studies

All animal experiments were performed at the Central Arkansas Veterans Healthcare System (John L. McClellan Memorial Veterans Hospital in Little Rock, AR) and have been approved by the Institutional Animal Care and Use Committee. Male CD-1 mice (8 weeks old, 32–37 g) were purchased from Charles River Laboratories (Wilmington, MA). The test compound was freshly dissolved in 0.9% saline, sterilized by ultrafiltration, and injected intraperitoneally (IP) in mice at one of three doses of 5, 20 or 50 mg/kg (n = 10 per dose). The additional control group (n = 10) was administered the vehicle (saline). The mice were euthanized 24 h after the injection, and blood was collected by cardiac puncture. Toxicity was assessed by measuring 14 blood markers of various organ functions as parts of the Comprehensive Diagnosis Kit (Abaxis, Union City, CA) and using VetScan VS2 instrument (Abaxis). The markers included: alanine aminotransferase (ALT), albumin (ALB), alkaline phosphatase (ALP), amylase (AMY), blood urea nitrogen (BUN), calcium (CA), creatinine (CRE), globulin (GLOB), glucose (GLU), phosphorus (PHOS), potassium (K^+), sodium (NA^+), total bilirubin (TBIL), and total protein (TP). Our criteria for toxicity were the combination of: (a) statistically significant difference from the untreated and vehicle (saline) controls, (b) going beyond normal lower and upper ranges, (c) dose-dependence of the toxic response, if any, and (d) consistency between several functional markers of the same organ. All animal experiments performed in the manuscript were conducted in compliance with UAMS, Little Rock, Arkansas guidelines.

4.11. TUNEL assay

Liver and kidney samples were embedded in paraffin and 5-μm sections were prepared. TUNEL assay was performed as previously described [40]. Briefly, the samples were stained using the *In Situ* Cell Death Detection Kit (Roche Diagnostics, Indianapolis, IN) according to the manufacturer's protocol. After staining, cells were counterstained with 4′,6-diamidino-2-phenylindol (DAPI) to visualize cell nuclei, mounted under coverslips with Prolong® Antifade kit (Invitrogen, Carlsbad, CA) and acquired using the Olympus IX-81

inverted microscope (Olympus America, Center Valley, PA) equipped with Hamamatsu ORCA-ER monochrome camera (Hamamatsu Photonics K.K., Hamamatsu City, Japan).

4.12. Macromolecular synthesis inhibition assay

Macromolecular synthesis inhibition was investigated using *S. aureus* ATCC 29213 (MIC = 1–0.5 μg/ml). Cells were grown at 35 °C overnight on trypticase soy agar plates containing 5% sheep blood, and isolated colonies were used to inoculate broth medium as described below for each assay. For each macromolecular synthesis reaction, *S. aureus* ATCC 29213 was exposed to 0.25, 0.5, 1, 2, 4, 8, or 16-fold the broth microdilution MIC of the compound. Positive controls were dosed at 8-fold their respective MIC.

4.13. DNA and RNA synthesis

When cells reached the early exponential phase in CAMHB, 100 μl of culture was added to triplicate 1.5 ml microfuge tubes containing various concentrations of test compound or control antibiotics (2.5 μl) at 40x the required final concentration. A “no drug” control was included for all experiments. Following a 30 min pre-incubation at room temperature to allow for drug inhibition of a pathway, either [^{3}H] thymidine, at 3.0 μCi per tube (DNA synthesis) or [^{3}H] uridine, at 0.5 μCi per tube (RNA synthesis) was added. Reactions were allowed to proceed at room temperature for 30 min and then stopped by adding 6 μl of cold 100% trichloroacetic acid (TCA). Reactions were incubated on ice for 30 min and the TCA-precipitated material was filtered through glass fiber filters, followed by three washes with 5 ml of cold 5% TCA and two washes with 5 ml of ethanol. After drying, the filters were placed in scintillation vials, liquid scintillation fluid was added, and counts were determined using a PerkinElmer Tri-Carb 4810 TR Liquid Scintillation Analyzer.

4.14. Cell wall synthesis

When cells reached an early exponential phase in CAMHBII, they were resuspended in M9 minimal medium (MEM) and 100 μl of culture was added to triplicate 1.5 ml microfuge tubes containing various concentrations of the test compound or control antibiotics (2.5 μl) at 40x the required final concentration. Following a 30-min pre-incubation at 37 °C to allow for drug inhibition of cell wall synthesis, [^{14}C] *N*-acetylglucosamine (0.4 μCi/reaction) was added to each tube and incubated for 45 min in a 37 °C heating block. Reactions were stopped through the addition of 100 μl of 8% SDS to each tube. Reactions were then heated at 95 °C for 30 min in a heating block, cooled, and briefly centrifuged. One hundred and 80 μL of each reaction were spotted onto pre-wet nitrocellulose membrane filters (0.8 μM). After washing three times with 5 ml of 0.1% SDS, the filters were rinsed two times with 5 ml of deionized water and allowed to dry. After drying, the filters were placed in scintillation vials, liquid scintillation fluid was added, and counts were determined using a PerkinElmer Tri-Carb 4810 TR Liquid Scintillation Analyzer.

4.15. Lipid synthesis

Bacterial cells were grown to early exponential growth phase in CAMHBII and 100 μl was added to 1.5 ml microfuge tubes (in triplicate) containing various concentrations of test compound or control antibiotics as described above. Following a 30-min pre-incubation at

room temperature to allow for inhibition of lipid synthesis, [^{3}H] glycerol was added at 0.5 μCi per reaction. Reactions were allowed to proceed at room temperature for 50 min and then stopped through the addition of 375 μl chloroform/methanol (1:2), followed by vortexing for 20 s after each addition. Chloroform (125 μl) was then added to each reaction and vortexed, followed by the addition of 125 μl dH_2O and vortexing. Reactions were centrifuged at 13,000 rpm in a microfuge for 10 min, and then 150 μl of the organic phase was transferred to a scintillation vial and allowed to dry in a fume hood for at least 1 h. Liquid scintillation fluid was added and samples were counted using a PerkinElmer Tri-Carb 4810 TR Liquid Scintillation Analyzer.

4.16. Protein synthesis

When cells reached the early exponential phase in CAMHB, they were resuspended in M9 minimal medium (MEM) and 100 μl of culture was added to triplicate 1.5 ml microfuge tubes containing various concentrations of test compound or control antibiotics (2.5 μl) at 40x the required final concentration. Following a 30-min pre-incubation at room temperature to allow for drug inhibition of protein synthesis, [^{3}H] leucine was added at 3.0 μCi per tube. Reactions were allowed to proceed at room temperature for 40 min and then stopped by adding 12 μl of cold 50% trichloroacetic acid (TCA)/20% casamino acids. Reactions were incubated on ice for 30 min and the TCA-precipitated material was filtered through glass fiber filters, followed by three washes with 5 ml of cold 5% TCA and two washes with 5 ml of ethanol. After drying, the filters were placed in scintillation vials, liquid scintillation fluid was added, and counts were determined using a PerkinElmer Tri-Carb 4810 TR Liquid Scintillation Analyzer.

Supplementary Material

Refer to Web version on PubMed Central for supplementary material.

Acknowledgements

This publication was made possible by the Research Technology Core of the Arkansas INBRE program, supported by a grant from the National Institute of General Medical Sciences, (NIGMS), P20 GM103429 from the National Institutes of Health to record the Mass Spectrometry data and grants 2I01BX002425. *In vivo* toxicity studies were supported by the National Institutes of Health grant 2P20 GM109005-06 and VA Merit Review grant 2I01 BX002425. This publication was made possible by the Arkansas INBRE Summer Research Grant, supported by a grant from the National Institute of General Medical Sciences, (NIGMS), P20 GM103429 from the National Institutes of Health.

References

[1]. Spellberg B, Guidos R, Gilbert D, Bradley J, Boucher HW, Scheld WM, Bartlett JG, Edwards J Jr., A. Infectious Diseases Society of, The epidemic of antibiotic-resistant infections: a call to action for the medical community from the Infectious Diseases Society of America, Clin. Infect. Dis 46 (2008) 155–164. [PubMed: 18171244]

[2]. Tal-Jasper R, Katz DE, Amrami N, Ravid D, Avivi D, Zaidenstein R, Lazarovitch T, Dadon M, Kaye KS, Marchaim D, Clinical and epidemiological significance of carbapenem resistance in acinetobacter baumannii infections, Antimicrob. Agents Chemother 60 (2016) 3127–3131. [PubMed: 26883694]

[3]. Marsit H, Koubaa M, Gargouri M, Ben Jemaa T, Gaddour H, Kotti F, Sammoudi A, Turki M, Ben Jemaa M, Hospital-acquired infections due to multidrug resistant Acinetobacter baumannii: how challenging is the management?, Fund. Clin. Pharmacol 30 (2016) 87–87.

[4]. Farha MA, Leung A, Sewell EW, D'Elia MA, Allison SE, Ejim L, Pereira PM, Pinho MG, Wright GD, Brown ED, Inhibition of WTA synthesis blocks the cooperative action of PBPs and sensitizes MRSA to beta-lactams, ACS Chem. Biol 8 (2013) 226–233. [PubMed: 23062620]

[5]. CDC, General Information about Staphylococcus aureus, in.

[6]. Moisse K, Antibiotic Resistance Could Bring 'End of Modern Medicine, ABC NEWS, 2012.

[7]. Mistry TL, Truong L, Ghosh AK, Johnson ME, Mehboob S, Benzimidazole-based FabI inhibitors: a promising novel scaffold for anti-staphylococcal drug development, ACS Infect. Dis 3 (2017) 54–61. [PubMed: 27756129]

[8]. CDC, Methicillin-resistant Staphylococcus aureus (MRSA), CDC, 1600 Clifton Road Atlanta, GA 30329–4027 USA, 2019.

[9]. Song S, Wood TK, Combatting persister cells with substituted indoles, Front. Microbiol 11 (2020) 1565. [PubMed: 32733426]

[10]. Saini H, Vadekeetil A, Chhibber S, Harjai K, Azithromycin-ciprofloxacin-impregnated urinary catheters avert bacterial colonization, biofilm formation, and inflammation in a murine model of foreign-body-associated urinary tract infections caused by Pseudomonas aeruginosa, Antimicrob. Agents Chemother 61 (2017) e01906–01916. [PubMed: 28031194]

[11]. Roy R, Tiwari M, Donelli G, Tiwari V, Strategies for combating bacterial biofilms: a focus on anti-biofilm agents and their mechanisms of action, Virulence 9 (2018) 522–554. [PubMed: 28362216]

[12]. Berditsch M, Afonin S, Reuster J, Lux H, Schkolin K, Babii O, Radchenko DS, Abdullah I, William N, Middel V, Strähle U, Nelson A, Valko K, Ulrich AS, Supreme activity of gramicidin S against resistant, persistent and biofilm cells of staphylococci and enterococci, Sci. Rep 9 (2019) 17938. [PubMed: 31784584]

[13]. Brinkman CL, Schmidt-Malan SM, Karau MJ, Greenwood-Quaintance K, Hassett DJ, Mandrekar JN, Patel R, Exposure of bacterial biofilms to electrical current leads to cell death mediated in part by reactive oxygen species, PloS One 11 (2016) e0168595. [PubMed: 27992529]

[14]. Zhang K, Li X, Yu C, Wang Y, Promising therapeutic strategies against microbial biofilm challenges, Frontiers in Cellular and Infection Microbiology 10 (2020).

[15]. Worthington RJ, Richards JJ, Melander C, Small molecule control of bacterial biofilms, Org. Biomol. Chem 10 (2012) 7457–7474. [PubMed: 22733439]

[16]. Joseph R, Naugolny A, Feldman M, Herzog IM, Fridman M, Cohen Y, Cationic pillararenes potently inhibit biofilm formation without affecting bacterial growth and viability, J. Am. Chem. Soc 138 (2016) 754–757. [PubMed: 26745311]

[17]. Moormeier DE, Bayles KW, Staphylococcus aureus biofilm: a complex developmental organism, Mol. Microbiol 104 (2017) 365–376. [PubMed: 28142193]

[18]. Khatoon Z, McTiernan CD, Suuronen EJ, Mah T-F, Alarcon EI, Bacterial biofilm formation on implantable devices and approaches to its treatment and prevention, Heliyon 4 (2018) e01067–e01067. [PubMed: 30619958]

[19]. Hagras M, Mohammad H, Mandour MS, Hegazy YA, Ghiaty A, Seleem MN, Mayhoub AS, Investigating the antibacterial activity of biphenylthiazoles against methicillin- and vancomycin-resistant Staphylococcus aureus (MRSA and VRSA), J. Med. Chem 60 (2017) 4074–4085. [PubMed: 28436655]

[20]. Wu Z-C, Boger DL, Maxamycins: durable antibiotics derived by rational redesign of vancomycin, Acc. Chem. Res 53 (2020) 2587–2599. [PubMed: 33138354]

[21]. Parmar A, Lakshminarayanan R, Iyer A, Mayandi V, Leng Goh ET, Lloyd DG, Chalasani MLS, Verma NK, Prior SH, Beuerman RW, Madder A, Taylor EJ, Singh I, Design and syntheses of highly potent teixobactin analogues against Staphylococcus aureus, methicillin-resistant Staphylococcus aureus (MRSA), and vancomycin-resistant enterococci (VRE) in vitro and in vivo, J. Med. Chem 61 (2018) 2009–2017. [PubMed: 29363971]

[22]. Guo Y, Bao C, Li F, Hou E, Qin S, Zhang Q, Liu J, Discovery, synthesis, and biological evaluation of dunnianol-based mannich bases against methicillin-resistant Staphylococcus aureus (MRSA), ACS Infect. Dis 6 (2020) 2478–2489. [PubMed: 32786272]

[23]. Qian Y, Allegretta G, Janardhanan J, Peng Z, Mahasenan KV, Lastochkin E, Gozun MMN, Tejera S, Schroeder VA, Wolter WR, Feltzer R, Mobashery S, Chang M, Exploration of the structural space in 4(3H)-Quinazolinone antibacterials, J. Med. Chem 63 (2020) 5287–5296. [PubMed: 32343145]

[24]. Delancey E, Allison D, Kc HR, Gilmore DF, Fite T, Basnakian AG, Alam MA, Synthesis of 4,4′-(4-formyl-1H-pyrazole-1,3-diyl)dibenzoic acid derivatives as narrow spectrum antibiotics for the potential treatment of acinetobacter baumannii infections, Antibiotics 9 (2020) 650.

[25]. Alnufaie R, Raj Kc H, Alsup N, Whitt J, Andrew Chambers S, Gilmore D, Alam MA, Synthesis and antimicrobial studies of coumarin-substituted pyrazole derivatives as potent anti-Staphylococcus aureus agents, Molecules 25 (2020) 2758.

[26]. Whitt J, Duke C, Ali MA, Chambers SA, Khan MMK, Gilmore D, Alam MA, Synthesis and antimicrobial studies of 4-[3-(3-Fluorophenyl)-4-formyl-1H-pyrazol-1-yl]benzoic acid and 4-[3-(4-Fluorophenyl)-4-formyl-1H-pyrazol-1-yl]benzoic acid as potent growth inhibitors of drug-resistant bacteria, ACS Omega 4 (2019) 14284–14293. [PubMed: 31508552]

[27]. Zakeyah AA, Whitt J, Duke C, Gilmore DF, Meeker DG, Smeltzer MS, Alam MA, Synthesis and antimicrobial studies of hydrazone derivatives of 4-[3-(2,4-difluorophenyl)-4-formyl-1H-pyrazol-1-yl]benzoic acid and 4-[3-(3,4-difluorophenyl)-4-formyl-1H-pyrazol-1-yl]benzoic acid, Bioorg. Med. Chem. Lett 28 (2018) 2914–2919. [PubMed: 30017319]

[28]. Brider J, Rowe T, Gibler DJ, Gottsponer A, Delancey E, Branscum MD, Ontko A, Gilmore D, Alam MA, Synthesis and antimicrobial studies of azomethine and N-arylamine derivatives of 4-(4-formyl-3-phenyl-1H-pyrazol-1-yl)benzoic acid as potent anti-methicillin-resistant Staphylococcus aureus agents, Med. Chem. Res 25 (2016) 2691–2697.

[29]. Allison D, Delancey E, Ramey H, Williams C, Alsharif ZA, Al-khattabi H, Ontko A, Gilmore D, Alam MA, Synthesis and antimicrobial studies of novel derivatives of 4-(4-formyl-3-phenyl-1H-pyrazol-1-yl)benzoic acid as potent anti-Acinetobacter baumannii agents, Bioorg. Med. Chem. Lett 27 (2017) 387–392. [PubMed: 28065568]

[30]. Barza M, Sulfonamides and Trimethoprim-Sulfamethoxazole, Williams & Wilkins, 1981, pp. 46–53.

[31]. Alnufaie R, Alsup N, Kc HR, Newman M, Whitt J, Chambers SA, Gilmore D, Alam MA, Design and synthesis of 4-[4-formyl-3-(2-naphthyl)pyrazol-1-yl]benzoic acid derivatives as potent growth inhibitors of drug-resistant Staphylococcus aureus, J. Antibiot 73 (2020) 818–827.

[32]. Meeker DG, Beenken KE, Mills WB, Loughran AJ, Spencer HJ, Lynn WB, Smeltzer MS, Evaluation of antibiotics active against methicillin-resistant Staphylococcus aureus based on activity in an established biofilm, Antimicrob. Agents Chemother 60 (2016) 5688–5694. [PubMed: 27401574]

[33]. Allison KR, Brynildsen MP, Collins JJ, Metabolite-enabled eradication of bacterial persisters by aminoglycosides, Nature 473 (2011) 216–220. [PubMed: 21562562]

[34]. Conlon BP, Nakayasu ES, Fleck LE, LaFleur MD, Isabella VM, Coleman K, Leonard SN, Smith RD, Adkins JN, Lewis K, Activated ClpP kills persisters and eradicates a chronic biofilm infection, Nature 503 (2013) 365–370. [PubMed: 24226776]

[35]. Whitt J, Duke C, Sumlin A, Chambers SA, Alnufaie R, Gilmore D, Fite T, Basnakian AG, Alam MA, Synthesis of hydrazone derivatives of 4-[4-Formyl-3-(2-oxochromen-3-yl)pyrazol-1-yl]benzoic acid as potent growth inhibitors of antibiotic-resistant Staphylococcus aureus and acinetobacter baumannii, Molecules 24 (2019) 2051.

[36]. Toxicological analysis using DNA fragmentation, in: Encyclopedia of Analytical Chemistry, pp. 1–18.

[37]. Cotsonas KA, Wu L, Macromolecular synthesis and membrane perturbation assays for mechanisms of action studies of antimicrobial agents, Curr Protoc Pharmacol Chapter 13 (2009) Unit 13A.17.

[38]. Martin JK, Sheehan JP, Bratton BP, Moore GM, Mateus A, Li SH-J, Kim H, Rabinowitz JD, Typas A, Savitski MM, Wilson MZ, Gitai Z, A dual-mechanism antibiotic kills gram-negative bacteria and avoids drug resistance, Cell 181 (2020) 1518–1532 e1514. [PubMed: 32497502]

[39]. Kim W, Steele AD, Zhu W, Csatary EE, Fricke N, Dekarske MM, Jayamani E, Pan W, Kwon B, Sinitsa IF, Rosen JL, Conery AL, Fuchs BB, Vlahovska PM, Ausubel FM, Gao H, Wuest WM, Mylonakis E, Discovery and optimization of nTZDpa as an antibiotic effective against bacterial persisters, ACS Infect. Dis 4 (2018) 1540–1545. [PubMed: 30132650]

[40]. Apostolov EO, Soultanova I, Savenka A, Bagandov OO, Yin X, Stewart AG, Walker RB, Basnakian AG, Deoxyribonuclease I is essential for DNA fragmentation induced by gamma radiation in mice, Radiat. Res 172 (2009) 481–492. [PubMed: 19772469]

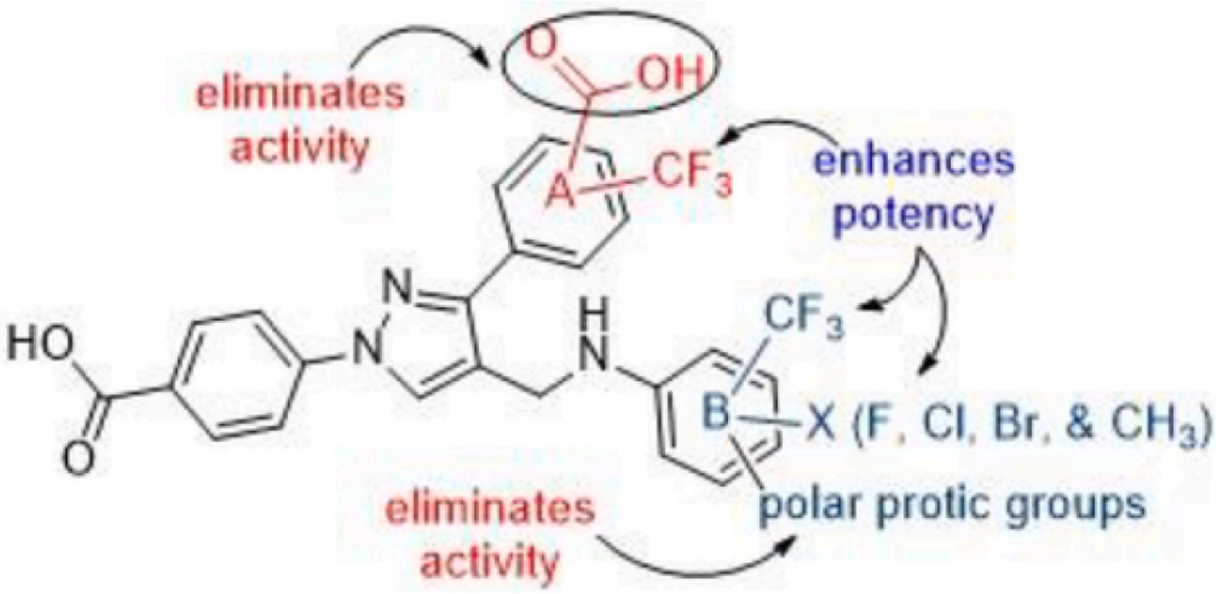

Fig. 1.
Structure activity relationship (SAR).

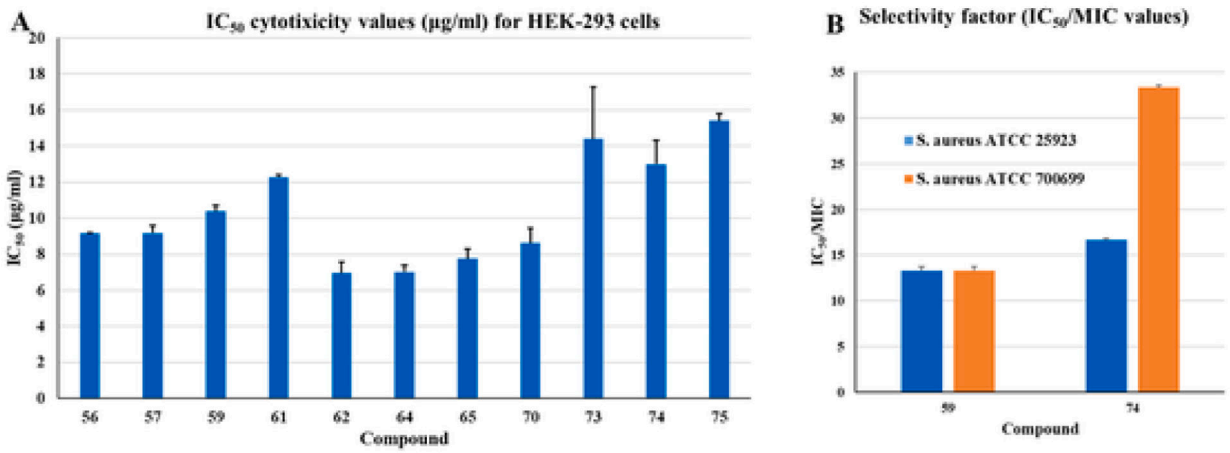

Fig. 2.

(A) IC_{50} values for the potent compounds and **(B)** Selectivity factor (IC_{50}/MIC values) for compounds **59** and **74** for *S. aureus* ATCC 25923 and *S. aureus* ATCC 700699 strains.

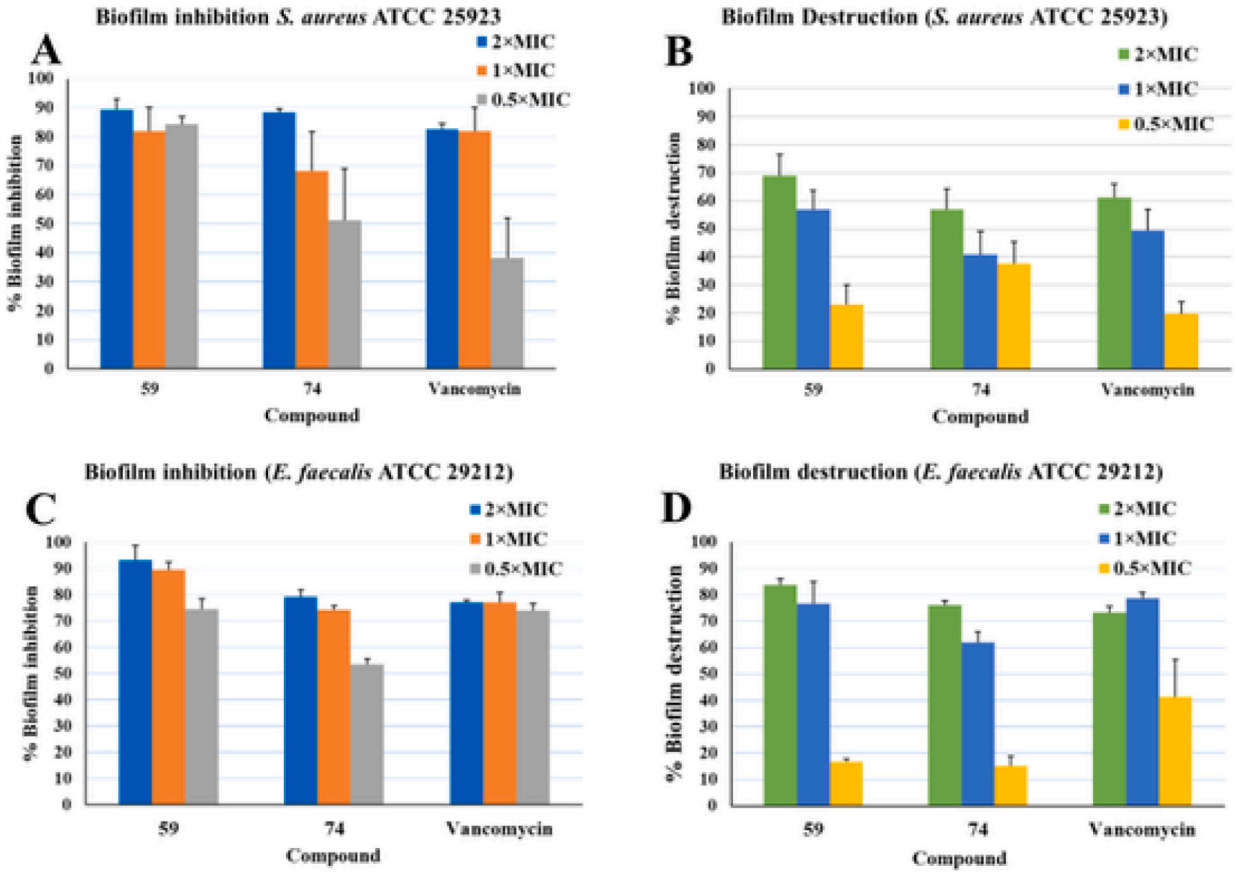

Fig. 3.

Biofilm inhibition and destruction assay **(A)** and **(B)** *S. aureus* ATCC 25923 **(C)** and **(D)** *E. faecalis* ATCC 29212.

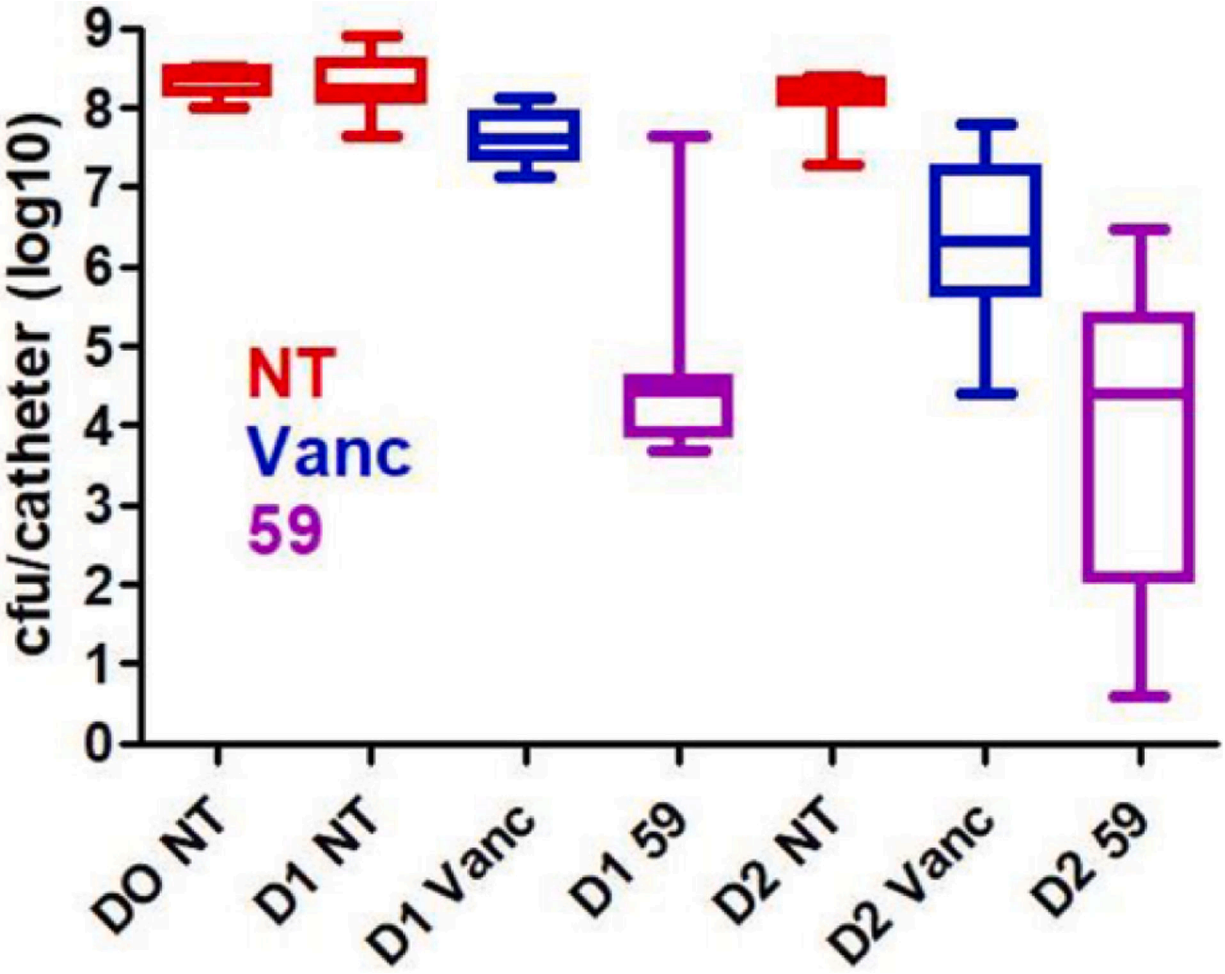

Fig. 4.

Elimination of catheter associated biofilm by compound **59**. NT = No Treatment, Vanc = Vancomycin, DO = Day 0, D1 = Day 1, and D2 = Day 2.

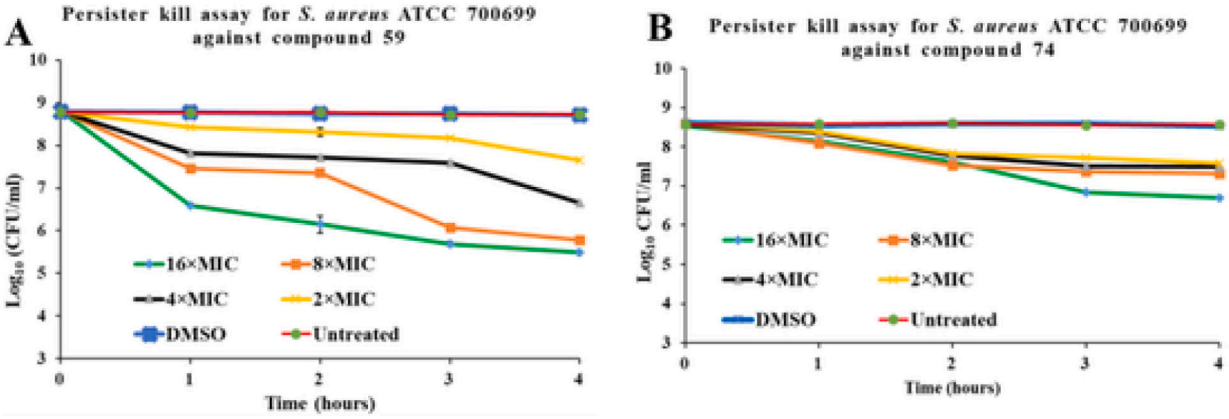

Fig. 5.

Persister cell time-kill assay for (A) compound **59** and (B) compound **74** against *S. aureus* ATCC 70699 (MRSA). The level of detection is 2×10^3 CFU/ml.

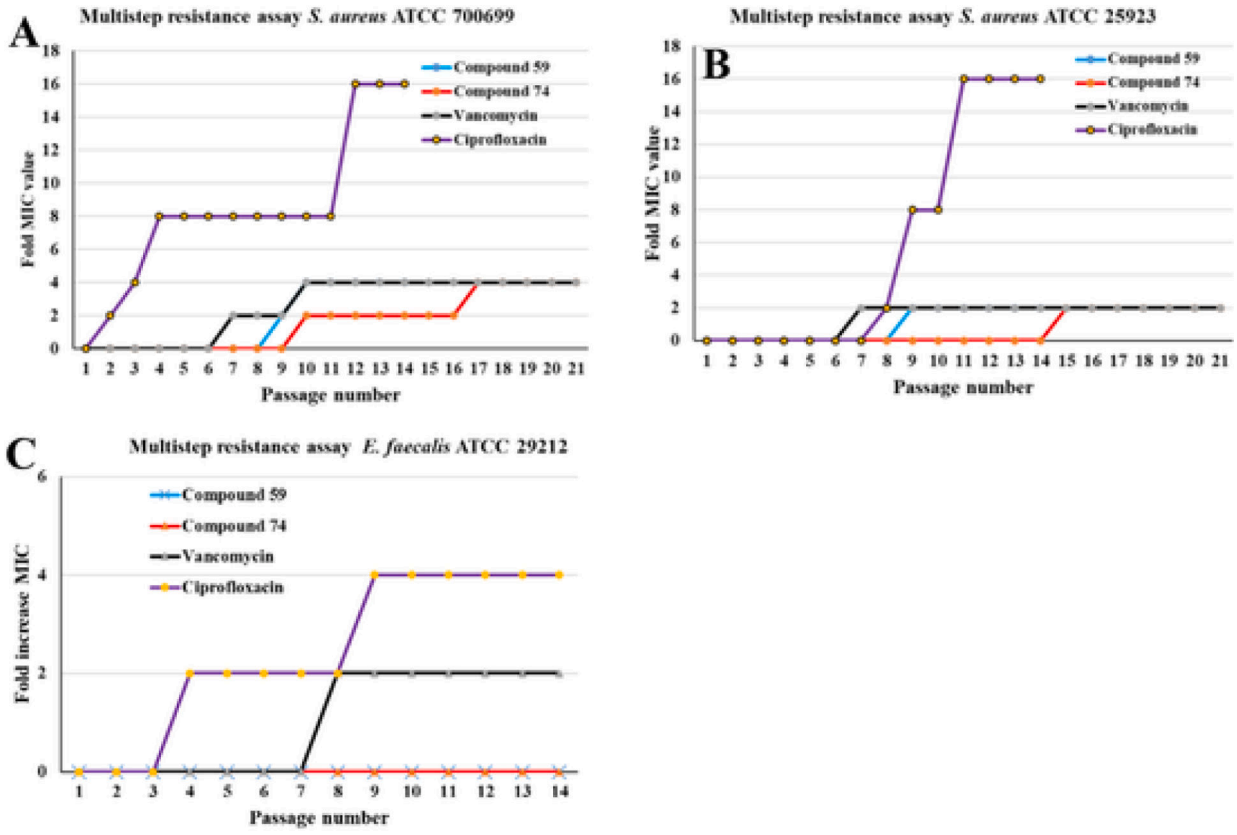

Fig. 6.

Multi-passage resistance studies for compounds **59** and **74** against **(A)** *S. aureus* ATCC 25923 (MSSA), **(B)** *S. aureus* ATCC 700699 (MRSA) and **(C)** *E. faecalis* ATCC 29212; note the different Y-axis range. Ciprofloxacin and vancomycin are positive controls. Studies were done for 21 days and 14 days as indicated.

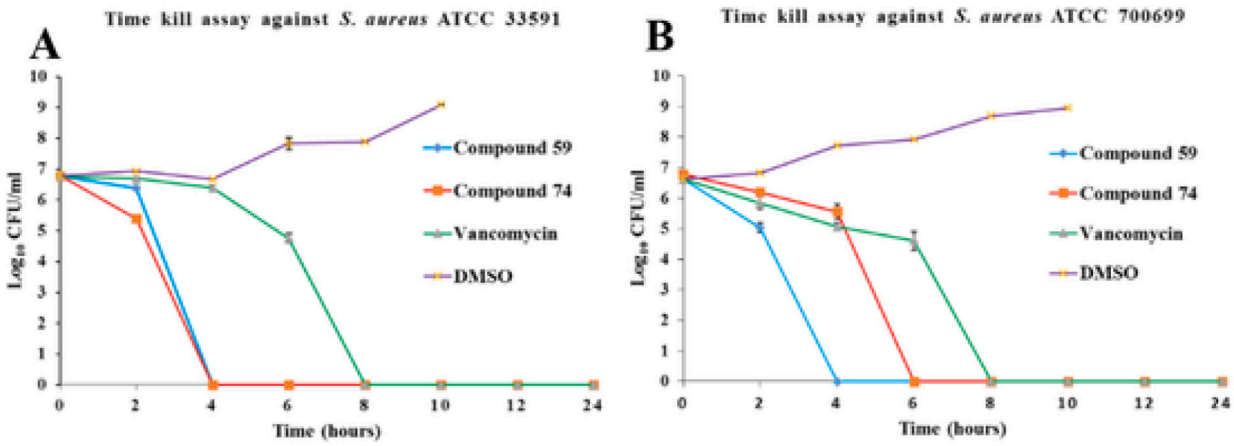

Fig. 7.

Time Kill Assay (TKA) for compounds **59** and **74**. **(A)** *S. aureus* ATCC 700699 **(B)** *S. aureus* ATCC 33591.

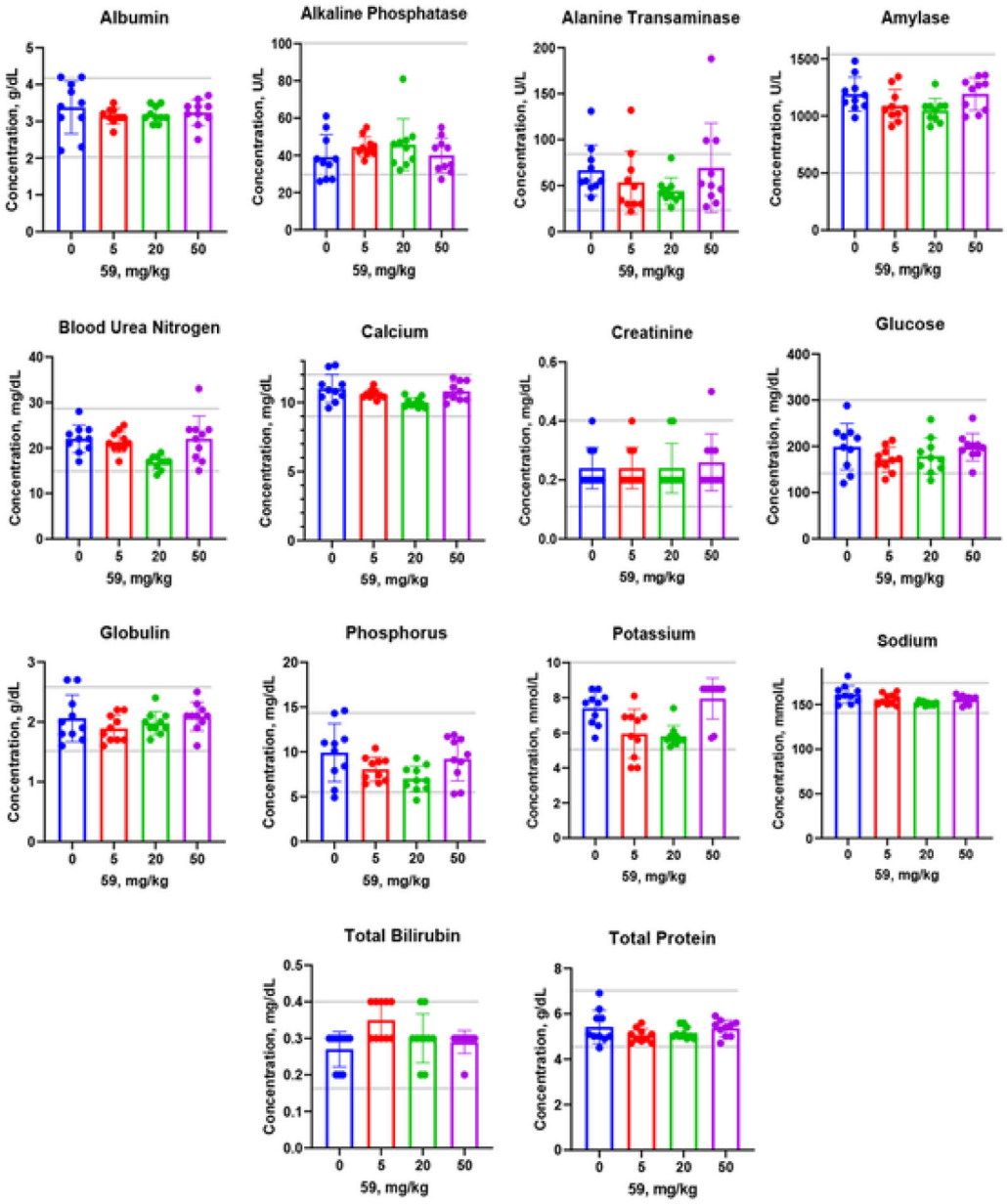

Fig. 8.

In vivo toxicity assessment of the compound **59**. Three doses (5, 20 and 50 mg/kg) were administered IP in CD-1 mice (n = 10 per dose). Blood samples were collected 24 h later, and plasma samples were tested by 14 parameters for organ functions. Data are presented as Mean ± SE. Normal ranges are shown by gray horizontal lines. None of the doses show any statistically significant difference compared with vehicle control (0 mg/kg dose in saline).

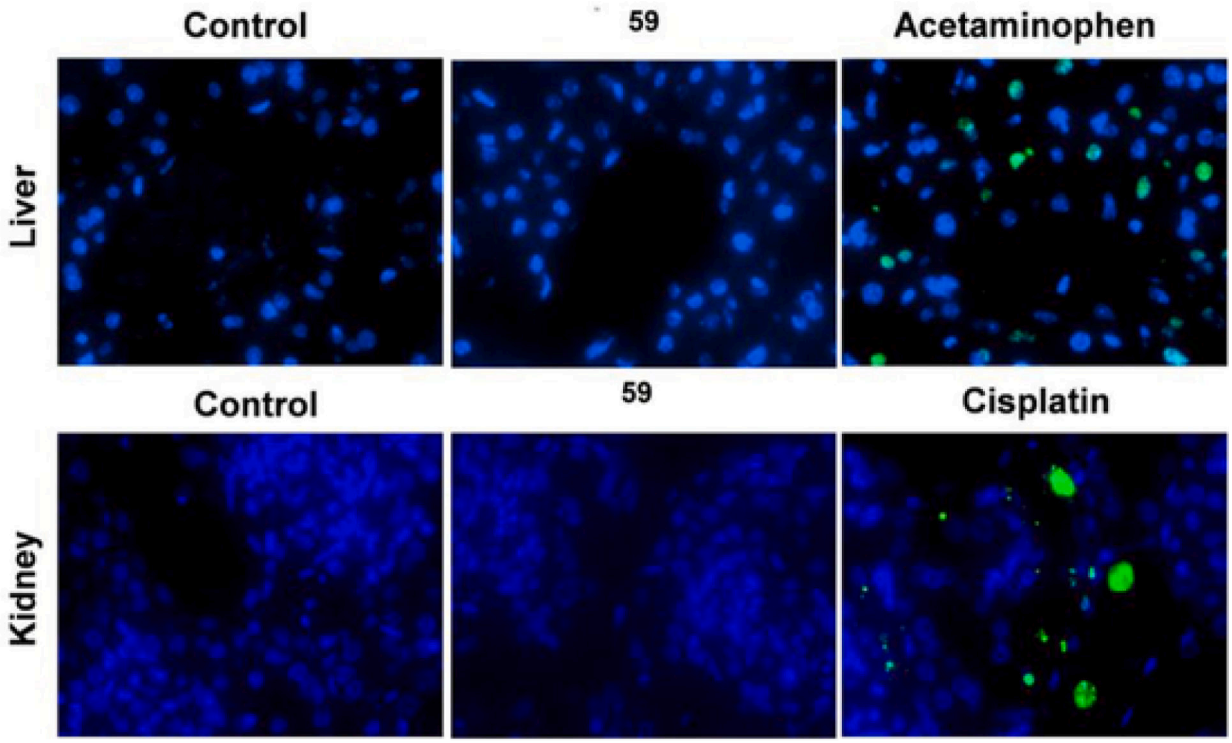

Fig. 9.

TUNEL assay in mouse liver and kidney samples injected with saline (Control) or compound (**59**, 50 mg/kg IP) in saline. Acetaminophen, 300 mg/kg, and Cisplatin, 20 mg/kg, were injected IP for 24 h and used as positive controls for the test. TUNEL-positive (dead) cells are shown with green color; nuclei in all cells are counterstained by blue color DAPI.

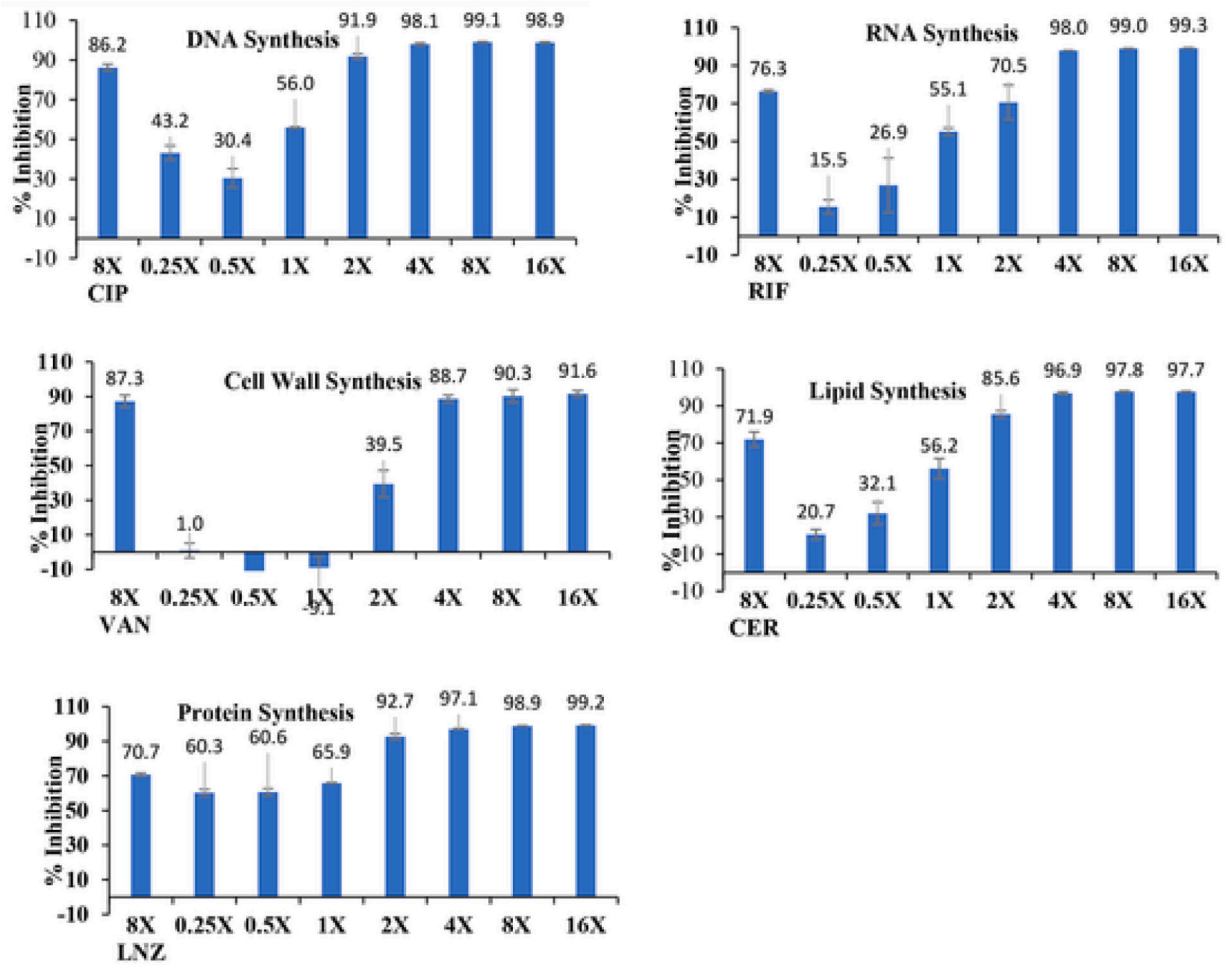

Fig. 10.

Inhibition of macromolecular synthesis for the mode of action for compound **59**. Ciprofloxacin (CIP), rifampicin (RIF), vancomycin (van), cerulenin (CER), and linezolid (LNZ) are the positive controls for DNA synthesis, RNA synthesis, Cell Wall Synthesis, Lipid Synthesis, and Protein Synthesis. All the positive controls were tested at 8xMIC and compound **59** was tested in the range of 0.25x to 16xMIC.

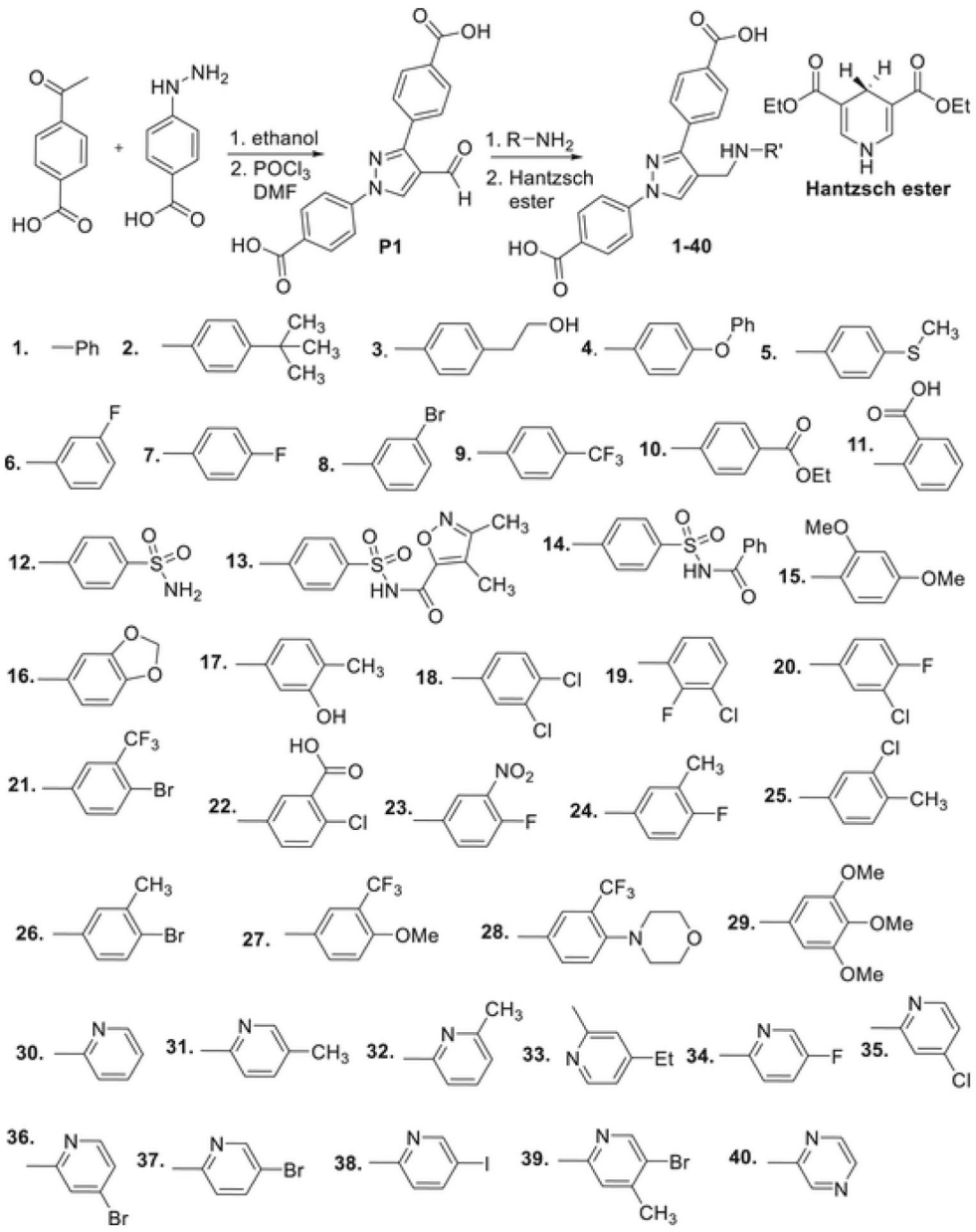

Scheme 1.

Synthesis of 1,3-dibenzoic acid-derived pyrazole anilines.

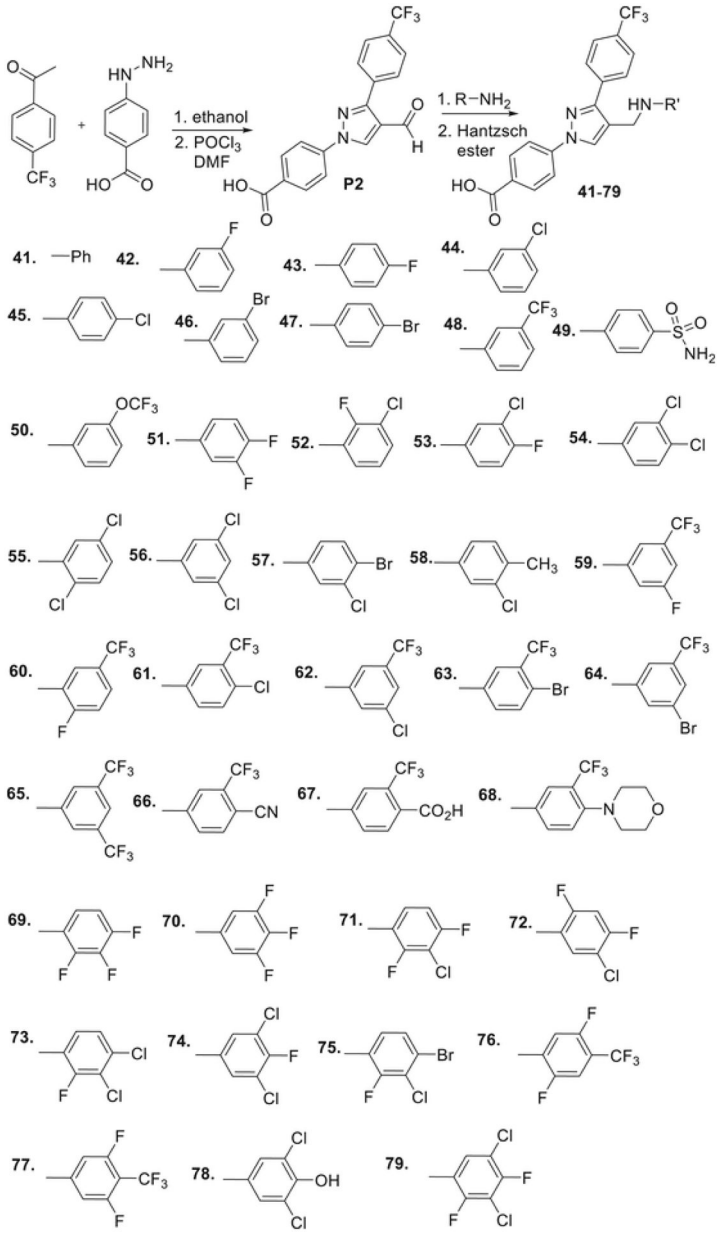

Scheme 2.
Structure of trifluoromethylphenyl-substituted pyrazole derivatives.

Table 1

Antimicrobial activity of trifluoromethyl-substituted derivatives. Gram-positive: antibiotic susceptible *S. aureus* ATCC 25923 (Sa23), antibiotic-resistant *S. aureus* BAA-2312 (Sa12): *S. aureus* ATCC 33591(Sa91), *S. aureus* ATCC 700699 (Sa99), *S. aureus* ATCC 33592 (Sa92), *S. epidermidis* ATCC 700296 (Se), *Bacillus subtilis* ATCC 6623 (Bs): vancomycin-resistant *E. faecium* ATCC 700221(Ef21) and antibiotic susceptible *E. faecalis* ATCC 29212 (Ef12).

#	Sa23	Sal2	Sa91	Sa99	Sa92	Se	Bs	Ef21	Efl2
41	12.5	12.5	6.25	6.25	6.25	12.5	3.12	6.25	25
42	3.12	3.12	3.12	3.12	3.12	6.25	1.56	6.25	25
43	6.25	3.12	6.25	6.25	12.5	12.5	1.56	6.25	25
44	1.56	1.56	0.78	0.78	1.56	3.12	0.78	0.78	12.5
45	1.56	1.56	1.56	1.56	1.56	3.12	0.78	1.56	6.25
46	0.78	0.78	0.78	1.56	0.78	3.12	0.78	1.56	6.25
47	0.78	0.78	0.78	0.78	1.56	3.12	0.78	0.78	6.25
48	1.56	1.56	0.78	0.39	0.78	1.56	0.78	1.56	6.25
49	50	50	50	50	50	50	50	NA	NA
50	0.78	0.78	0.78	0.78	0.78	3.12	0.78	0.78	3.12
51	1.56	1.56	1.56	3.12	1.56	6.25	0.78	3.12	12.5
52	1.56	0.78	1.56	1.56	1.56	3.12	0.78	0.78	3.12
53	0.78	0.78	0.78	1.56	0.78	3.12	0.78	1.56	6.25
54	0.78	0.78	0.78	0.78	0.78	1.56	0.78	0.78	1.56
55	0.78	0.78	0.78	0.78	0.78	1.56	0.78	0.78	3.12
56	0.78	0.78	0.78	0.78	0.78	0.78	0.78	0.78	1.56
57	0.78	0.78	0.78	0.78	0.78	0.78	0.78	0.78	1.56
58	0.78	0.78	0.78	0.78	0.78	1.56	0.78	0.78	3.12
59	0.39	0.78	0.39	0.78	0.78	1.56	0.78	0.78	1.56
60	1.56	0.78	0.78	0.78	1.56	3.12	0.78	1.56	6.25
61	0.78	0.78	0.78	0.78	0.78	0.78	0.78	0.78	0.78
62	0.78	0.78	0.78	0.78	0.78	1.56	0.78	0.78	6.25
63	3.12	3.12	0.78	3.12	3.12	12.5	3.12	0.78	1.56
64	0.78	0.78	3.12	0.78	0.78	1.56	0.78	0.78	0.78
65	0.78	0.78	0.78	0.78	0.78	1.56	0.78	0.78	0.78
66	1.56	1.56	0.78	1.56	0.78	3.12	0.78	6.25	12.5

#	Sa23	Sal2	Sa91	Sa99	Sa92	Se	Bs	Ef21	Efl2
67	50	50	NA	NA	NA	50	NA	NA	NA
68	0.78	1.56	0.78	0.78	0.78	1.56	0.78	0.78	1.56
69	1.56	1.56	1.56	1.56	1.56	3.12	0.78	3.12	NA
70	0.78	0.78	0.78	0.78	0.78	1.56	0.78	0.78	1.56
71	1.56	1.56	1.56	1.56	1.56	1.56	0.78	1.56	6.25
72	1.56	0.78	1.56	0.78	1.56	3.12	0.78	1.56	6.25
73	0.78	0.78	0.78	0.78	0.78	0.78	0.78	0.78	1.56
74	0.78	0.78	0.78	0.78	0.78	0.78	0.78	0.78	0.78
75	0.78	0.78	0.78	0.78	0.78	0.78	0.78	0.78	1.56
76	0.78	0.78	0.78	0.78	0.78	1.56	0.78	0.78	3.12
77	1.56	1.56	1.56	1.56	1.56	3.12	0.78	6.25	12.5
78	50	50	50	50	50	50	12.5	NA	50
79	0.78	0.78	0.78	0.78	0.78	0.78	0.78	0.78	0.78
V	0.78	0.78	1.56	3.12	1.56	1.56	0.19	>50	3.12

Table 2

MIC values of **59** against the clinical isolates of *E. faecalis*, *E. faecium*, and *S. aureus*. Positive controls: Oxacillin (Oxa), Vancomycin (Van), and Meropenem (Mer). VRE = Vancomycin resistant enterococci.

Collection number	Bacteria	Phenotype	MIC (μg/ml)			
			59	**Oxa**	**Van**	**Mer**
1088051	*E. faecalis*	VRE	2	64	>32	2
1091563	*E. faecalis*	VRE	4	64	>32	2
1091720	*E. faecalis*	VRE	4	64	>32	8
1094112	*E. faecalis*	VRE	4	>64	>32	8
1100440	*E. faecalis*	VRE	4	>64	>32	4
1088168	*E. faecium*	VRE	4	>64	>32	>128
1088228	*E. faecium*	VRE	4	>64	>32	>128
1088925	*E. faecium*	VRE	4	>64	>32	>128
1089544	*E. faecium*	VRE	4	>64	>32	>128
1091282	*E. faecium*	VRE	2	>64	>32	>128
ATCC 29213	*S. aureus*	MSSA	2	0.25	1	0.06
1088060	*S. aureus*	MSSA	4	0.5	0.5	0.06
1088105	*S. aureus*	MSSA	2	0.25	1	0.12
1088626	*S. aureus*	MSSA	2	0.25	0.5	0.06
1088064	*S. aureus*	MRSA	2	64	0.5	4
1088610	*S. aureus*	MRSA	4	64	0.5	4
1088888	*S. aureus*	MRSA	4	>64	1	8
1089106	*S. aureus*	MRSA	4	64	1	2